SIMULATION AND VISUALISATION OF SOLAR CAR MOTION ALONG THE ROAD

by
Murad Eminov

A thesis
submitted in partial fulfilment
of the requirements for the degree of
Master of Science in Information Technology
Kiel University of Applied Sciences
(Fachhochschule Kiel)

February, 2015

Statement of Originality

I hereby declare that:

- this thesis and the work reported herein was composed by and originated entirely from me,
- information derived and verbatim from the published and unpublished work of others has been properly acknowledged and cited in the bibliography,
- this thesis has not been submitted for a higher degree at any other University or Institution.

Date, Name, Matricle Number, Signature:

18.02.2016, 922154, Murad Eminov

Dedicated to my parents

ACKNOWLEDGEMENTS

I would like to thank Prof.Dr.Robert Manzke for his support and encouragement on carrying current work. His previous high assessment of my Master's Project, which was devoted to application of Information Technology to the domain of Renewable Energy, encouraged me to further develop the idea and add new concepts to it in my current Thesis. I am also grateful to him for accepting to become my first supervisor.

Many thanks to Prof.Dr.Christoph Weber for his helpful discussion on prospects of solar energy usage and also for encouraging me to carry out the present work. I'm especially grateful to him for informing me about solar car projects at Bochum University of Applied Sciences which eventually led me to establish the direct contact with SolarCar Team implementing the solar cars. I'm also very grateful to him for accepting to become my second supervisor.

I'm grateful to Prof.Dr.Rauf Gardashov for his guidance, supervision and control of my understanding the developed the mathematical model of solar radiation as well as its further development to take into account all the physical forces acting to the solar car during the motion. Also, many thanks to him for his valuable opinions regarding the finally achieved 3D visualisation reflecting the both the physics of the solar as well the energy potential.

Also, I would like to express my gratitude to Mr.Sebastian Weigel, the strategy team leader of SolarCar Team of Bochum University of Applied Sciences for presenting me the technical parameters of solar cars developed by his team, which I used to carry out the simulation and visualisation.

Finally, I express my gratitude to Mrs.Khadja Huseynova for her technical assistance, in helping to choose better visualisation scene view angles and color combinations for terrain, road and the solar car.

ABSTRACT

The importance of solar energy as an alternative to the fossil fuel increases year after year. Therefore, it is reasonable to assume that solar cars using solar energy as an alternative to fossil fuel will become widely used in the future. The solar cars convert the solar energy falling on their photovoltaic panels to the kinetic energy of motion. The solar cars will have to be operated on the roads that had already been built for conventional cars. Therefore, it is important to know the solar energy falling to the photovoltaic cell on the solar car for any geographical location of road and for any instance of time. In current thesis, the model for simulation of solar car motion along the road is developed. This model is composite of two models. The first is the "mathematical model of solar radiation falling onto the panel of solar car" which determines the amount solar energy consumed by electric motor of car for any instant of time and at any point of road. Here, the solar zenith and azimuth is determined by the way, which is based on the solution of Kepler's equation of the Earth motion around the Sun and has high computational accuracy that differs it from the commonly used one. The second is "mathematical model of solar car motion" which determines the law of motion by solving the differential equation of motion by taking into account all the forces (driving, gravity, reaction, resistance) acting to the car. The derived exact solution of the differential equation of car motion for straight-line trajectory is applied for curved road. As a study case, the developed model is implemented to simulate the solar car "Power Core-Sun Cruiser" motion on the chosen three roads 1) Hamburg-Berlin; 2) Baku-Shamakhi; 3) Zakatala-Tbilisi for specific days of year (equinox, solstice). The characteristic of motion essentially depend on solar energy entry and road characteristics i.e. time of the year, motion start time, turbidity and cloudiness of atmosphere, road location and tilt. By using the simulated data the ArcGIS based 3D visualization of car motion along the chosen roads is carried out. The visualization shows that the motion is released accordingly to the laws of physics.

TABLE OF CONTENTS

LIST OF TABLES

LIST OF FIGURES

CHAPTER 1

INTRODUCTION

1.1 Problem Context

Renewable energy, particularly solar energy has drawn a great attention to different industries, in particular to automotive industry. The importance of using solar energy as an alternative to conventional fuel energy increases. Solar energy has several benefits compared to conventional fuel energy. An important benefit is that solar power provides reliable energy. The exact time when the sun will rise and set can be precisely predicted, even though predicting cloudiness can sometimes be less accurate. This makes solar power a highly reliable energy source.

From economical perspective, the solar power is a type of alternative energy that no one can turn into monopoly. While being implemented along with simplicity of solar panels, this concept also notably contributes to energy security of the countries to implement the solar energy. The solar energy usage also ensures energy independence from the conventional fuel energy, since having solar panels on the roof of the car, the solar car user will receive essentially independent source of electricity that will come at no cost.

As a result of rapid growth of the world population, the issues relating to energy have become a priority [1]. Despite, the estimations of United Nations Population Division (UNO), as well as International Institute for Applied Systems Analysis (IIASA) showing large variety of expected results, it can be assumed that the world population will reach approximately 9 billion people by 2050.

Reaching higher living standards in the World is among the priorities in the future as well. The increasing number of the World population as well as the growing need for higher living standards point out to the expected tendency of increase in energy demand in the future. In spite of fossil fuels being a part of today's energy source, the efforts in more intensive usage of solar energy in the future need to be done. Although, rapid transition from fossil fuel energy usage to solar energy usage is not expected in short-term, this will be ultimately achieved in long-term.

From ecological perspective, the fossil fuel exhaust gases have negative influence on human body and may cause different diseases such as lung diseases [2]. These issues seriously put usability and profitability of fossil fuel energy under question. In densely polluted regions a human can intake around 50 million particulates into his or her organism. Despite the valid standards have clear bounds regarding the acceptable particulates a fossil fuel energy based vehicle permitted to emit to the environment, numerous research have displayed that the harmful impact of particulates is in inverse proportion with their sizes. Since the relation between the surface of exhaust particulate and the volume and mass of it is becoming greater as the smaller gets the particulate, this reasons the importance to decrease the number of exhaust particulates instead of their total mass. This makes automotive industry cope with the obligations on using specific filters on fossil powered applications.

Therefore, transition to alternative energy usage, especially to solar energy is an important problem, since solar power usage doesn't cause any emission.

In particular, the road transport is looking forward for the efficient electric processes to take over the conventional fossil fuel usage.

In transport area, as well as in the industry, many technologies would be accelerated in their deployment because of the solar car energy implementation [3]. Due to improvements in the battery exchange, we can suppose that the future cars will become either electric vehicles(EVs) or Plug-in Hybrid Electric Vehicles (PHEVs). PHEVs can consume electric power for daily usage, but can also permit usage of conventional fossil fuel for long distance trips.

The development of new generation of PV cells with higher efficiency and reduced cost will contribute to wide use of solar cars.

The transition to solar energy will dramatically increase the high efficiency of photovoltaic cells.

Photovoltaic devices are receiving growing interest in both industry and research institutions due to the great demand for clean and renewable energy.

A solar cell (also called a photovoltaic cell) is an electrical device that converts the energy of light directly into direct current electricity (dc) using semiconductors that exhibit the photovoltaic effect. The Figure 1.1 below shows the basic operation of a solar cell.

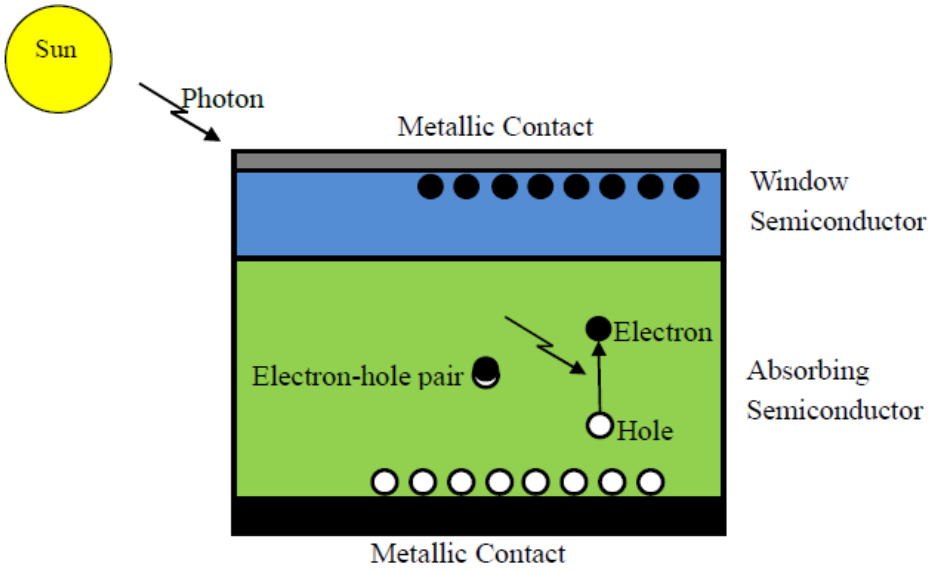

Figure 1.1: Basic operation of a solar cell.

When a semi conductive material absorbs a photon, electron gains energy so it can move more easily. The energy gain of this electron forms a hole in the energy level that it was before. This means that a single photon is capable to generate two types of currents: the movement of the electron, and the filling of the hole. For the case of this explanation we could consider the electron and the hole as two particles with the same amount of energy but different signs. The movement of these hole-electron pairs is what creates the current. In order to collect these electrons and holes a different type

of semiconductor called window is used. This semiconductor has two functions: allow the transit of the photon and generate an electric field capable of separating the electron from the hole. In this way, a metal connected to the window can collect the electrons and a metal connected to the absorber can collect the holes. In summary, electrons in a solar cell absorb photon energy in sunlight which excites them to the conduction band from the valence band. This generates hole-electron pairs, which are being separated by a potential barrier (such as a p-n junction) and induces a current, as shown in Figure 1.2 below.This is how the energy from the sun is converted. The efficiency of a given solar cell will depend on how transparent is the window semiconductor, how absorbing is the absorber semiconductor and how many electrons and holes are collected. The simplest model of a silicon p-n junction solar cell is given in Figure 1.2. below.

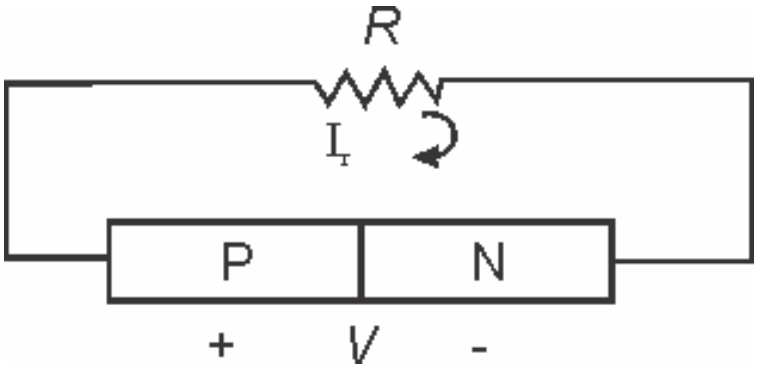

Figure 1.2: Simplest model of Si p-n- junction solar cell

Because of the intermittent nature of solar energy (solar radiation is not available during the night), efficient energy storage systems are critically needed to make the optimal of the electricity generated from these sun cells since they can promote the reliability and effective use of the entire power system by storing energy when in excess while releasing it when in high demand. Thus, the energy of the photovoltaic cells can either be used directly or be used to recharge storage devices (batteries and capacitors) which in turn can power the application electronics when the Sun is not shining. As shown in Figure 1.3, a typical photovoltaic solar energy harvesting system includes PV cells which are often electrically connected and encapsulated as module

(1), inverter (2) to convert dc electricity produce by PV-cell to ac electricity as well as energy storage systems (3), such as batteries or electrochemical capacitors.

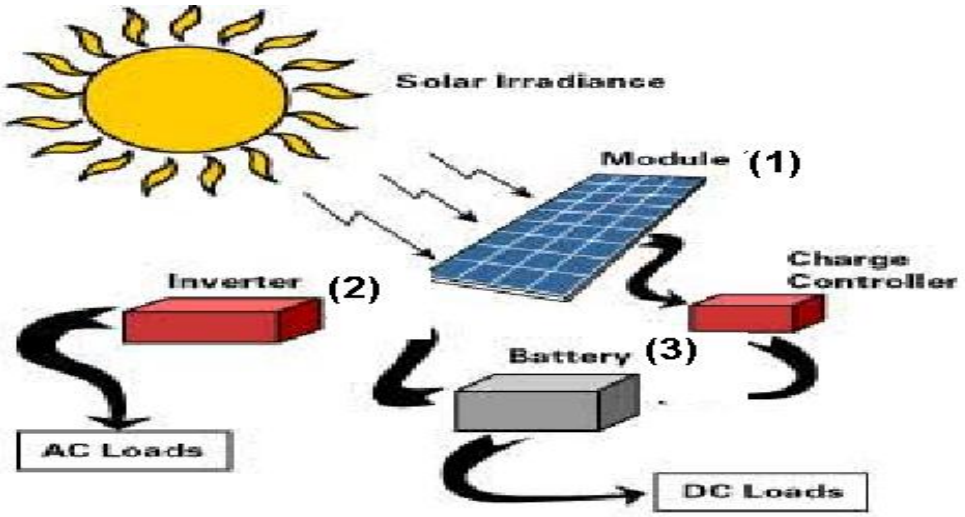

Figure 1.3: The scheme of sun harvesting system CdTe/CdS PV-cell

In practice nearly all photovoltaic energy conversion uses semiconductor materials in the form of p-n- and hetero-junctions.

Despite the high cost, some 40% of first generation solar cells the solar cells produced, in the world, were single crystal silicon related to first generation solar cells and, according to the manufacturer's data in 2009, the highest module efficiency available for single-crystalline silicon is 20%. Second generation solar cells are based on heterojunctions of thin layers of different semiconductor among which CdS/Cu_2S, CdS/CdTe, CdS/ $CuInSe_2$ (or CIS) combinations are the most promising solar cells are developed so far [4][5]. In such cells CdS -n-type semiconductor with band gap of ~2.5 eV is commonly used as a window layer, while CdTe was found to be a very suitable absorbing layer for solar cells due to its direct band gap of ~1.5 eV close to the optimum band gap for PVs. The CdS/CdTe based solar cells have reached an efficiency of 16.5% which is close to the predicted efficiency limit of 17.5%. This kind of solar cells have been used for a long time and still being widely used

nowadays. However, due to many issues associated with the fabrication procedures of CdTe-CdS solar cells they are not much more efficient than silicon solar cells as we might expect.

Electrochemical capacitors that are also designated supercapacitors [6][7] derive their energy storage capacity from interaction between electrode and electrolyte at the interfacial region. Supercapacitors are currently a prominent area of research for energy storage devices as they have high power density, long cycling life, and short charging time. Moreover, they have higher energy density than conventional dielectric capacitors. Supercapacitors can be used either alone as a primary power source or as an auxiliary one with rechargeable batteries for high-power applications, such as industrial mobile equipment and hybrid/electric vehicles.

The solar array consists of hundreds of photovoltaic solar cells converting sunlight into electricity. In order to construct an array, PV cells are placed together to form modules which are placed together to form an array. In Figure 1.4 it is shown a cell, module, and array. The larger arrays in use can produce over 2 kilowatts (2.6 hp).

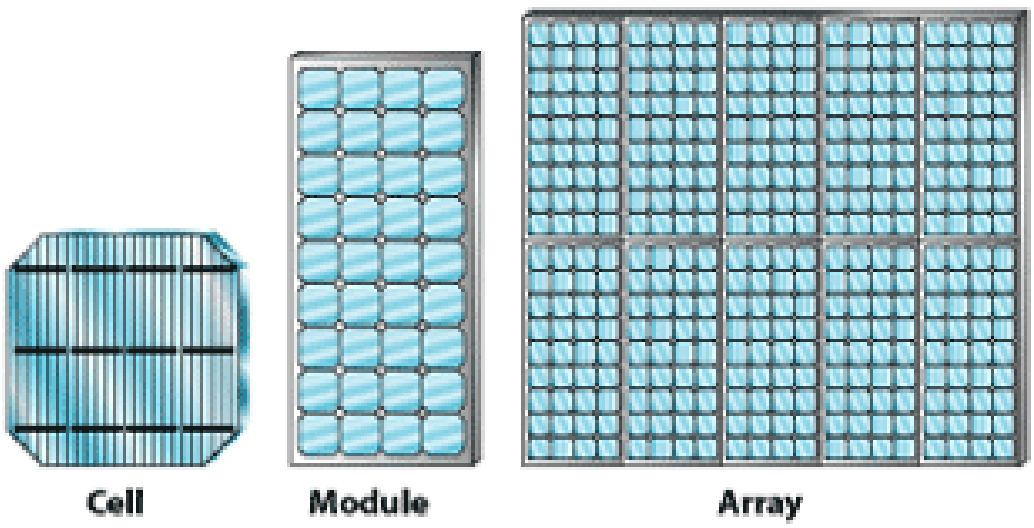

Figure 1.4: Cells, modules and arrays [8].

Overview of hybrid solar cars

Solar cars have began gaining interest among car buyers mainly because of their advantages in no fuel usage, therefore causing no air pollution and economical perspective on saving resources on buying fuel etc. A hybrid solar car consists of the following elements as described in [9] and [10] (Figure 1.5 below):

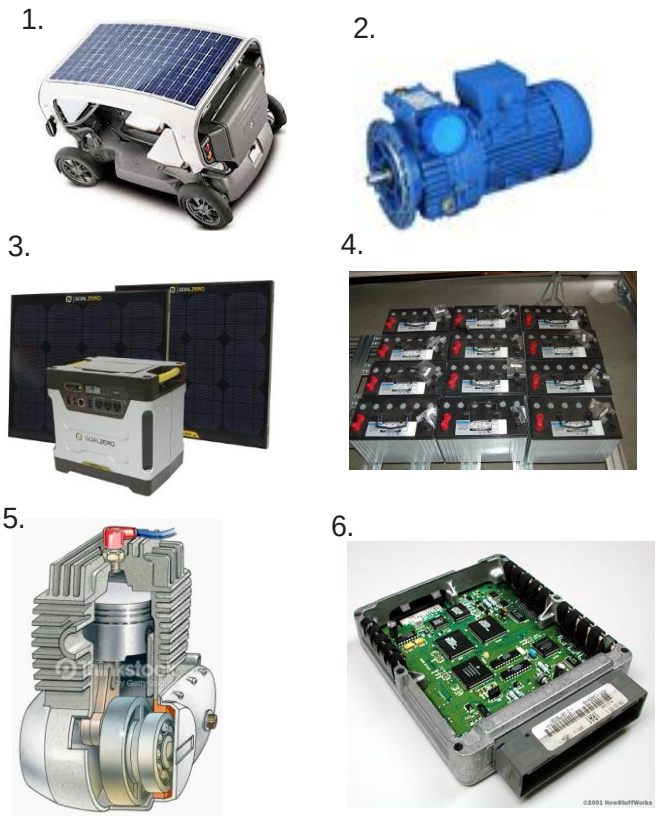

Figure 1.5: Main elements of hybrid solar car: 1-PV panel, 2-Electric motor, 3- Electric generator, 4-Battery bank, 5-IC Engine, 6-ECU controlling.

Photovoltaic panel converts the falling solar radiation into electricity which is being accumulated in batteries. Then, this electrical energy is used for the solar car motion. Electric motor or brushless DC motor is used to convert the electrical energy into mechanical energy. During the brake or road slope the Electric Generator can regenerate energy. A very important element of solar car, the battery bank can supply 24 V direct current to both electric motor and electronic devices of solar car. The IC

engine is used for driving during the night or minimum electric energy. The ECU (Electronic Control Unit) is a circuit which controls the provided energy to the motor in order to control speed variations.

The factors such as solar cars being environmentally friendly as well as their exploitation not requiring spending on fuel will contribute to widely usage of solar cars. Therefore, it is important to know the distribution of solar radiation on existing roads. The currently existing roads had been constructed taking into account the abundance of solar radiation. In many cases, the roadsides were planted with trees for aesthetic purposes. As the solar cars will become widely used, the solar cars will travel over the existing roads. Therefore, distribution of solar radiation over the existing roads and simulation of solar car motion is necessary for development of optimal management for solar cars.

1.2 Thesis Statement

1.2.1 Objectives

The aim of the present thesis work is to develop a mathematical model of solar radiation falling onto the panel of solar car at any point of the road and any instance of time and simulation of the solar car motion on basis of solution of differential equation of motion which takes into account all the forces acting to the solar car during the motion: driving force, reaction force, resistance force (aerodynamic resistance and rolling resistance) and gravity force along the routes Baku-Shamakhi, Hamburg-Berlin and Zakatala-Tbilisi.

An ArcGIS v 10.3 based visualization of the simulated data which presents the motion of solar car more visually is also an objective of the present work.

1.2.2 Procedures

The present work has been carried out through accomplishing the following procedures:

- Development of solar radiation model for calculation of the amount of solar energy falling onto the panel of solar car;
- Simulation of solar car motion on the basis of solution of differential equation of motion which takes into account all the forces acting to the car (driving force, reaction force, resistance force (aerodynamic resistance and rolling resistance);
- The realization of the Fortran based program for simulation of solar car motion using solar radiation data;
- Visualization of solar car motion using the simulated data;

As a study case three roads, one in Germany, and two in Caucasus which allows demonstrating the influence of longitude differences on falling solar energy amount, were chosen.

The simulation was carried out using the technical parameters of solar car "Sun Cruiser" which is designed by SolarCar Team of Bochum University of Applied Sciences [11].

In order to achieve high accuracy the solar zenith and azimuth have been calculated by solving the Kepler's equation of the Earth motion around the Sun. The solution of the differential equation of motion for curved road has been carried out by using the exact solution of differential equation for straight line trajectory.

To achieve a better presentation, ArcGIS based visualization of solar car motion along the chosen roads has been implemented. The abovementioned procedures are shown in the following scheme.

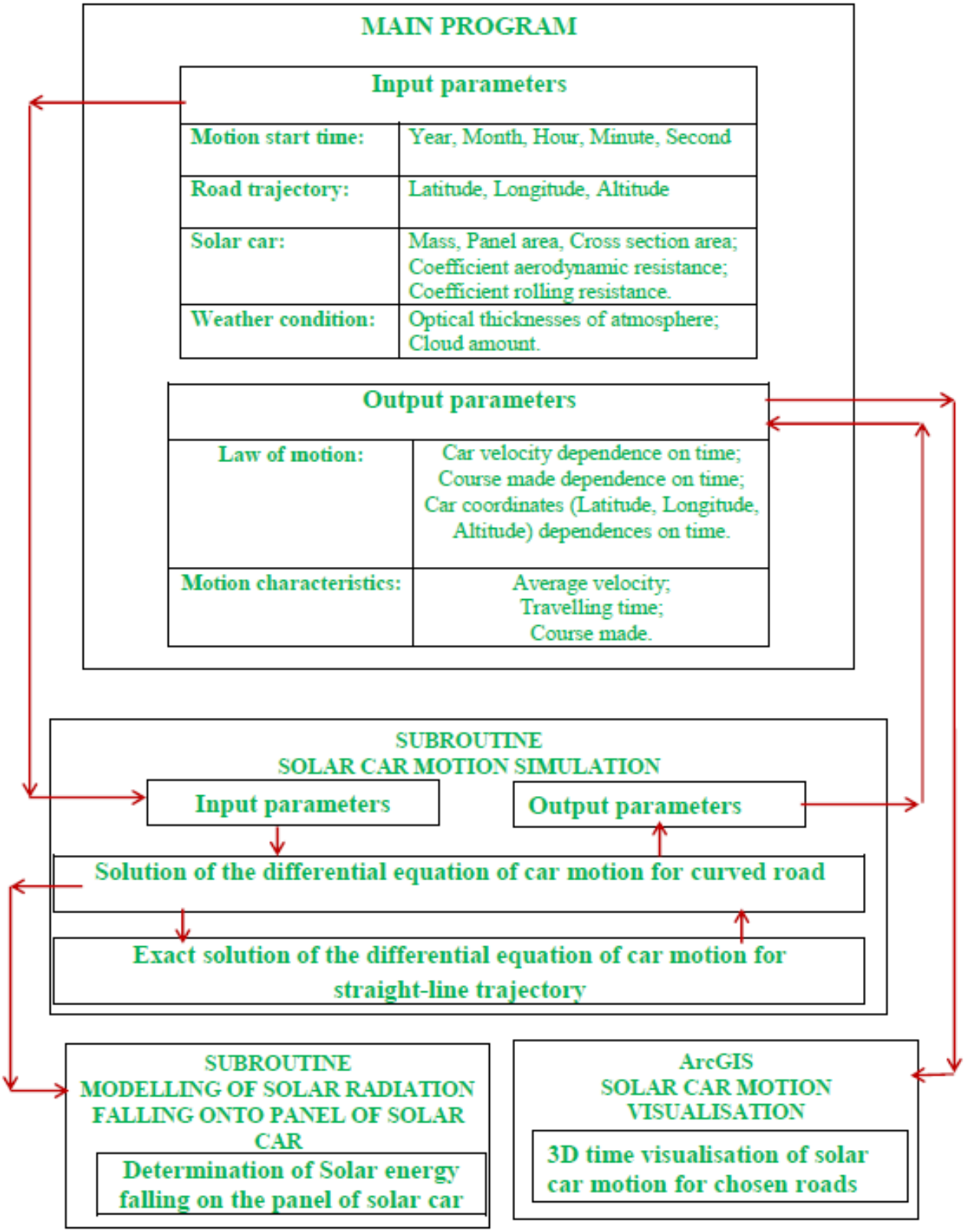
MAIN PROGRAM
Input parameters
Motion start time:
Year, Month, Hour, Minute, Second
Road trajectory:
Latitude, Longitude, Altitude
Solar car:
Mass, Panel area, Cross section area;
Coefficient aerodynamic resistance;
Coefficient rolling resistance.
Weather condition:
Optical thicknesses of atmosphere;
Cloud amount.
Output parameters
Law of motion:
Car velocity dependence on time;
Course made dependence on time;
Car coordinates (Latitude, Longitude, Altitude) dependences on time.
Motion characteristics:
Average velocity;
Travelling time;
Course made.
SUBROUTINE
SOLAR CAR MOTION SIMULATION
Input parameters
Output parameters
Solution of the differential equation of car motion for curved road
Exact solution of the differential equation of car motion for straight-line trajectory
SUBROUTINE
MODELLING OF SOLAR RADIATION FALLING ONTO PANEL OF SOLAR CAR
Determination of Solar energy falling on the panel of solar car
ArcGIS
SOLAR CAR MOTION VISUALISATION
3D time visualisation of solar car motion for chosen roads

1.3 Prior Work

1.3.1 Web-Based Program Package For Modelling Of Solar Energy Falling Onto The Panel Of Solar Car Along The Road

Web-based based visualization of a solar car motion under falling solar energy was previously achieved on 2D Google Maps in [12] by means of combining the Application Program Interface (API) calling scripts that is inserted into the program code with the scripts used to bring into the motion the 2D icon (a blue circle) representing a solar car with the scripts that make the circle move between the geographical coordinates (latitudes and longitudes) over the instances of time taking into account the location of the Sun.

In Figure 1.6 below it is given a working interface of web-based application for visualization of solar car motion under the falling solar radiation. The web-based application uses Google Maps API which retrieves 2D Google basemap onto the canvas element to carry out the visualization. A JQuery plugin DateTimePicker was implemented in order to set the desired visualization date.

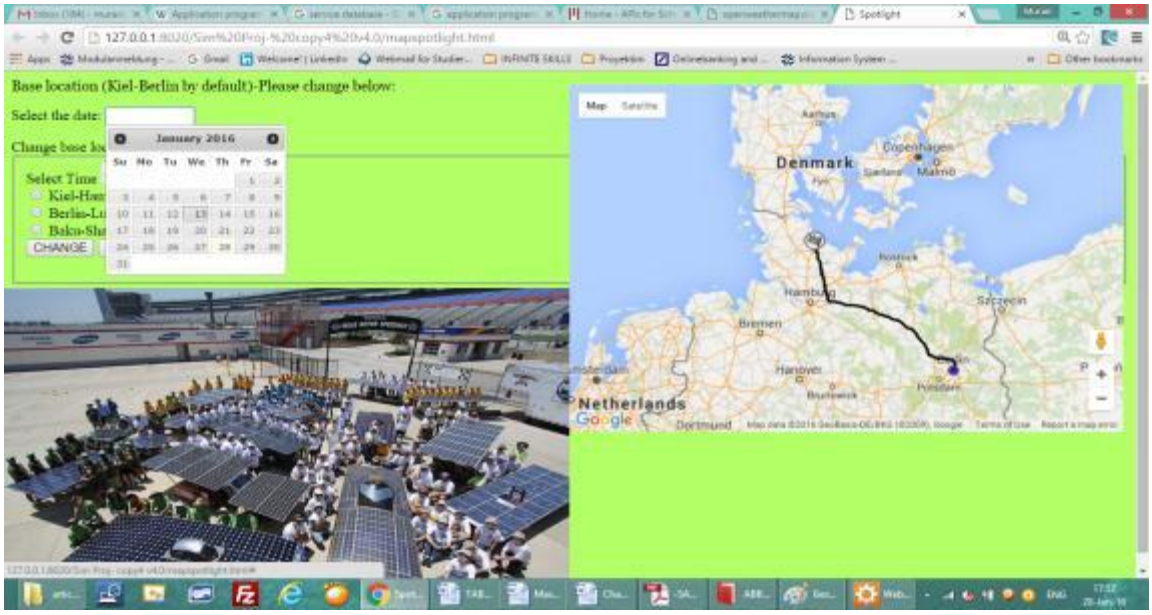

Figure 1.6: Web-based visualization of solar car motion [12].

However, the web-based simulation and visualization was carried out under the assumption that the solar car is moving along the chosen roads Kiel-Berlin and Baku-Shemakhi under directly falling solar radiation and along the plain road (when solar radiation falling onto the solar panel is maximum).

The current thesis introduces a more realistic mathematical model simulating the falling solar radiation which also takes into account all the acting forces to the solar car (driving force, reaction force, resistance force (aerodynamic resistance and rolling resistance) as well as the road tilt, which affects the amount of falling solar radiation onto the panel.

As well, a more realistic visualizations based on the results from the mathematical model is carried out in 3D ArcScene for the roads Hamburg-Berling, Baku-Shemakhi, Zakatala-Tbilisi, where it can clearly be seen the motion of solar car which is affected by all the forces acting to the car (driving force, reaction force, resistance force (aerodynamic resistance and rolling resistance)) on the roads, which have tilts.

1.3.2 Possible visualization of cloud layers for previously carried out 2D Web based visualization of solar car motion along the road

In web-based visualization implementing API, a visualization of cloudiness that has impact on the falling solar radiation can be achieved by means of OpenWeatherMap API (http://openweathermap.org/).

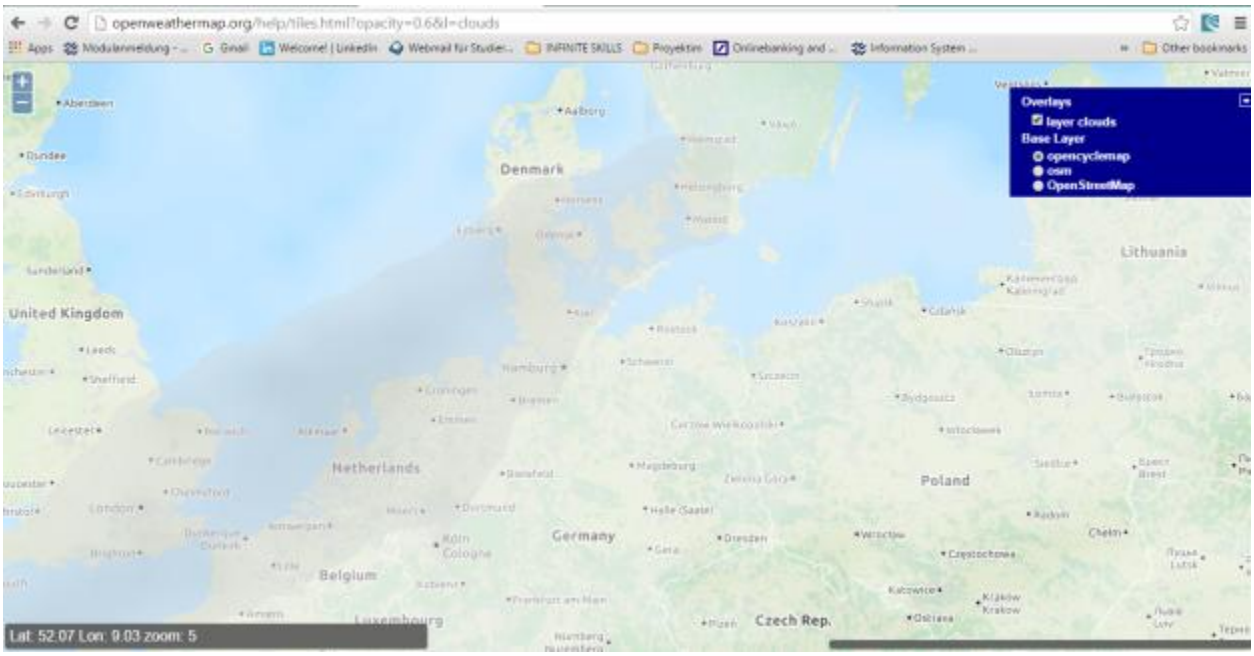

Figure 1.7: Visualization of cloudiness layer with OpenWeatherMap API

OpenWeatherMap API offers rich capabilities to visualize the data of the clouds layers which can give up to16-days forecast obtained from the stations. The API currently has the capability to visualize the historical data for up to 200, 000 cities through JSON, XML and HTML calls.

The API can as well be implemented to visualize other essential data such as Precipitation, Clouds, Pressure, Temperature, Wind etc.

CHAPTER 2

MATHEMATICAL MODEL OF SOLAR RADIATION FALLING ONTO THE PANEL OF SOLAR CAR

Developed by us mathematical model consists of four stages. The first stage: for the given moment of time the location of the Earth on the elliptical orbit around the Sun is found; The second stage: for this moment of time the latitude and the longitude of the Sun are determined; The third stage: in any point on the Earth and at this moment of time the Solar zenith and azimuth are found; The fourth stage: for this moment of time and point the amount of global (direct + diffuse) solar radiation falling onto the panel of car is calculated.

The Fortran code subroutine to realise this model is given in Appendix B.

2.1 Determination of the Earth Location in orbit

The location of the Earth in orbit is determined by the solution of Kepler's equation of orbital motion:

$$M = E - e\sin E \qquad (2.1)$$

where, E - eccentric anomaly, M -mean anomaly. Eccentric anomaly E is related to the true anomaly φ equation:

$$\varphi = 2\arctan\left(\sqrt{\frac{1+e}{1-e}}\ \tan\frac{E}{2}\right) + \frac{\pi}{2} \qquad (2.2)$$

where, $e = 0.016729$ - eccentricity of the Earth's orbit. Mean anomaly M related to the time t (*seconds*), reckoned from the moment of the vernal equinox: $M = \frac{\sqrt{GM_S}}{a^{3/2}}\ t \approx$

$0.199 \times 10^{-6} \cdot t$; here, $M_s = 1.989 \times 10^{30}\ kg$ - mass of the Sun, $M_s = 1.989 \times 10^{30}\ N \cdot (m/kg)^2$ - gravitational constant, $a = 1.496 \times 10^{8}\ km$ -major axis of the elliptic Earth's orbit. The joint solution of equations (2.1) and (2.2) gives the dependence of the angle φ on the time t: $\varphi = \varphi(t)$, i.e the location of the Earth in orbit at any given time. For the solution of Kepler's equation various methods (Taff 1985) have been developed. The capabilities of modern computers allow us to solve numerically the equations (2.1) and (2.2) with great accuracy.

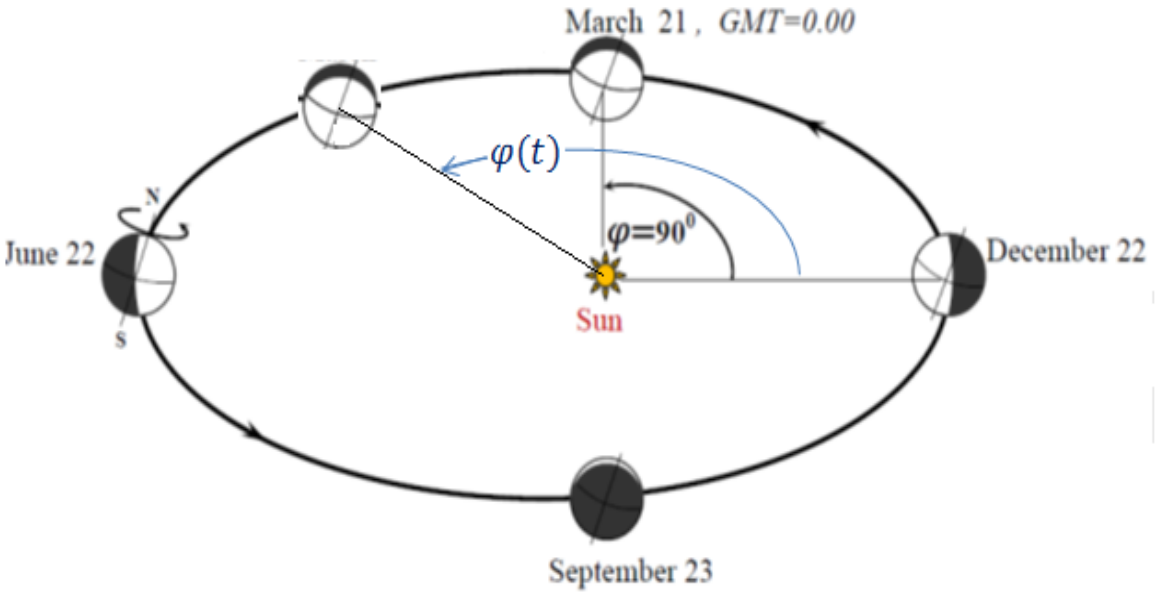

Figure 2.1: The motion of the Earth around the Sun

2.2 Determination of the solar latitude and longitude

Suppose that, at the moment of the vernal equinox ($t = 0$), (around March 21), the Greenwich Mean Time (GMT) is: $GMT0$. The precise value of $GMT0$ is determined by astronomical calculations and varies from year to year. At the moment $t = 0$, the meridian of Greenwich will have an angle $\varphi_{\mathrm{GMT}\,0} = \frac{\omega}{2\pi} \cdot \mathrm{GMT0}$ from the direction of

AB (Figure. 2.1), where, $\omega = \frac{2\pi}{T_{sid}}$, $T_{sid} = 23.96\ h. = 23.96 \times 3600\ sec. = 86256\ sec.$ - sidereal rotation period of the Earth. Then, at time $t > 0$ the Greenwich meredian will form with the direction of *AB*, the angle:

$$\varphi_G = \varphi_{GMT\,0} + \omega \cdot t \tag{2.3}$$

As it can be seen, the angle φ_G, determining the longitude of the Sun depends on two parameters: t and $GMT0$. From spherical triangles in Figure: 2.1, we determine the latitude θ_{Sun} and the longitude φ_{Sun} of the Sun:

$$\left.\begin{aligned} \theta_{Sun} &= \arcsin[-\sin(\delta)\cos(\varphi)] \\ \varphi_{Sun} - \varphi_G &= \arcsin[-\sin(\varphi)\cos(\theta_{Sun})] \end{aligned}\right\} \tag{2.4}$$

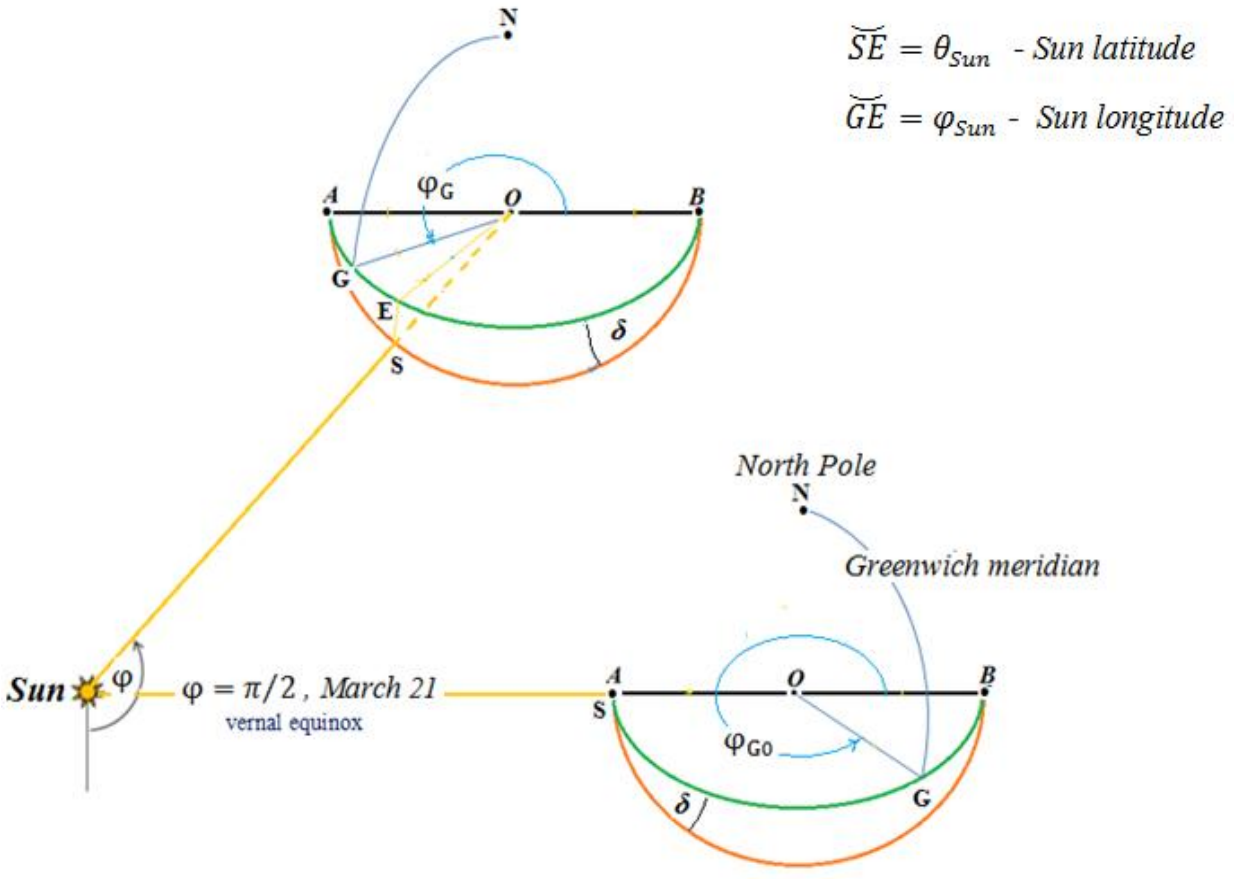

Figure 2.2: The determination of solar zenith and azimuth

Thus, the formulas (4) determine the dependence of the latitude θ_{Sun} and the longitude φ_{Sun} on time t

$$\begin{cases} \theta_{\text{Sun}} = \theta_{\text{Sun}}(t) \\ \varphi_{\text{Sun}} = \varphi_{\text{Sun}}(t) \end{cases} \tag{2.5}$$

since, the angle φ depends on time t.

2.3 Determination of solar zenith and azimuth

To determine the zenith i_{sun} and the azimuth ϕ_{sun} angles of the Sun at the given point $M(lat = \theta_M, lon = \varphi_M)$ on the Earth at the given moment of time, let us turn to Figure 2.3. As we see from the spherical triangular NMS:
$\angle NMS = \phi_{sun}$; $\angle MNS = \varphi_{sun}$; $\angle NOM = 90^0 - \theta_M$; $\angle NOS = 90^0 - \theta_{sun}$ and $arc\ \overset{\smile}{MS} = \angle MOS = i_{sun}$. Applying to the triangular NMS cos-theorem, we obtain:

$$\cos\overset{\smile}{MS} = \cos\overset{\smile}{NM}\cos\overset{\smile}{NS} + \sin\overset{\smile}{NM}\sin\overset{\smile}{NS}\cos(\varphi_{sun} - \varphi_M) \tag{2.6}$$

$$\cos\overset{\smile}{NS} = \cos\overset{\smile}{NM}\cos\overset{\smile}{MS} + \sin\overset{\smile}{NM}\sin\overset{\smile}{MS}\cos\phi_{sun} \tag{2.7}$$

From (2.6) and (2.7) we find:

$$\cos i_{sun} = \sin\theta_M \sin\theta_{sun} + \cos\theta_M \cos\theta_{sun} \cos(\varphi_{sun} - \varphi_M) \tag{2.8}$$

$$\cos\phi_{sun} = (\sin\theta_{sun} - \sin\theta_M \cos i_{sun}) / \cos\theta_M \sin i_{sun} \tag{2.9}$$

The formulas (2.8) and (2.9) determine the zenith i_{sun} and azimuth ϕ_{sun} angles of the Sun on the dependence of point $M(\theta_M, \varphi_M)$ and the time t.

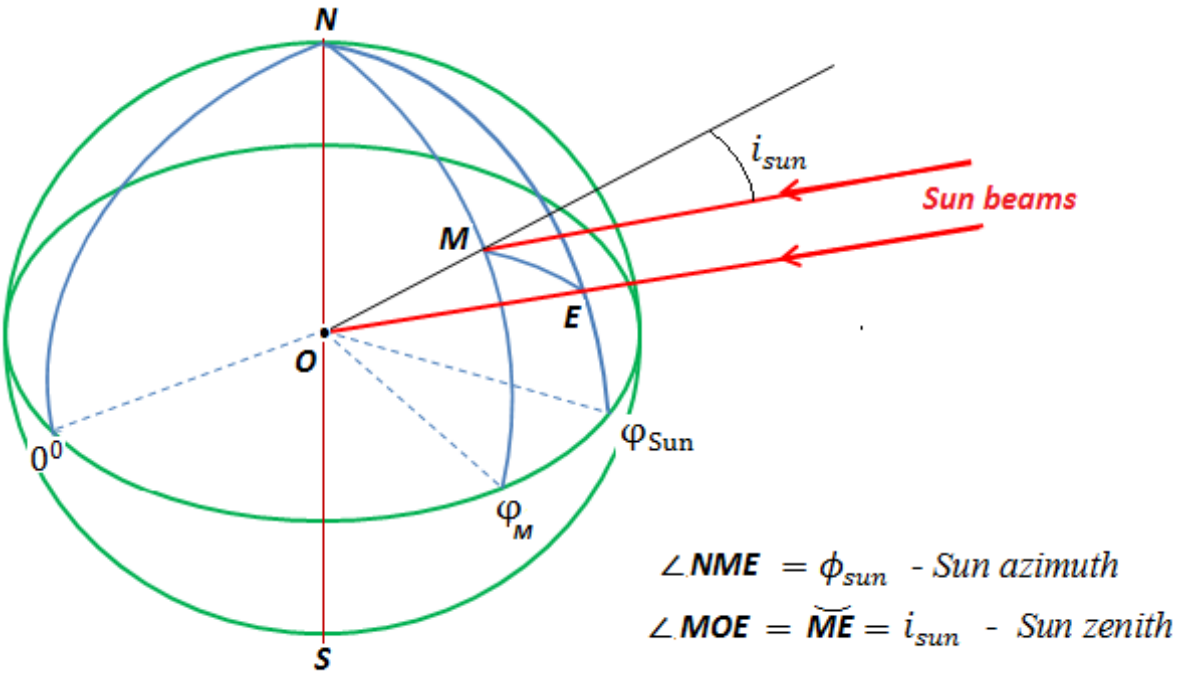

Figure 2.3: The calculation of solar zenith and azimuth

2.4 Determination of Solar energy falling on the panel of solar car

In the case of clear atmosphere, the amount of direct solar radiation reaching the solar car panel is defined by the formula (Figure: 2.4)

$$S_{pan}\,(i_{sun}) = S_0\, cos\, \chi_n \exp\left(-\frac{\tau}{cos\, i_{sun}}\right) \qquad (2.10)$$

where, S_0 = 1367 W/m^2 –solar constant (i.e. the amount of incoming solar electromagnetic radiation per unit area that would be incident on a plane perpendicular to the rays, at upper boundary of atmosphere);

χ_n – angle between the sunbeam and normal to the panel.

τ - atmosphere optical thickness, which is for clear atmosphere $= 0.3$. Note that τ is connected with Linke turbidity factor T_L : $T_L = \tau/\tau_R$. Here $\tau_R = 0.2$ –is

Rayleigh optical depth of atmosphere (where takes place only pure molecular scattering).

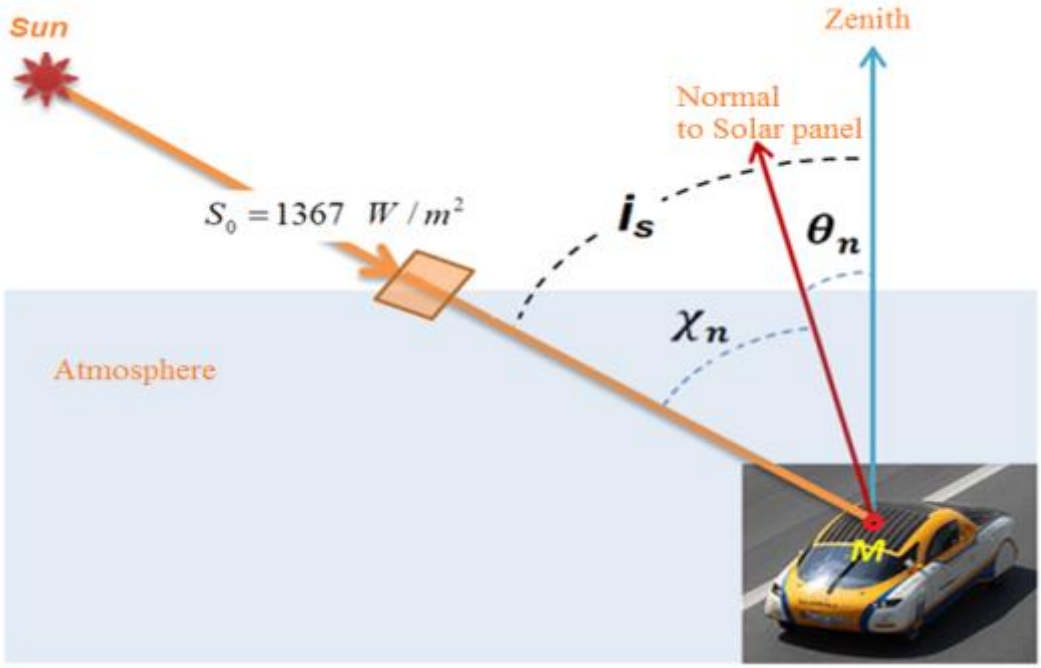

Figure 2.4: Determination of solar energy falling on the panel of solar car.

As we can see from Figure 2.4, the amount of solar radiation falling onto the perpendicular to the Sun beam plane at the Earth level is

$$S_{per}(i_{sun}) = S_0 \exp\left(-\frac{\tau}{\cos i_{sun}}\right) \tag{2.11}$$

So

$$S_{pan}(i_{sun}) = S_{per}(i_{sun}) \cos \chi_n \tag{2.12}$$

The angle χ_n is defined through the zenith i_{sun}, azimuth ϕ_{sun} of the Sun and zenith ϑ_n, azimuth ϕ_n of normal to panel (or to road tilt), by the equation of spherical trigonometry

$$\cos \chi_n = \cos i_{sun} \cos \vartheta_n + \sin i_{sun} \sin \vartheta_n \cos(\phi_{sun} - \phi_n) \tag{2.13}$$

The zenith i_{sun} and azimuth ϕ_{sun} of the Sun depend on point M on the road and instant of time t and are defined by the formulas of (2.8) and (2.9). To define those

angles**,** methods having different degree of accuracy have been developed. We calculate those angles on the method which is based on solution of Kepler's equation and has more accuracy [13-15].

To calculate the diffuse sky radiation falling on the panel under cloudless atmosphere**,** the experimentally determined quantity - the ratio of direct radiation in global - $\eta(i_{sun})$, has been used.

$$\eta(i_{sun}) = \frac{S_{Hor}(i_{sun})}{S_{Hor}(i_{sun}) + D_{Hor}(i_{sun})} \tag{2.14}$$

where,

$$S_{Hor}(i_{sun}) = S_0 exp\left(-\frac{\tau}{cos\, i_{sun}}\right) \tag{2.15}$$

is the direct solar radiation falling to horizontal plane. The values of $\eta(i_{sun})$ is presented in the Table 2.1. Then the diffuse radiance determined from (1.14) is:

$$D_{Hor}(i_{sun}) = \frac{\eta(i_{sun})}{1-\eta(i_{sun})} \cdot S_{Hor}(i_{sun}) \tag{2.16}$$

Table 2.1: The ratio of direct radiation in global

i_{sun},^{0}	0	20	30	40	50	60	65	70	75	80	85	90
$\eta(i_{sun})$	0.18	0.18	0.18	0.18	0.19	0.22	0.26	0.32	0.41	0.55	0.70	0.98

Thus the global irradianse is determined as:

$$Q_{Hor}(i_{sun}) = S_{Hor}(i_{sun}) + D_{Hor}(i_{sun}) \tag{2.17}$$

The diffuse Sky radiation $D_P(i_{sun})$, falling on the panel of solar car, at the first approximation can be taken as $D_P(i_{sun}) = D_H(i_{sun})$.

Thus, the global (direct + diffuse) solar radiation falling to the panel is calculated as:

$$Q_{Pan}(i_{sun}) = S_{Pan}(i_{sun}) + D_{Pan}(i_{sun}) \tag{2.18}$$

In the case of ***continuous cloudiness*** the amount $Q_{Hor,1}$ of falling onto horizontal area solar radiation (*irradiance*) depends on solar zenith, cloud types and of its ***water*** content and is changed in wide interval. The representative value of $Q_{Hor,1}$ on dependence of solar zenith i_{sun} is presented in Table 2.2.

Table 2.2: Irradiance of horizontal area in continuous cloudiness

$i_{sun}, ^0$	0	20	30	40	50	60	65	70	75	80	85	90
$Q_{Hor,1}$ $(Watt/m^2)$	210	189	166	143	134	125	120	114	108	103	98	85

In the case of ***partly cloudy*** atmosphere with *cloud amount* $10p$ $(0 \leq p \leq 1)$ the irradiance $Q_{Hor,p}$ is defined on the formula:

$$Q_{Hor,p}(i_{sun}) = Q_{Hor}(i_{sun}) \cdot (1-p) + Q_{Hor,1}(i_{sun}) \cdot p \qquad (2.19)$$

In this case at first approximation the irradiance of solar panel $Q_{Pan,p}$ can be taken as $Q_{Pan,p}(i_{sun}) \approx Q_{Hor,p}(i_{sun})$.

2.5 Solar energy characteristic in the chosen cities.

The amount of solar energy falling to any point of Earth depends on location of this point, time of year (seasons) and weather condition. For clear atmosphere the solar energy is decreasing upward to North. The described above mathematical model determines the spatio-temporal dependency of falling solar energy. For a chosen cities Hamburg, Berlin (Germany), Baku, Shamakhi, Zakatala (Azerbaijan) and Tbilisi (Georgia) the amounts of solar energy for specific days of year calculated on developed method are presented below. The geographical coordinates (from north to equator) of those cities are given in Table 2.3.

City	*Hamburg*	*Berlin*	*Tbilisi*	*Zakatala*	*Shamakhi*	*Baku*
Latitude	53.565278	52.516667	41.716667	41.633611	40.630278	40.395278
Longitude	10.001389	13.383333	44.783333	46.643333	48.641389	49.882222
Elevation	22	48	749	582	716	136

Table 2.3: The locations of the chosen cities

As we see the differences in latitude of Germany cities from Azerbaijan cities is about 12^0 , which is main causes of differences in solar energy between cities of those countries.

The daily amounts of solar energy calculated on the developed here method for the specific days (equinox and solstice) of year are given in Table 4 and in Figures 2.5-2.10. The analyses of table 4 show that at equinox (vernal and autumnal) the amount of solar energy in cities of Azerbaijan is approximately 30% greater than in cities of Germany.

21 March (vernal equinox)					
City	**Day length (*hour*)**	**Daily (perpendicular) irradiance** *(kWatt/m^2)*	**Daily direct (horizontal) irradiance** *(kWatt/m^2)*	**Daily diffuse (horizontal) irradiance** *(kWatt/m^2)*	**Daily global (horizontal) irradiance** *(kWatt/m^2)*
Hamburg	12.0	6.76	3.16	1.05	4.21
Berlin	12.0	6.87	3.29	1.07	4.36
Tbilisi	12.0	7.82	4.51	1.28	5.79
Zakatala	12.0	7.83	4.52	1.28	5.80
Shamakhi	12.0	7.90	4.63	1.29	5.93
Baku	12.0	7.91	4.65	1.30	5.95

Table 2.4: Characteristics of solar radiation for specific days in chosen cities:
21 March (vernal equinox)

22 September (autumnal equinox)					
City	**Day length (*hour*)**	**Daily (perpendicular) irradiance** *(kWatt/m^2)*	**Daily direct (horizontal) irradiance** *(kWatt/m^2)*	**Daily diffuse (horizontal) irradiance** *(kWatt/m^2)*	**Daily global (horizontal) irradiance** *(kWatt/m^2)*
Hamburg	12.0	6.79	3.19	1.06	4.25
Berlin	12.0	6.92	3.33	1.07	4.41
Tbilisi	12.0	8.27	4.76	1.20	5.97
Zakatala	12.0	8.18	4.72	1.22	5.95
Shamakhi	12.0	8.33	4.86	1.22	6.09
Baku	12.0	8.01	4.72	1.30	6.02

Table 2.5: Characteristics of solar radiation for specific days in chosen cities: 22 September (autumnal equinox)

At the summer solstice the amounts of solar energy in cities of Germany and Azerbaijan are roughly the same. But at the winter solstice the amounts of solar energy in cities of Azerbaijan are greater 3.6 times than Germany cities.

22 June (summer solstice)					
City	**Day length (*hour*)**	**Daily (perpendicular) irradiance** *(kWatt/m^2)*	**Daily direct (horizontal) irradiance** *(kWatt/m^2)*	**Daily diffuse (horizontal) irradiance** *(kWatt/m^2)*	**Daily global (horizontal) irradiance** *(kWatt/m^2)*
Hamburg	16.8	11.25	7.29	1.93	9.22
Berlin	16.6	11.23	7.34	1.94	9.28
Tbilisi	15.0	11.31	7.97	1.81	9.78
Zakatala	15.0	11.19	7.91	1.83	9.75
Shamakhi	14.9	11.24	7.98	1.81	9.79
Baku	14.9	10.84	7.75	1.92	9.68

Table 2.6: Characteristics of solar radiation for specific days in chosen cities:

22 June (summer solstice)

22 December (winter solstice)					
City	**Day length (*hour*)**	**Daily (perpendicular) irradiance** *(kWatt/m^2)*	**Daily direct (horizontal) irradiance** *(kWatt/m^2)*	**Daily diffuse (horizontal) irradiance** *(kWatt/m^2)*	**Daily global (horizontal) irradiance** *(kWatt/m^2)*
Hamburg	7.2	1.45	0.28	0.29	0.57
Berlin	7.4	1.68	0.35	0.33	0.68
Tbilisi	9.0	4.20	1.42	0.60	2.02
Zakatala	9.0	4.14	1.41	0.61	2.02
Shamakhi	9.1	4.15	1.48	0.66	2.14
Baku	9.1	4.15	1.48	0.66	2.14

Table 2.7: Characteristics of solar radiation for specific days in chosen cities:
22 December (winter solstice)

The behaviours of solar energy components during the day for the specific days (equinox and solstice) of year are presented in Figures 2.5-2.10.

As we see for equinox days and winter solstice the direct irradiance of perpendicular to Sun beams plane greater than global irradiance of horizontal area about 30% and 80%, respectively. However, for summer solstice near midday global horizontal irradiance is a little greater than perpendicular.

If we add diffuse radiance to direct perpendicular then it will greater than global. Consequently, if solar panel follows the Sun as a sunflower the irradiance will be maximum. But designing the collar car panel in such manner does not seems has perspectives because of worsening the aerodynamic of car.

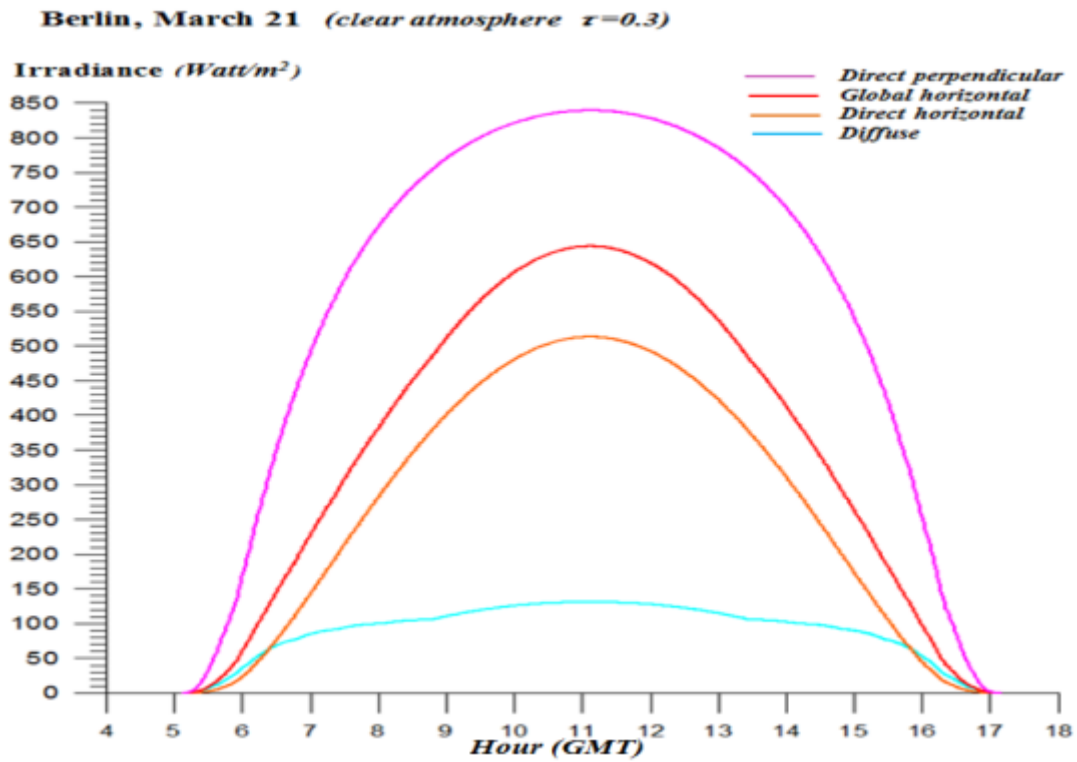

Figure 2.5: Solar energy components changes during the day in March 21 (vernal equinox) in Berlin.

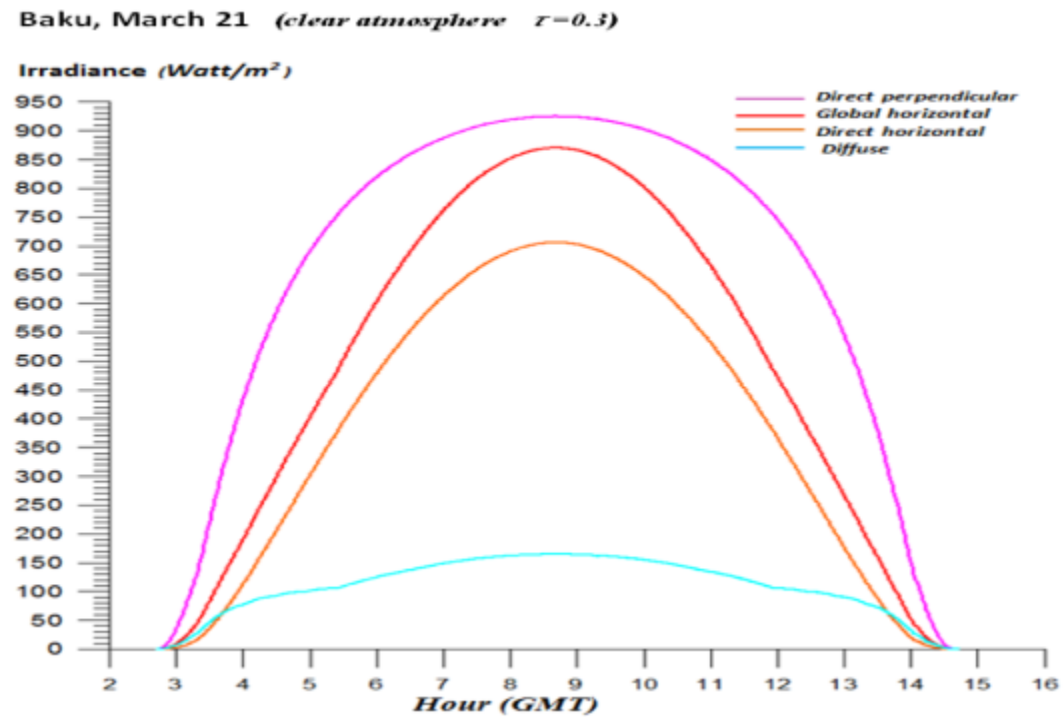

Figure 2.6: Solar energy components changes during the day in March 21 (vernal equinox) in Baku.

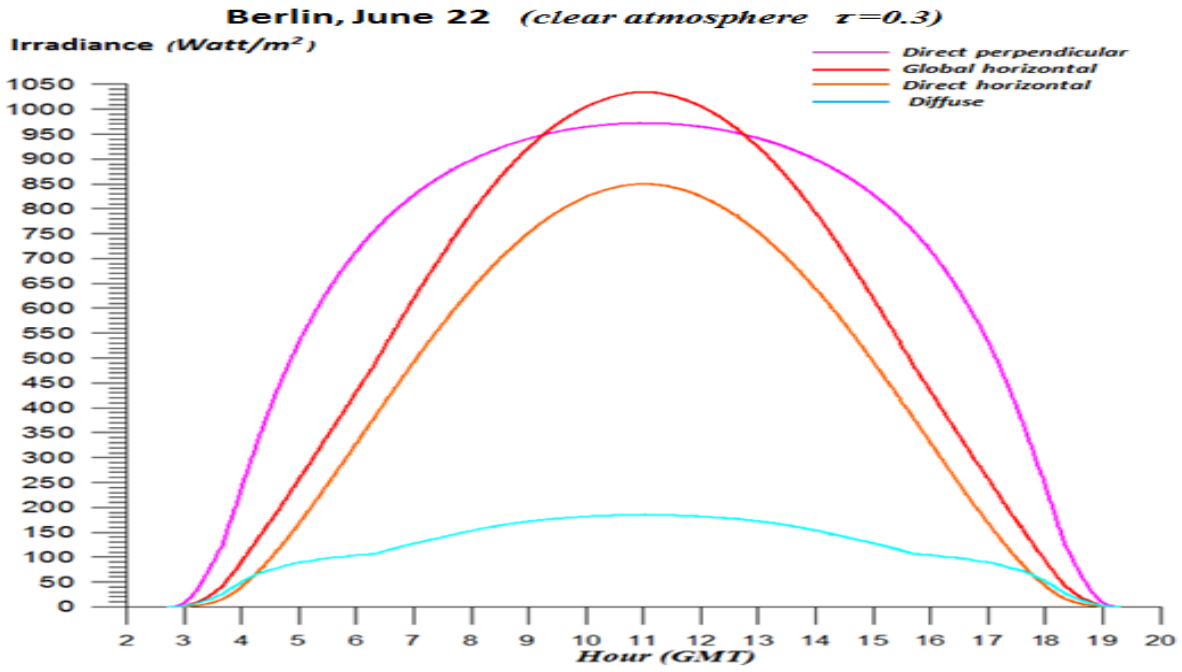

Figure 2.7: Solar energy components changes during the day in June 22 (summer solstice) in Berlin.

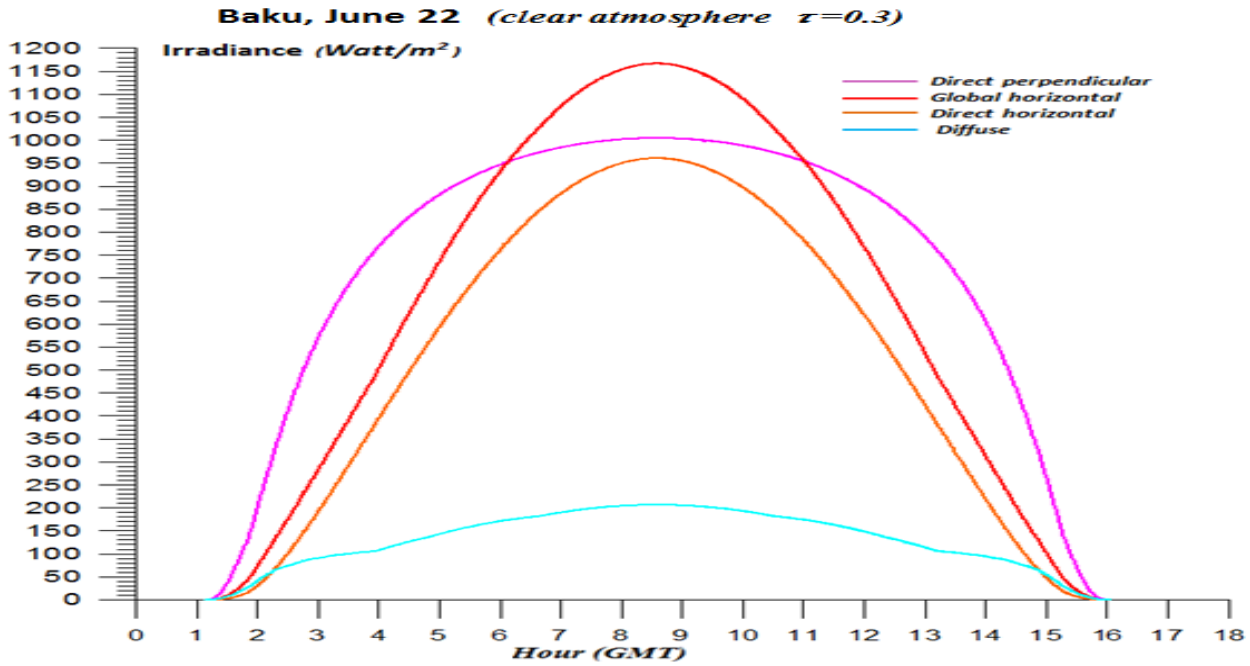

Figure 2.8: Solar energy components changes during the day in June 22 (summer solstice) in Baku.

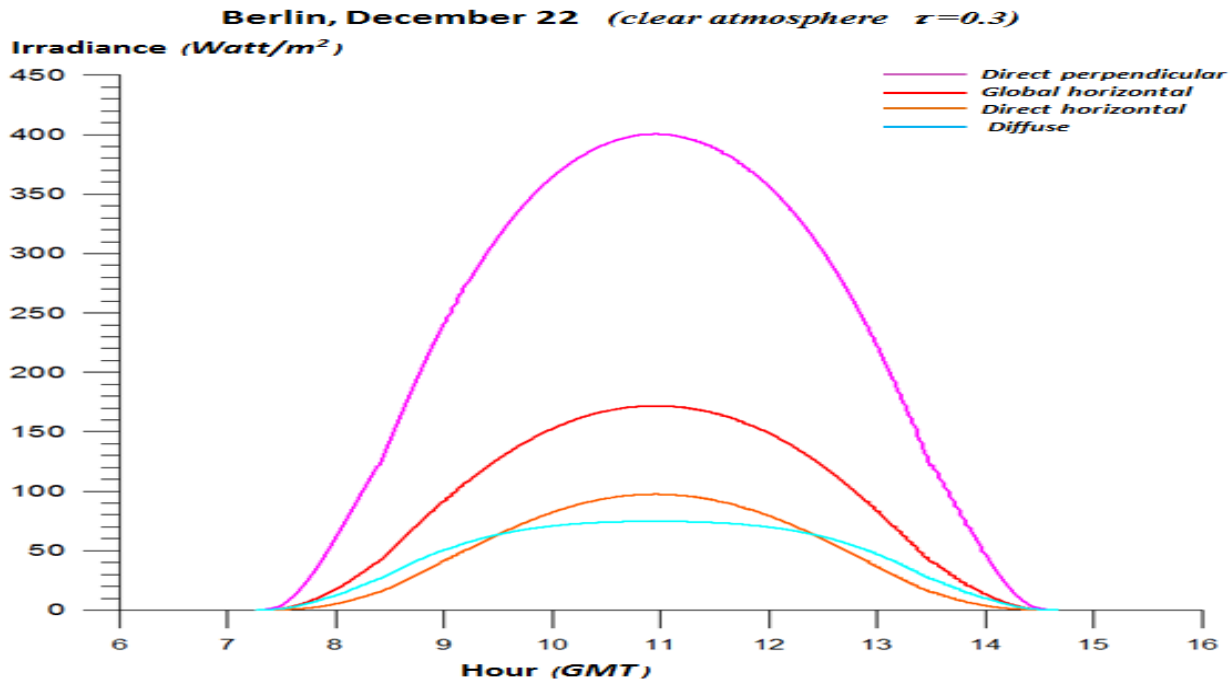

Figure 2.9: Solar energy components changes during the day in December 22 (winter solstice) in Berlin.

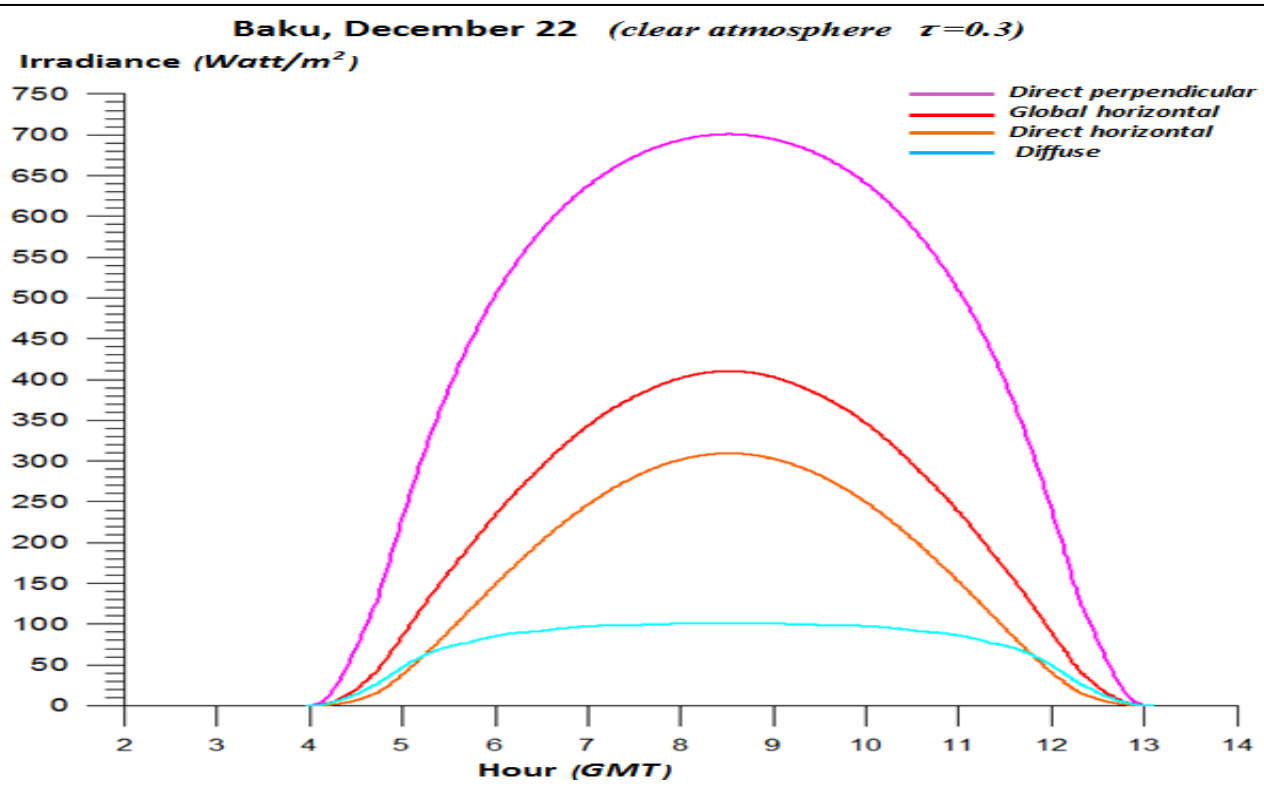

Figure 2.10: Solar energy components changes during the day in December 22 (winter solstice) in Baku.

The correctness of developed here model has been tested by measurements of solar radiation with high accuracy pyrometer in the city Zakatala. The registration of solar radiation has been made with time interval 100 second. The fragment of measurements for two specific days (partly cloudy and continuous cloudiness) is presented in figure 1.11. As we see continuous cloudiness reduces the irradiance about $\delta Q = \frac{6.90-1.33}{6.90} \approx 0.807 \approx 81\%$.

The comparison of measured and calculated on the model values of irradiance is given in Figure 2.12. In the day of measurements (22 July, 2015) the week top level clouds as is showed in Figure 2.13, are taken place.

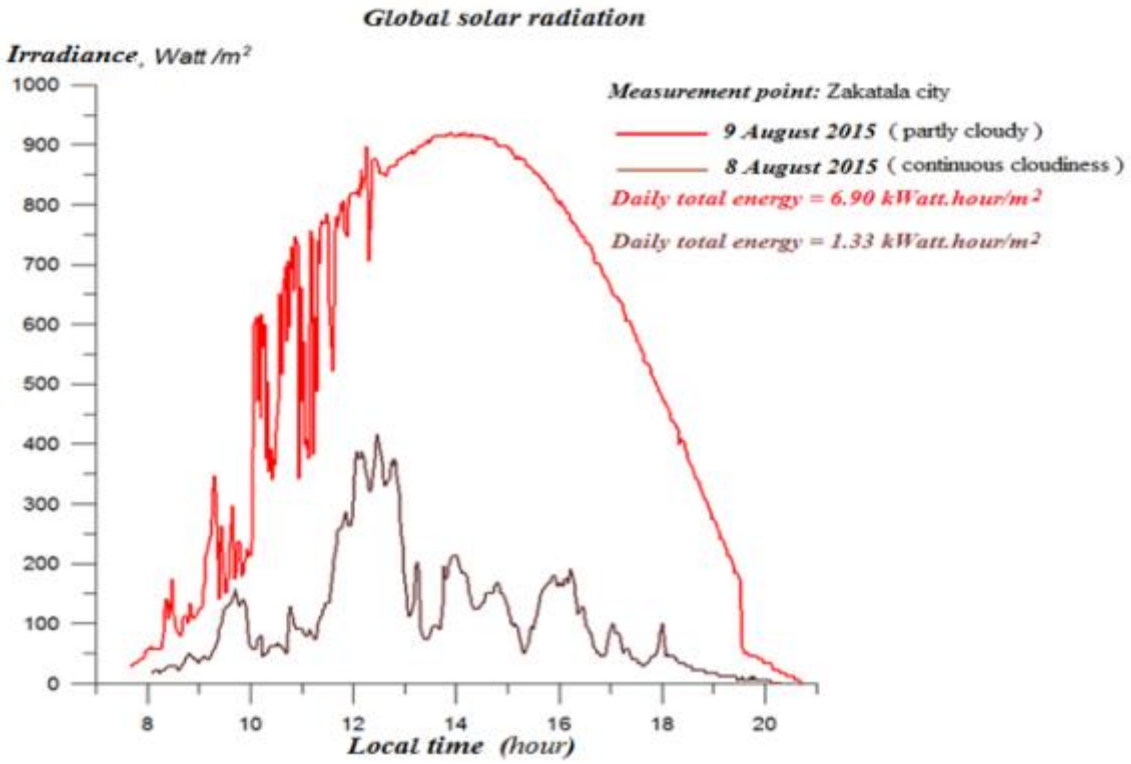

Figure 2.11: The measured values of global solar radiation falling onto horizontal plane.

As we see, for same moments of times (near 12 h. and 16 h.) the measured irradiance is greater than calculated on model for cloudless atmosphere. This event can be physically explained as a result of two effects. First, the weak top level clouds

enlarges the angular size of Sun (due to strongly oblongness of indicatrix of cloud particles); second, the brightness of clouds are higher than brightness of clear part of sky. The first increases direct irradiance and the second-diffuse and as a result the global irradiance is increasing. The daily amount of the measured total energy differs from calculated $\delta E = \frac{7.34-7.09}{7.34} \approx 0.034 \approx 3.4\%$, that conform the correctness of the model.

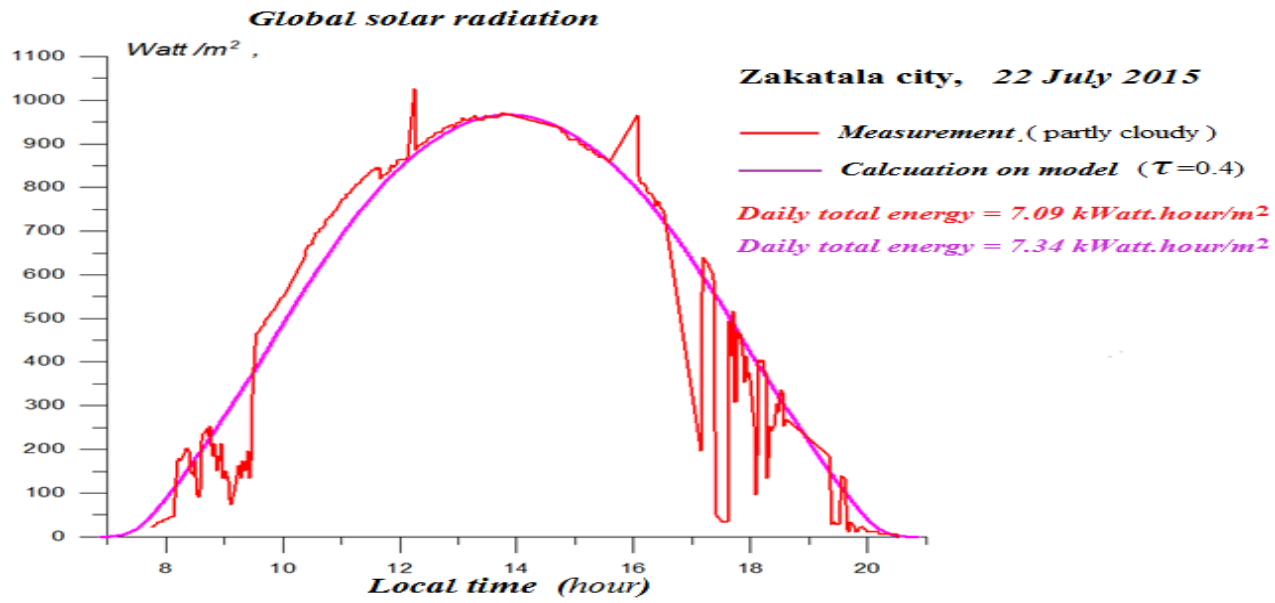

Figure 2.12: The measured and calculated on the method values of global solar radiation falling onto horizontal plane.

Figure 2.13: The state of atmosphere when the global irradiance was greater than for clear atmosphere (week top level clouds; solar zenith≈ 43^0)

CHAPTER 3

DIFFERENTIAL EQUATION OF MOTION OF SOLAR CAR AND IT'S SOLUTION

We consider the motion of the car in the coordinate system associated with the Earth, so that the coordinate centre coincides with the Earth centre, the plane Oxy coincides with equator plane, axis Ox directed to the Greenwich meridian, axis Oy directed to East meridian of 90^0, axis Oz coincides with the Earth rotation axis and is directed to the North pole (Figure 3.1). Using of this coordinate system, in opposite to the local coordinate system used in [12], allows us to take into account Earth curvature and simulate the car motion to arbitrary large distance. The Fortran code subroutine to realise this car motion simulation is given in Appendix A.

Let the equation of the road (line) be: $\vec{r} = \vec{r}(s)$, where, $\vec{r}$ - radius vector of arbitrary point M on the road; s - the path length from initial point M_0 to M (Figure 3.2).

When the car moves on the road, the radius vector $\vec{r}$ of car (which is assumed as a point M) is changed depending on time, i.e. $\vec{r} = \vec{r}(t)$. The differential equation of the car motion is obtained from the Newton law**:**

$$m\frac{d\vec{v}}{dt} = \vec{F} \tag{3.1}$$

Where, $\vec{v} = \frac{d\vec{r}}{dt}$ – velocity of the car, $\vec{F}$ is the resultant of acting forces. To determine the resultant $\vec{F}$ we must identify all the forces acting to the car. The main forces acting to a car are shown in Figure 3.2.

In solar car, the driving power is generated by electrical motor.

Electrical Motor Efficiency. If power output is measured in *Watt (W),* electrical motor efficiency η_{ef} can be expressed as:

$$\eta_{ef} = \frac{P_{out}}{P_{in}} \tag{3.2}$$

where, P_{out} - mechanical output power ($[P_{out}] = Watt$); P_{in} - electrical input power ($[P_{in}]=Watt$) [18]. Modern electrical motors meet the efficiencies η_{ef} greater than 0.9.

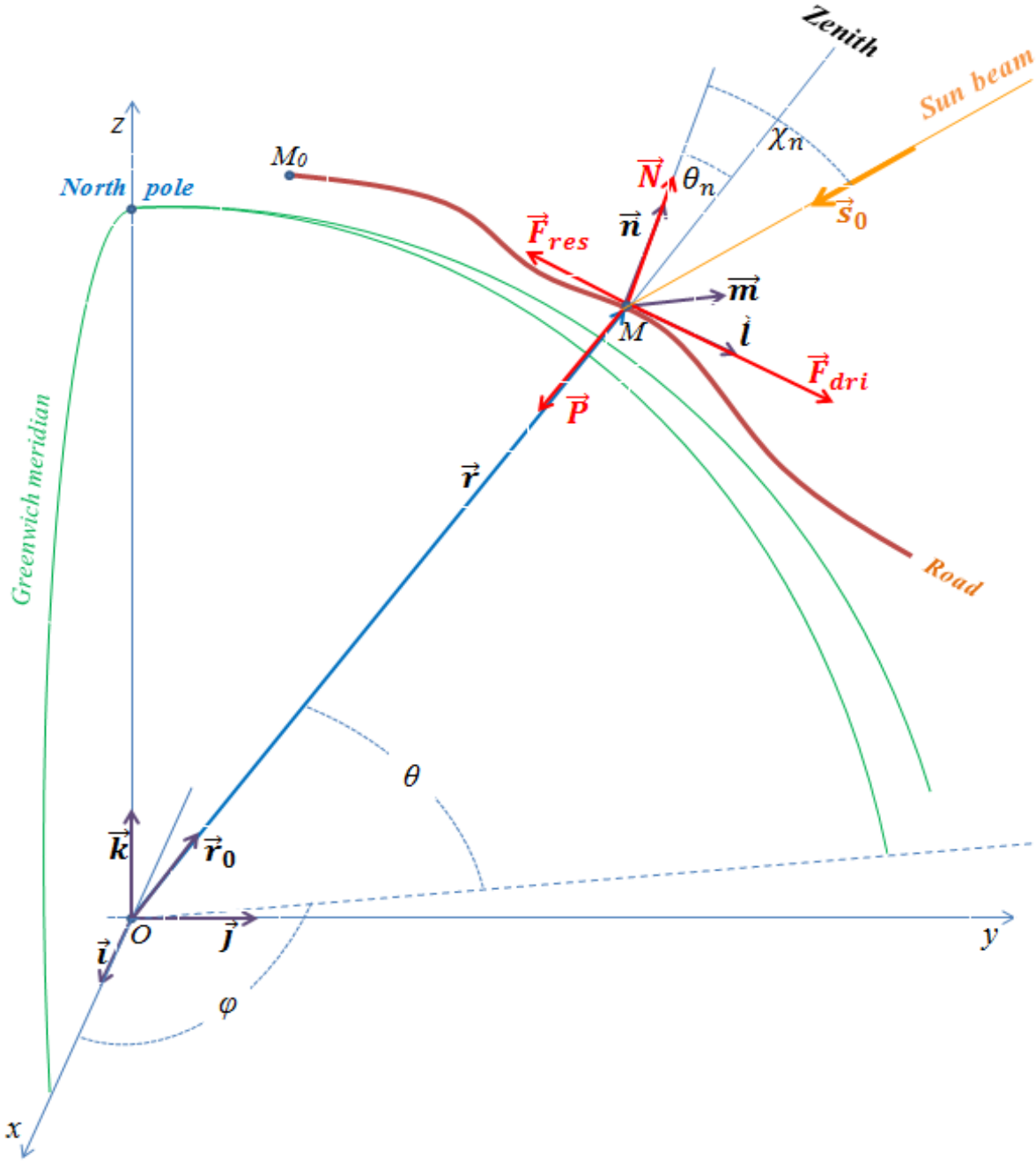

Figure 3.1: The choosing of coordinate system and identification of forces acting to the solar car on the road

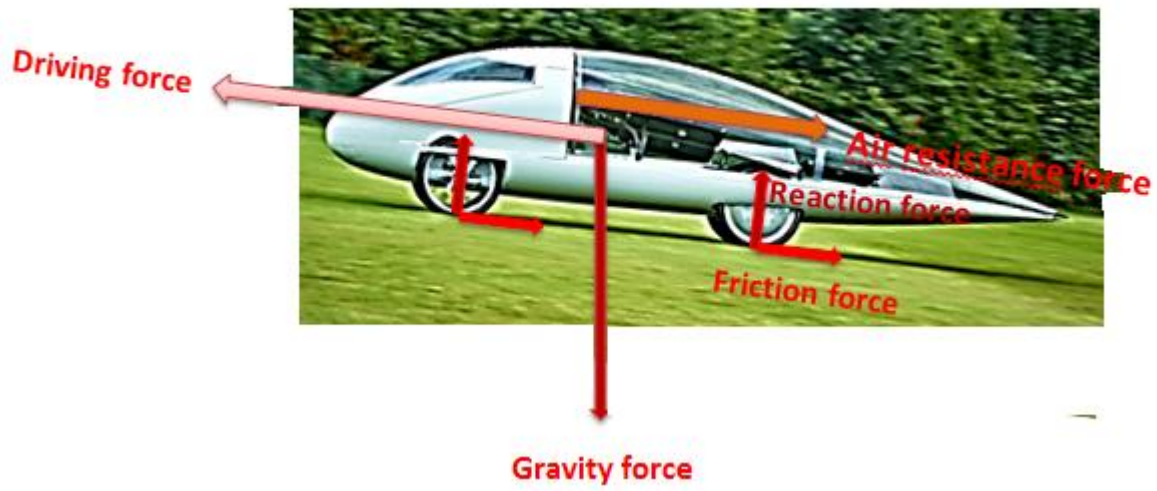

Figure 3.2: Forces acting to the solar car on the road during motion

3.1 Determination of resultant force.

The main forces acting to the car during the motion are followings:

Driving force. The origin of driving force F_{dri} is a power P_{out} generated by electric motor. If only a solar energy is used, then

$$P_{out} = \eta_{ef} \, C_{ef} W_{sol} S_{pan} \tag{3.3}$$

where, W_{sol} – power of solar radiance falling per m^2 of solar panel ($[W_{sol}] = watt/m^2$) ; S_{pan} – area of solar panel ($[S_{pan}] = m^2$) ; C_{ef} – coefficient of efficiency ($[C_{ef}]$ = *non dimensional*) which is the rate of solar energy transformed to electric by solar cells. For modern solar cells: $C_{ef} \approx 0.30$. In the case, when hybrid energy supply of engine is used, then

$$P_{out} = \eta_{ef} \left(C_{ef} W_{sol} S_{pan} + P_{accum} \right) \tag{3.4}$$

where, P_{accum} – power consumption from accumulator. Consequently, the module of

the driving force is determined by the formula:

$$F_{dri} = \frac{P_{out}}{v} = \frac{\eta_{ef}\left(C_{ef} W_{sol} S_{pan} + P_{accum}\right)}{v} \quad (3.5)$$

The direction of driving force coincides with the direction of velocity vector $\vec{v}$, which is tangent to road line. Then

$$\vec{F}_{dri} = \frac{P_{out}}{v} \cdot \vec{l} \quad (3.6)$$

where, $\vec{l}$ – unite vector in direction of $\vec{v}$.

We suppose that power P_{out} is transmitted to wheel torque without loss. In opposite case, the losses can be taken into account by entering the corresponding coefficient or correction of coefficient η_{ef}.

Gravity force. All bodies upon the Earth experience a force of gravity that is directed "downwards" towards the centre of the Earth. The force of gravity on the Earth is always equal to the weight of the body [19]. The gravity force module $F_{grav} = mg$, where m- mass of car ([m] =kg); $g = 9.8\, m/s^2$ - gravitational acceleration. At the considered point the gravity force is directed to the centre of the Earth:

$$\vec{F}_{grav} = -mg \cdot \vec{r}_0 \quad (3.7)$$

Reaction force. Because car is exerting force on the road, the road will push the car with opposite force in the direction on the normal to road surface [20]. This force is called reaction force and it balances the normal component of gravity force:

$$\vec{N} = mg\,(\vec{r}_0 \cdot \vec{n}) \cdot \vec{n} \quad (3.8)$$

where, $\vec{n}$ – unite normal vector to road surface, directed upward.

Resistance force. Resistance force $\vec{F}_{res}$ reacts against the motion and consist of air resistance force $\vec{F}_{air}$ and rolling friction force $\vec{F}_{rol}$:

$$\vec{F}_{res} = \vec{F}_{air} + \vec{F}_{rol}$$

The forces $\vec{F}_{air}$, $\vec{F}_{rol}$ are directed opposite to the vector $\vec{v}$, i. e. on direction: $-\vec{l}$.

$$\vec{F}_{res} = -(F_{air} + F_{rol}) \cdot \vec{l} \tag{3.9}$$

The air resistance force depends on aerodynamic parameters of car and air speed (which at calm weather is equal to car speed v) [21] . It is experimentally derived that, at the car speeds less than sound speed

$$F_{air} = C_w \frac{\rho_{air} S_{cros}}{2} v^2 \tag{3.10}$$

where, C_w - air resistance coefficient ($[C_w]$=*non dimensional*) ; $\rho_{air} = 1.22\ kg/m^3$ density of atmosphere air; S_{cros} – cross section area of car ($[S_{cros}]= m^2$) ;
It should be noted that the air resistance force does not depend on car mass.

The rolling friction force F_{rol} is proportional to the magnitude of reaction force $N = |\vec{N}|$:

$$F_{rol} = C_{rr}\ N = C_{rr} mg\ (\vec{r}_0 \cdot \vec{n}) \tag{3.11}$$

where, C_{rr} - rolling resistance coefficient [22]. For special Michelin solar car/eco-marathon tires the values of $C_{rr} = 0.0025$.

Thus the resultant $\vec{F}$ we have:

$$\vec{F} = \vec{F}_{dri} + \vec{F}_{grav} + \vec{N} + \vec{F}_{res} \quad \text{or more explicitly}$$

$$\vec{F} = \frac{P_{out}}{v} \cdot \vec{l} - mg \cdot \vec{r}_0 + mg\ (\vec{r}_0 \cdot \vec{n}) \cdot \vec{n} - \left(C_w \frac{\rho_{air} S_{cros}}{2} v^2 + C_{rr} mg(\vec{n} \cdot \vec{r}_0) \right) \cdot \vec{l} \tag{3.12}$$

3.2. Differential equation of motion

From (3.1) and (3.12) we obtain the differential equation of car motion:

$$m \frac{d\vec{v}}{dt} = \left[\frac{P_{out}}{v} - \left(C_w \frac{\rho_{air} S_{cros}}{2} v^2 + C_{rr} mg\ \vec{n} \cdot \vec{r}_0 \right) \right] \cdot \vec{l} - mg \cdot \vec{r}_0 + mg\ (\vec{r}_0 \cdot \vec{n}) \cdot \vec{n} \tag{3.13}$$

If substitute $\vec{v} = v \cdot \vec{l}$ then we have:

$$m \left(\vec{l} \frac{dv}{dt} + v \frac{d\vec{l}}{dt} \right) = \left[\frac{P_{out}}{v} - \left(C_w \frac{\rho_{air} S_{cros}}{2} v^2 + C_{rr} mg\ \vec{n} \cdot \vec{r}_0 \right) \right] \cdot \vec{l}$$

$$-mg \cdot \vec{r}_0 + mg\ (\vec{r}_0 \cdot \vec{n}) \cdot \vec{n} \qquad (3.14)$$

Scalar multiplying both side by $\vec{l}$ and taking into account that: $\vec{l} \cdot \vec{l} = 1$, $\vec{n} \cdot \vec{l} = 0$ (because $\vec{n} \perp \vec{l}$) and $\vec{l} \cdot \frac{d\vec{l}}{dt} = 0$ (derivative of unit vector is perpendicular to itself) we obtain:

$$m\ \frac{dv}{dt} = \left[\frac{P_{out}}{v} - \left(C_w\ \frac{\rho_{air}\ S_{cros}}{2} v^2 + C_{rr} mg\ (\vec{n} \cdot \vec{r}_0)\right)\right] - mg\left(\vec{r}_0 \cdot \vec{l}\right) \qquad (3.15)$$

or

$$m\ \frac{dv}{dt} = \frac{P_{out}}{v} - C_w\ \frac{\rho_{air}\ S_{cros}}{2} v^2 + \left(-C_{rr} mg\ (\vec{n} \cdot \vec{r}_0) - mg\left(\vec{r}_0 \cdot \vec{l}\right)\right) \qquad (3.16)$$

If we denote

$$a = \frac{C_w \rho_{air}\ S_{cros}}{2m} \quad ; \quad b = -C_{rr}\, g\ (\vec{n} \cdot \vec{r}_0) - g\left(\vec{r}_0 \cdot \vec{l}\right)\ ;\ c = \frac{P_{out}}{m} \qquad (3.17)$$

we have:

$$\frac{dv}{dt} = \frac{c}{v} - av^2 + b \qquad (3.18)$$

As we can see from (3.17) that $a > 0$; $c > 0$. The sign of b depends on the coefficient C_{rr} and the road tilt and for small tilts $b < 0$.

Let to define explicitly dot products in expression of coefficient b. The unite vector $\vec{r}_0$ of arbitrary point $M(x, y, z)$ on the road is determined as:

$$\vec{r}_0 = \frac{\vec{r}}{|\vec{r}|} = \frac{1}{\sqrt{x^2 + y^2 + z^2}} \left(x \cdot \vec{\imath} + y \cdot \vec{\jmath} + z \cdot \vec{k}\right) \qquad (3.19)$$

The Cartesian coordinates x, y and z of point M is expressed by it's geographical coordinates θ *(latitude)* , φ *(longitude)*, and h *(altitude)* as:

$$\begin{cases} x = (R + h)\cos\theta\cos\varphi \\ y = (R + h)\cos\theta\sin\varphi \\ z = (R + h)\sin\theta \end{cases} \qquad (3.20)$$

where, $R = 6371000$ *meter* – mean radius of the Earth.

The unite normal vector $\vec{n}$ is perpendicular to road surface i.e. to unite vectors $\vec{l}$ and $\vec{m}$; at that $\vec{m} \perp \vec{r}_0$ because of roads are constructed so that to have no lateral tilt.

Consequently,

$$\vec{m} = \frac{\vec{r}_0 \times \vec{l}}{\left|\vec{r}_0 \times \vec{l}\right|} \tag{3.21}$$

$$\vec{r}_0 \times \vec{l} = \begin{vmatrix} \vec{i} & \vec{j} & \vec{k} \\ r_{0x} & r_{0y} & r_{0z} \\ l_x & l_y & l_z \end{vmatrix}$$

$$= \left(r_{0y} l_z - r_{0z} l_y\right) \cdot \vec{i} + \left(r_{0z} l_x - r_{0x} l_z\right) \cdot \vec{j} + \left(r_{0x} l_y - r_{0y} l_x\right) \cdot \vec{k} \tag{3.22}$$

$$\left|\vec{r}_0 \times \vec{l}\right| = \sqrt{\left(r_{0y} l_z - r_{0z} l_y\right)^2 + \left(r_{0z} l_x - r_{0x} l_z\right)^2 + \left(r_{0x} l_y - r_{0y} l_x\right)^2} \tag{3.23}$$

and

$$\vec{n} = \vec{l} \times \vec{m} = \begin{vmatrix} \vec{i} & \vec{j} & \vec{k} \\ l_x & l_y & l_z \\ m_x & m_y & m_z \end{vmatrix}$$

$$= \left(l_y m_z - l_z m_y\right) \cdot \vec{i} + \left(l_z m_x - l_x m_z\right) \cdot \vec{j} + \left(l_x m_y - l_y m_x\right) \cdot \vec{k} \tag{3.24}$$

Because, $\vec{l}$, $\vec{m}$ and $\vec{n}$ are mutually perpendicular unite vectors we have:

$\left|\vec{l}\right| = 1$, $|\vec{m}| = 1$ and $|\vec{n}| = 1$; $\vec{l} \perp \vec{m}$, $\vec{n} \perp \vec{m}$ and $\vec{l} \perp \vec{n}$.

Note that, in general, the vector $\vec{n}$ did not coincide with binormal vector of road curve $\vec{r} = \vec{r}(s)$; $\vec{n}$ is one of perpendicular to $\vec{l}$ unite vectors which is perpendicular simultaneously to band of road i.e. $\vec{n} \perp \vec{m}$.

In general case of curved trajectory the coefficients a, b, and c in the differential equation (3.18) depend on point M at the road and therefore this equation can be solved only numerically. But for straight-line trajectory those coefficients are constants and equation is solved exactly.

3.3 Exact solution of the differential equation of car motion for straight-line trajectory

If the distance from initial point M_0 to terminal point M_1 is smaller than Earth curvature then curvature's effect can be neglected. Additionally, if the road is straight-line then the coefficients a , b , and c in the differential equation (3.18) are constants. In this case the equation (3.18) can be exactly solved by following way.

$$\frac{dv}{dt} = \frac{c - av^3 + bv}{v} \tag{3.25}$$

$$\int_{v_0}^{v} \frac{v\,dv}{c - av^3 + bv} = t + const \tag{3.26}$$

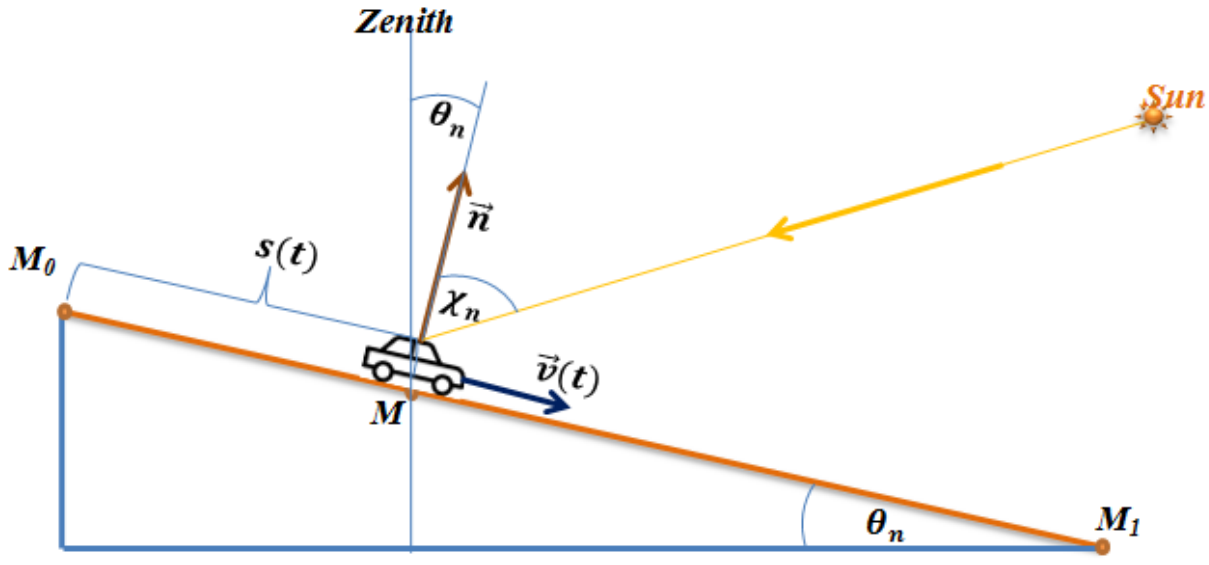

Figure 3.3: Car motion on straight-line trajectory

If we take *initial condition* such as:

$$v = v_0 \quad at \quad t = 0 \tag{3.27}$$

then (3.26) becomes:

$$\int_{v_0}^{v} \frac{v\,dv}{c - av^3 + bv} = t$$

or

$$\int_{\boldsymbol{v_0}}^{\boldsymbol{v}} \frac{\boldsymbol{v\,dv}}{\boldsymbol{v^3 + pv + q}} = \boldsymbol{-at} \qquad (\mathbf{3.28})$$

where, new coefficients p and q are defined as:

$$p = -\frac{b}{a} \quad ; \qquad q = -\frac{c}{a} \qquad (3.29)$$

so, $a \neq 0$, i.e. exist the air resistance.

Differential form of equation (3.28) is:

$$\frac{\boldsymbol{v\,dv}}{\boldsymbol{v^3 + pv + q}} = \boldsymbol{-a\,dt} \qquad (3.30)$$

The equation (3.28) defines dependence of the velocity of car on time $v = v(t)$.

To determine the dependence of course made of car on time s= $s(t)$ we can either evaluate numerically the integral $s(t) = \int_0^t v(t)dt$ by using $v = v(t)$ from (3.28) or follow the procedure. Multiplying by v both side of (3.30) and using $vdt = ds$ we obtain:

$$\frac{v^2\,dv}{v^3 + pv + q} = -a\,ds \qquad (3.31)$$

or

$$\int_{v_0}^{v} \frac{v^2\,dv}{v^3 + pv + q} = -a\,s(v) \qquad (3.32)$$

This integrals can be evaluated by the method of expansion in rational fractions.

Evaluation of the integrals $\int_{v_0}^{v} \frac{v\,dv}{v^3+pv+q}$ **and** $\int_{v_0}^{v} \frac{v^2\,dv}{v^3+pv+q}$

The result of integral depend on structure of roots of cubic equation

$$v^3 + pv + q = 0.$$

Case 1. Discriminant of equation $\mathbf{D_3 = -108\left(\frac{q^2}{4} + \frac{p^3}{27}\right) < 0}$**.** Then the equation $v^3 + pv + q = 0$ has one real root v_1 and two v_2 , v_3 complex conjugate ($v_2 = \bar{v}_3$). In this case $v^3 + pv + q = (v - v_1)(v^2 + \alpha v + \beta) = 0$ and the discriminant $\boldsymbol{d_2 = \alpha^2 - 4\beta}$ of the quadratic equation $v^2 + \alpha v + \beta = 0$ also negative $\boldsymbol{d_2 < 0}$ **.** Here

$$\alpha = v_1 \quad ; \quad \beta = p + v_1^2 \tag{3.33}$$

The procedure of expansion in rational fractions and integration is as follows.

$$\frac{v}{v^3 + pv + q} = \frac{A}{v - v_1} + \frac{Bv + C}{v^2 + \alpha v + \beta} \tag{3.34}$$

The coefficients A, B and C are determined from equality of left and right sides of (3.34), which gives:

$$v = A\,(v^2 + \alpha v + \beta) + (Bv + C)(v - v_1)$$

or

$$\begin{cases} A + B = 0 \\ \alpha A - Bv_1 + C = 1 \\ \beta A - Cv_1 = 0 \end{cases} \tag{3.35}$$

By solving (3.35) and taking into account (3.33) we find:

$$A = \frac{v_1}{p + 3v_1^2} \quad ; \quad B = -\frac{v_1}{p + 3v_1^2} \; ; \; C = \frac{p + v_1^2}{p + 3v_1^2} \tag{3.36}$$

Then

$$\int \frac{v}{v^3 + pv + q}\,dv = A\int \frac{1}{v - v_1}\,dv + \int \frac{Bv + C}{v^2 + \alpha v + \beta}\,dv$$

$$= A\ln|v - v_1| + \frac{B}{2}\ln(v^2 + \alpha v + \beta) + \frac{2C - \alpha B}{\sqrt{4\beta - \alpha^2}}\arctan\left(\frac{2v + \alpha}{\sqrt{4\beta - \alpha^2}}\right)$$

or finally

$$\int \frac{v}{v^3+pv+q}dv = \frac{v_1}{p+3v_1^2}\ln\left(\frac{|v-v_1|}{\sqrt{v^2+v_1v+p+v_1^2}}\right)$$
$$+\frac{2p+3v_1^2}{(p+3v_1^2)\sqrt{4p+3v_1^2}}\arctan\left(\frac{2v+v_1}{\sqrt{4p+3v_1^2}}\right)+const \qquad (3.37)$$

According to (3.29)

$$-at = \frac{v_1}{p+3v_1^2}\ln\left(\frac{|v-v_1|\sqrt{v_0^2+v_1v_0+p+v_1^2}}{|v_0-v_1|\sqrt{v^2+v_1v+p+v_1^2}}\right)$$
$$+\frac{2p+3v_1^2}{(p+3v_1^2)\sqrt{4p+3v_1^2}}\left[\arctan\left(\frac{2v+v_1}{\sqrt{4p+3v_1^2}}\right)-\arctan\left(\frac{2v_0+v_1}{\sqrt{4p+3v_1^2}}\right)\right] \qquad (3.38)$$

Thus the equation (3.38) implicitly determine the dependence of car velocity on time: $v = v(t)$.

Let now determine the dependence of course made of car on time s= $s(t)$

$$\int_{v_0}^{v}\frac{v^2\,dv}{v^3+pv+q} = -a\,s(v) \qquad (3.39)$$

Evaluating the integral by the method of expansion in rational fractions as before we find

$$-a\,s(v) = \frac{v_1^2}{p+3v_1^2}\ln\left(\left|\frac{v-v_1}{v_0-v_1}\right|\right)+\frac{p+2v_1^2}{p+3v_1^2}\ln\left(\frac{v^2+v_1v+p+v_1^2}{v_0^2+v_1v_0+p+v_1^2}\right)$$
$$+\frac{pv_1}{(p+3v_1^2)\sqrt{4p+3v_1^2}}\left[\arctan\left(\frac{2v+v_1}{\sqrt{4p+3v_1^2}}\right)-\arctan\left(\frac{2v_0+v_1}{\sqrt{4p+3v_1^2}}\right)\right] \qquad (3.40)$$

This equation determine the course made by car on dependence of velocity $= s(v)$. Substituting the dependence $v = v(t)$ defined from (3.38) we finally find $s = s(v) = s\big(v(t)\big) = s(t)$. To illustrate the behaviour of solutions of the equations (3.38) and (3.40) the graphs of dependences $v = v(t)$ and $s = s(t)$ are presented in Figures 3.4 and 3.5. As we see, because of constancy of consumption power, the velocity and course made are monotonically raised. Note that, in the calculation the parameters of car are taken for “PowerCore SunCruiser”, which is described in more details in the next chapter.

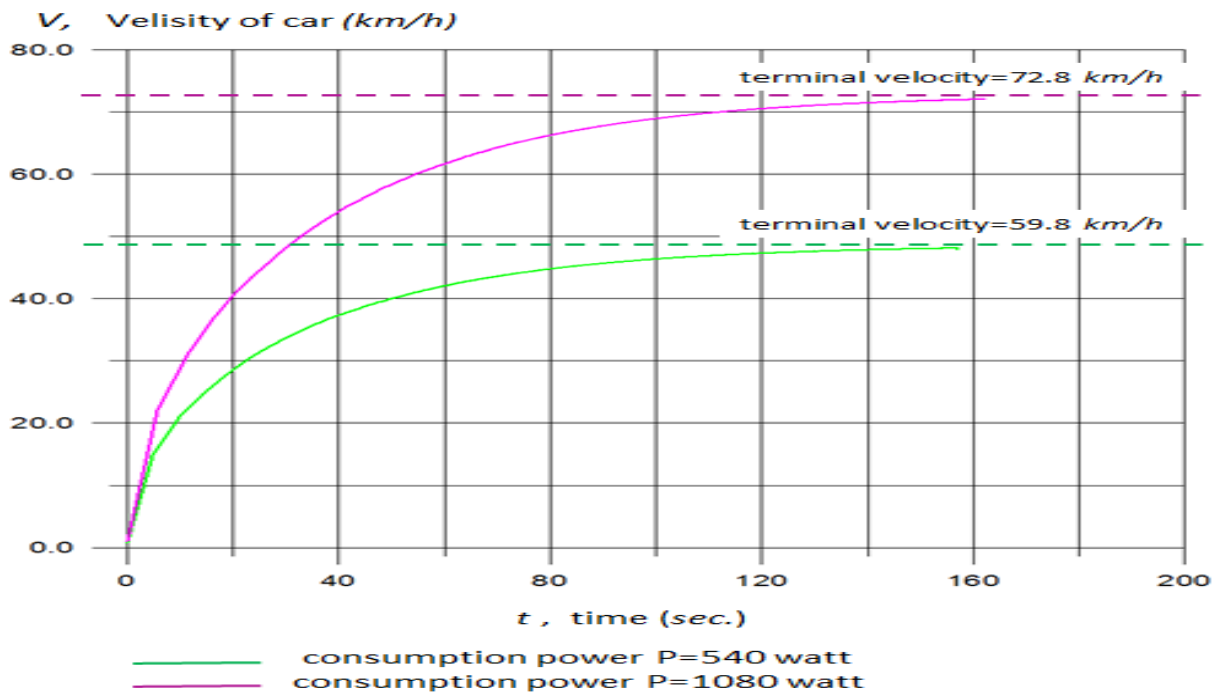

Figure 3.4: Solar car velocity dependences for two cases of constantly consumption power.

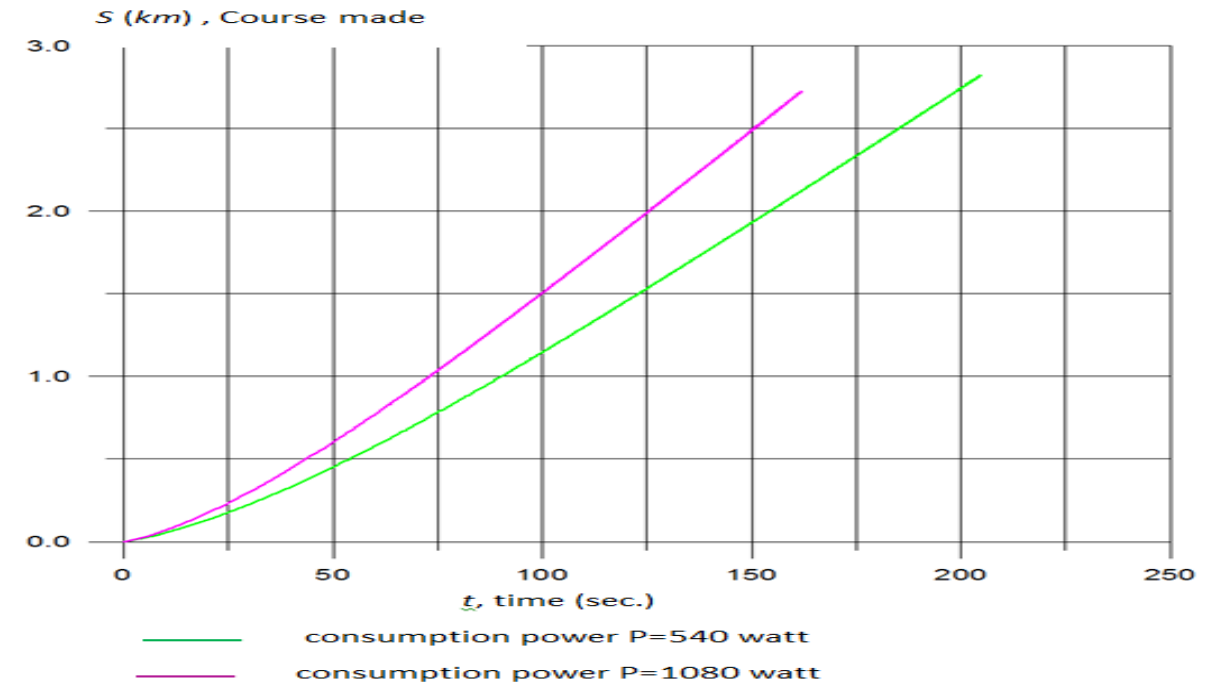

Figure 3.5: Solar car course made dependences for two cases of constantly consumption power.

Subcase. Let, additionally the condition $q = 0$ (which means $P_{out} = 0$) is satisfied, i.e. the motion is only realised under the gravity force. Because of $D_3 < 0$ then should be $p > 0$ (rolling resistance prevails over gravity). Motion of car is realized due to initial velocity v_0 . Evaluation of integrals give:

$$-a\,t = \int_{v_0}^{v} \frac{v\,dv}{v^3 + pv + q} = \int_{v_0}^{v} \frac{v\,dv}{v^3 + pv} = \int_{v_0}^{v} \frac{dv}{v^2 + p}$$

$$= \frac{1}{\sqrt{p}} \left[\arctan\left(\frac{v}{\sqrt{p}}\right) - \arctan\left(\frac{v_0}{\sqrt{p}}\right) \right]$$

and for velocity we have:

$$v = \sqrt{p}\tan\left[\arctan\left(\frac{v_0}{\sqrt{p}}\right) - a\sqrt{p}t\right] \qquad (3.38^*)$$

Analogically,

$$-a\,s(v) = \int_{v_0}^{v} \frac{v^2\,dv}{v^3 + pv + q} = \int_{v_0}^{v} \frac{v^2\,dv}{v^3 + pv} = \int_{v_0}^{v} \frac{v\,dv}{v^2 + p}$$

$$= \frac{1}{2}\ln\left(\frac{v^2 + p}{v_0^2 + p}\right) \qquad (3.40^*)$$

Note that in this subcase the motion begin with initial velocity $v|_{t=0} = v_0$ and motion is terminated at $t_* = \arctan\left(\frac{v_0}{\sqrt{p}}\right)/\left(a\sqrt{p}\right)$ with the terminal velocity $v|_{t=t_*} = 0$ and course made $s_* = \frac{1}{2a}\ln\left(\frac{v_0^2+p}{p}\right)$. The character of mototin is demonstrated in Figures 3.6 and 3.7. For intial velocities $v_0 = 50\ km/h$ and $v_0 = 70\ km/h$ the motion is terminated after the time $t_* = 664\ sec$. And $t_* = 706\ sec$. with cource made $s_* = 2.70\ km$ and $s_* = 3.39\ km$, respectively.

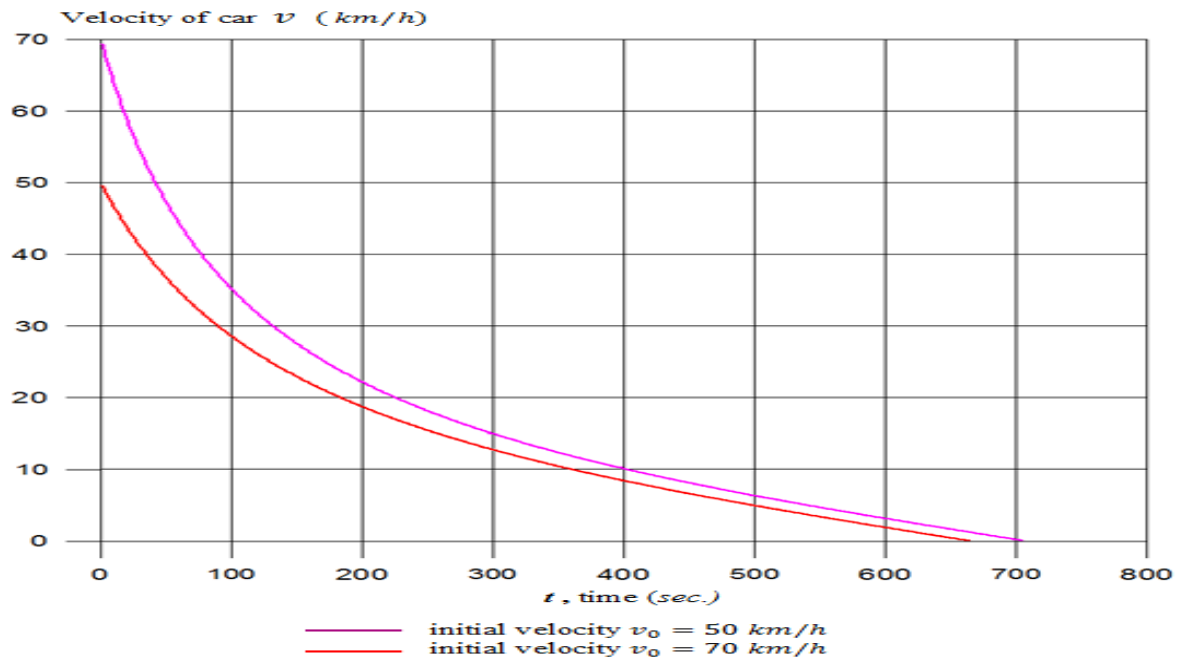

Figure 3.6: Solar car velocity dependences for two values of initial velocities.

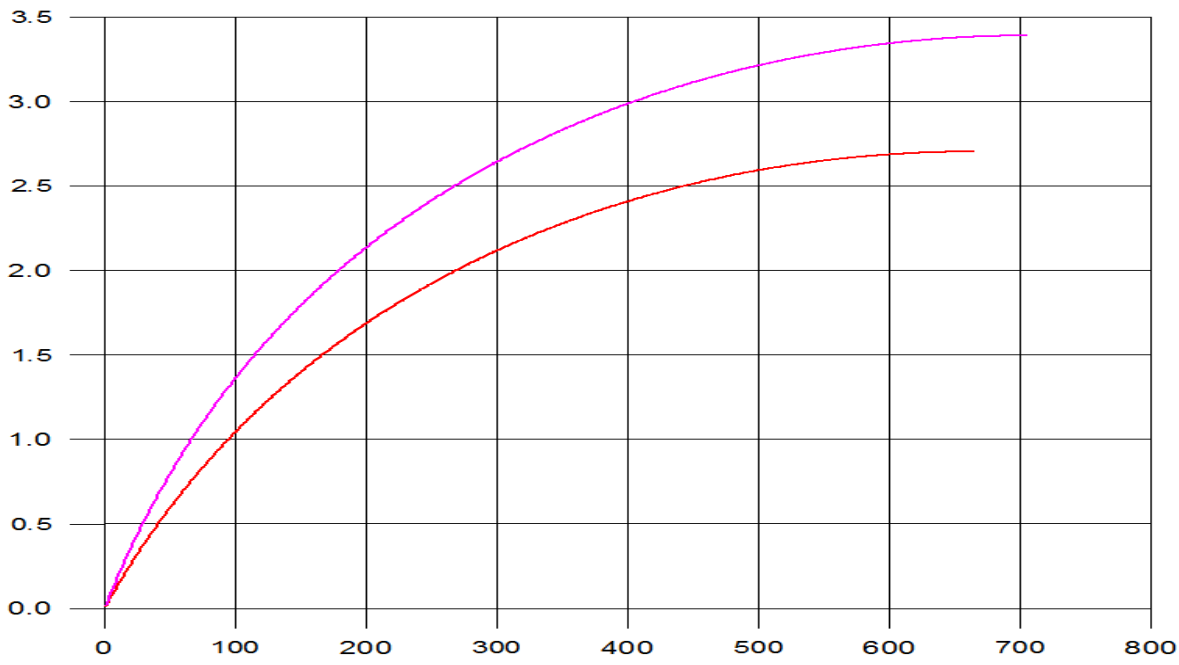

Figure 3.7: Solar car course made dependences for two values of initial velocities.

Case 2. Discriminant of equation $\boldsymbol{D_3 = -108\left(\frac{q^2}{4} + \frac{p^3}{27}\right) > 0}$**.** Then the equation $v^3 + pv + q = 0$ has three real different roots $v_1 \neq v_2 \neq v_3$. In this case $v^3 + pv + q = (v - v_1)(v^2 + \alpha v + \beta) = (v - v_1)(v - v_2)(v - v_3) = 0$ and the discriminant $\boldsymbol{d_2 = \alpha^2 - 4\beta}$ of the quadratic equation $v^2 + \alpha v + \beta = 0$ also positive $\boldsymbol{d_2 > 0}$**.**

The procedure of expansion in rational fractions and integration is as follows.

$$\frac{v}{v^3 + pv + q} = \frac{A}{v - v_1} + \frac{B}{v - v_2} + \frac{C}{v - v_3} \tag{3.41}$$

The coefficients A, B and C are determined from equality of left and right sides of (3.41), which gives:

$$v = A\,(v - v_2)(v - v_3) + B\,(v - v_1)(v - v_3) + C\,(v - v_1)(v - v_2)$$

or

$$\begin{cases} A + B + C = 0 \\ (v_3 + v_2)A + (v_3 + v_1)B + (v_2 + v_1)C = 1 \\ v_3 v_2 A + v_3 v_1 B + v_2 v_1 C = 0 \end{cases} \tag{3.42}$$

By solving (3.42) we find:

$$\begin{cases} A = \dfrac{v_1(v_2 - v_3)}{v_1^2(v_2 - v_3) + v_2^2(v_3 - v_1) + v_3^2(v_1 - v_2)} \\ B = \dfrac{v_2(v_3 - v_1)}{v_1^2(v_2 - v_3) + v_2^2(v_3 - v_1) + v_3^2(v_1 - v_2)} \\ C = \dfrac{v_3(v_1 - v_2)}{v_1^2(v_2 - v_3) + v_2^2(v_3 - v_1) + v_3^2(v_1 - v_2)} \end{cases} \tag{3.43}$$

Then

$$\int \frac{v}{v^3 + pv + q}\,dv = A\int \frac{1}{v - v_1}\,dv + B\int \frac{1}{v - v_2}\,dv + C\int \frac{1}{v - v_3}\,dv$$
$$= A\ln|v - v_1| + B\ln|v - v_2| + C\ln|v - v_3| + const \tag{3.44}$$

and the dependence $v = v(t)$ is determined from:

$$A\ln\left|\frac{v - v_1}{v_0 - v_1}\right| + B\ln\left|\frac{v - v_2}{v_0 - v_2}\right| + C\ln\left|\frac{v - v_3}{v_0 - v_3}\right| = -at \tag{3.45}$$

The evaluation of integral (3.32) gives the dependence $s = s(v)$ as the following form:

$$-as(v) = Av_1 \ln\left|\frac{v - v_1}{v_0 - v_1}\right| + Bv_2 \ln\left|\frac{v - v_2}{v_0 - v_2}\right| + Cv_3 \ln\left|\frac{v - v_3}{v_0 - v_3}\right| \qquad (3.46)$$

Subcase. Let additionally the condition $q = 0$ (which means $P_{out} = 0$) is satisfied, i,e. the motion is happened due to gravity force component along the direction of motion which depends on road tilt angle α. Because of $D_3 > 0$ then should be $p < 0$ (gravity carrying the motion prevails over rolling resistance). Evaluations of integrals give:

$$-a\,t = \int_{v_0}^{v} \frac{v\,dv}{v^3 + pv + q} = \int_{v_0}^{v} \frac{v\,dv}{v^3 + pv} = \int_{v_0}^{v} \frac{dv}{v^2 - (-p)} = \int_{v_0}^{v} \frac{dv}{v^2 - \left(\sqrt{-p}\right)^2}$$

$$= \frac{1}{2\sqrt{-p}}\left[\ln\left|\frac{v - \sqrt{-p}}{v + \sqrt{-p}}\right| - \ln\left|\frac{v_0 - \sqrt{-p}}{v_0 + \sqrt{-p}}\right|\right] \qquad (3.45^*)$$

Analogically,

$$-a\,s(v) = \int_{v_0}^{v} \frac{v^2\,dv}{v^3 + pv + q} = \int_{v_0}^{v} \frac{v^2\,dv}{v^3 + pv} = \int_{v_0}^{v} \frac{v\,dv}{v^2 + p} = \frac{1}{2}\ln\left|\frac{v^2 + p}{v_0^2 + p}\right| \qquad (3.46^*)$$

The character of mototin in this subcase is demonstrated in Figures 3.8 and 3.9. Independently of initial velocity v_0 the velosity is raised in time with desending acceleration and after 10 minutes becomes almost constant and the course made increase linearly.

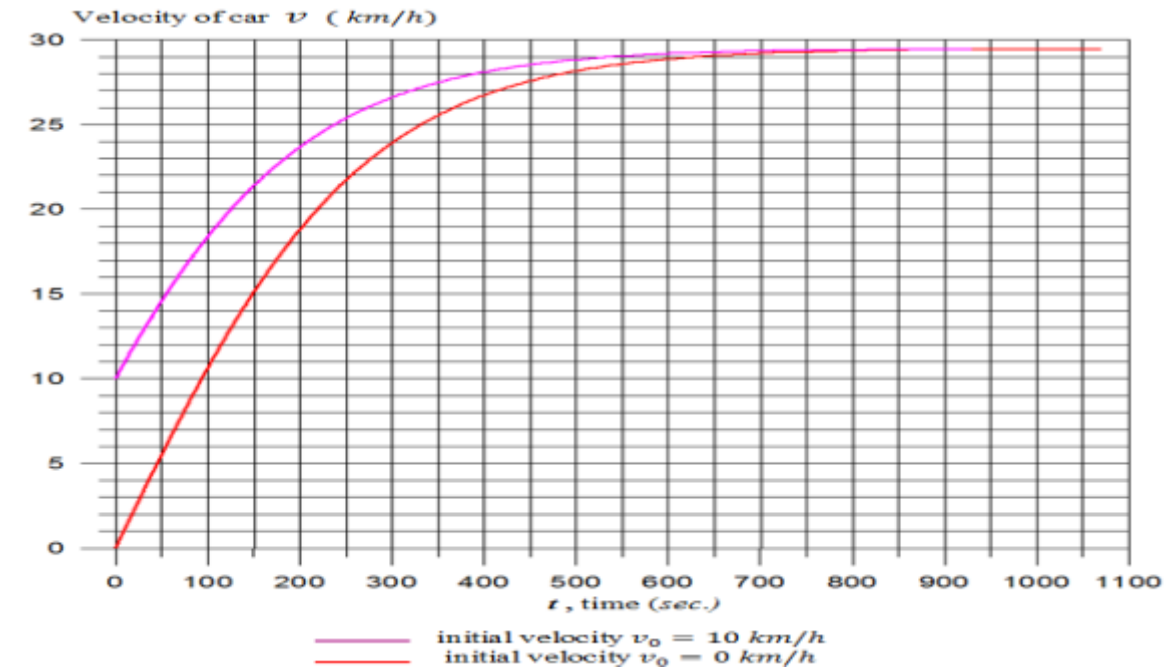

Figure 3.8: Solar car velocity dependences for two values of initial velocities.

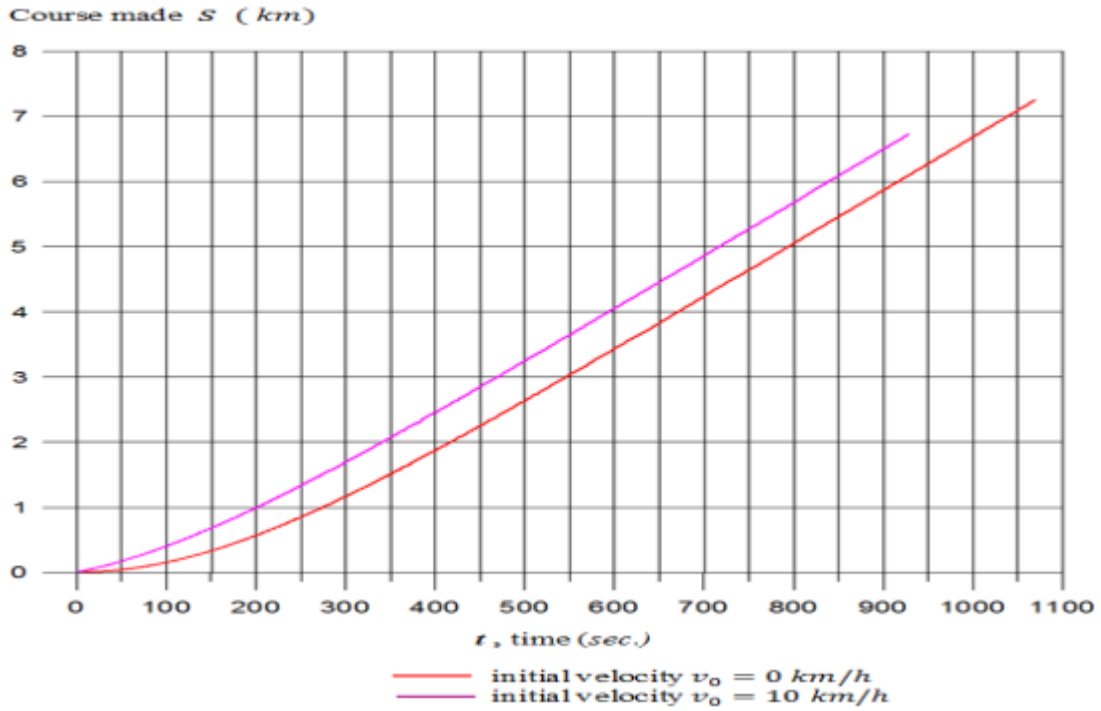

Figure 3.9: Solar car course made dependences for two values of initial velocities.

Case 3. Discriminant of equation $D_3 = -108\left(\frac{q^2}{4} + \frac{p^3}{27}\right) = 0$. Then the equation $v^3 + pv + q = 0$ has three real different roots so that: $v_1 \neq v_2 = v_3$. In this case $v^3 + pv + q = (v - v_1)(v^2 + \alpha v + \beta) = (v - v_1)(v - v_2)^2 = 0$ and the discriminant $\boldsymbol{d_2 = \alpha^2 - 4\beta = 0}$.

The procedure of expansion in rational fractions and integration is as follows.

$$\frac{v}{v^3 + pv + q} = \frac{A}{v - v_1} + \frac{B}{v - v_2} + \frac{C}{(v - v_2)^2} \tag{3.47}$$

The coefficients A, B and C are determined from equality of left and right sides of (3.47), which gives:

$$v = A\,(v - v_2)^2 + B\,(v - v_1)(v - v_2) + C\,(v - v_1)$$

or

$$\begin{cases} A + B = 0 \\ -2v_2A - (v_1 + v_2)B + C = 1 \\ v_2^2A + v_1v_2B - v_1C = 0 \end{cases} \tag{3.48}$$

By solving (3.48) we find:

$$\begin{cases} A = \dfrac{v_1}{(v_2 - v_1)^2} \\ B = -\dfrac{v_1}{(v_2 - v_1)^2} \\ C = \dfrac{v_2}{v_2 - v_1} \end{cases} \tag{3.49}$$

Then,

$$\int \frac{v}{v^3 + pv + q}\,dv = A\int \frac{1}{v - v_1}\,dv + B\int \frac{1}{v - v_2}\,dv + C\int \frac{1}{(v - v_2)^2}\,dv$$

$$= A\ln\frac{|v - v_1|}{|v - v_2|} + \frac{C}{v - v_2}\ln + const \tag{3.50}$$

and the dependence $v = v(t)$ is determined from:

$$A\ln\left|\frac{(v - v_1)(v_0 - v_2)}{(v - v_2)(v_0 - v_1)}\right| + C\,\frac{(v_0 - v)}{(v - v_2)(v_0 - v_2)} = -at \tag{3.51}$$

The evaluation of integral (3.32) gives the dependence $s = s(v)$ as the following form:

$$-as(v) = Av_1 \ln\left|\frac{v - v_1}{v_0 - v_1}\right| - Av_2 \ln\left|\frac{v - v_2}{v_0 - v_2}\right|$$
$$+ C \ln\left|\frac{v - v_2}{v_0 - v_2}\right| - Cv_2 \frac{(v_0 - v)}{(v - v_2)(v_0 - v_2)} \qquad (3.52)$$

3.4 Solution of the differential equation of car motion for curved trajectory

In the general case of curved trajectory for determination of law of motion, i.e. $v = s(t)$ and $= s(t)$, the curved trajectory can be represented as the chain of short straight-line trajectories (Figure 3.10).

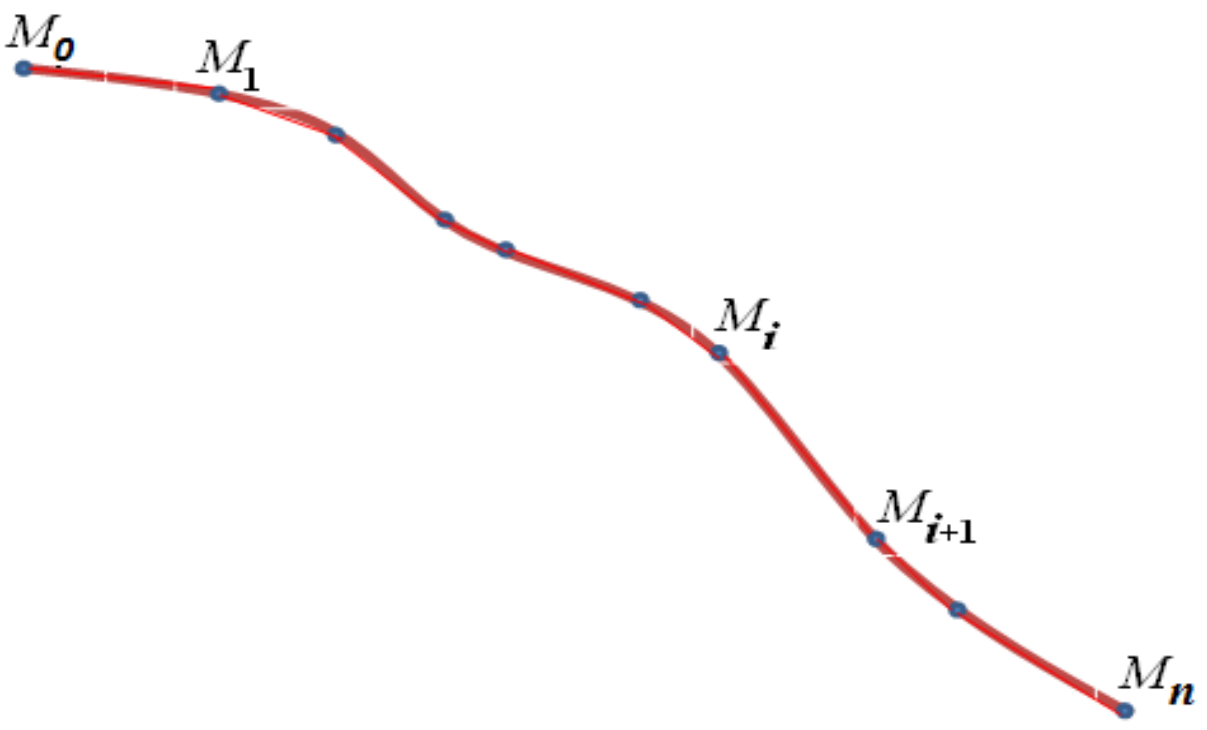

Figure 3.10: Curved trajectory as a chain of small straight-line trajectories.

If the lengths of intervals M_iM_{i+1} $(i = 0,1,2,3 \ldots)$ are sufficiently small then the

coefficients a , b , and c in the differential equation (3.18) can be takin as a constant in this interval and to determine the law of motion two way may be used. First way, exact solution obtained in previous section is applied to every interval M_iM_{i+1} . At that initial conditions at point M_i for interval M_iM_{i+1} should be taken as terminal values at point M_i of solution for interval $M_{i-1}M_i$. Second way, the differential equation (3.18) (or (3.30)) can be solved numerically. The equation (3.18) can be written as

$$dv = \left(\frac{c}{v} - av^2 + b\right)dt \tag{3.53}$$

and approximately

$$\Delta v = \left(\frac{c}{v} - av^2 + b\right)\Delta t \tag{3.54}$$

Let t_i $(i = 0,1,2,3,\dots n)$ is the moment of time when car is passing from point $M_i = (x_i, y_i, z_i)$ and , $s_i = length(\widetilde{M_oM_i})$, $\Delta s_i = length\left(\widetilde{M_iM_{i+1}}\right)$. If we take $\Delta t_i = t_{i+1} - t_i$ and $\Delta v_i = v_{i+1} - v_i$ where $v_i = v(t_i)$ then from (3.54) the following algorithm for determination t_i and v_i is obtained:

$$\begin{cases} v_0 = v_{initial\ \ velocity} \quad , \quad at\ \ t = 0 \\ \Delta t_i = \Delta s_i / v_i \\ v_{i+1} = v_i + \left(\frac{c_i}{v_i} - av_i^2 + b_i\right)\cdot \Delta t_i \end{cases} \tag{3.54}$$

The coordinates $(x_i\ , y_i\ , z_i)$ of point M_i on the road and the shadow function (which determines the shadowing of Sun by relief, surrounding of point M_i), are calculated from DEM of the territory. As we can see from (3.17) coefficient $a > 0$ and is constant at every point of road and coefficients b_i and c_i are defined:

$$b_i = -C_{rr}\, g\ (\vec{n}_i \cdot \vec{r}_{0i}) - g\left(\vec{r}_{0i} \cdot \vec{l}_i\right)\ ;\ \ c_i = \frac{P_{out\ i}}{m} \tag{3.55}$$

The unite vector $\vec{l}$ at the point M_i is calculated on formula:

$$\vec{l}_i = \frac{(x_{i+1} - x_i)\cdot \vec{\imath} + (y_{i+1} - y_i)\cdot \vec{\jmath} + (z_{i+1} - z_i)\cdot \vec{k}}{\sqrt{(x_{i+1} - x_i)^2 + (y_{i+1} - y_i)^2 + (z_{i+1} - z_i)^2}} \tag{3.55}$$

The unite vectors $\vec{r}_0$ and $\vec{n}$ at the point M_i are calculated on formulas which follow from their definition [see (3.19), (3.21) and (3.24)]:

$$\vec{r}_{0i} = \frac{1}{\sqrt{x_i^2 + y_i^2 + z_i^2}} \left(x_i \cdot \vec{\imath} + y_i \cdot \vec{\jmath} + z_i \cdot \vec{k} \right) \tag{3.56}$$

$$\vec{m}_i = \frac{\vec{r}_{0i} \times \vec{l}_i}{\left| \vec{r}_{0i} \times \vec{l}_i \right|} \quad ; \quad \vec{n}_i = \vec{l}_i \times \vec{m}_i \tag{3.57}$$

In the next chapter in order to simulate solar car motion the exact solution for straight line road is used.

CHAPTER 4

SIMULATION AND VISUALIZATION OF SOLAR CAR MOTION

4.1 Simulation of solar car motion

The simulation of solar car motion was carried out for the chosen three routes:
1) Hamburg-Berlin (Germany) 2) Baku-Shamakhi (Azerbaijan) 3) Zakatala-Tbilisi(Azerbaijan-Georgia) . The road Hamburg-Berlin is located at the latitudes 52.5^0-53.5^0 and it is about 12^0 upward to North than the roads Baku-Shamakhi and Zakatala-Tbilisi. Due to the latitude differences the amount of solar radiation over those roads is essentially various for different seasons of year, as it was mentioned in the Chapter 2. The 3D presentations of those roads are given in Figures 4.1-4.3.

The simulation of solar car motion is carried out by solution of differential equation of the motion as described in Chapter 3 method. The curved road is presented as broken line (chain of small straight-lines, Figure 3.10). At every straight-line section of road the differential equation of motion is exactly solved by using formulas (3.38), (3.40) and (3.45), (3.46) and dependencies $v = v(t)$ and $s = s(t)$ are found. The initial velocity at the point M_0 is taken as $v_0 = 0$; at the point M_{i+1} of segment $[M_{i+1}, M_{i+2}]$ is taken $v_{i+1,0} = v_{i,e}$, where $v_{i,e}$ is the velocity at the endpoint of segment $[M_i, M_{i+1}]$, which is found from exact solution at this segment.

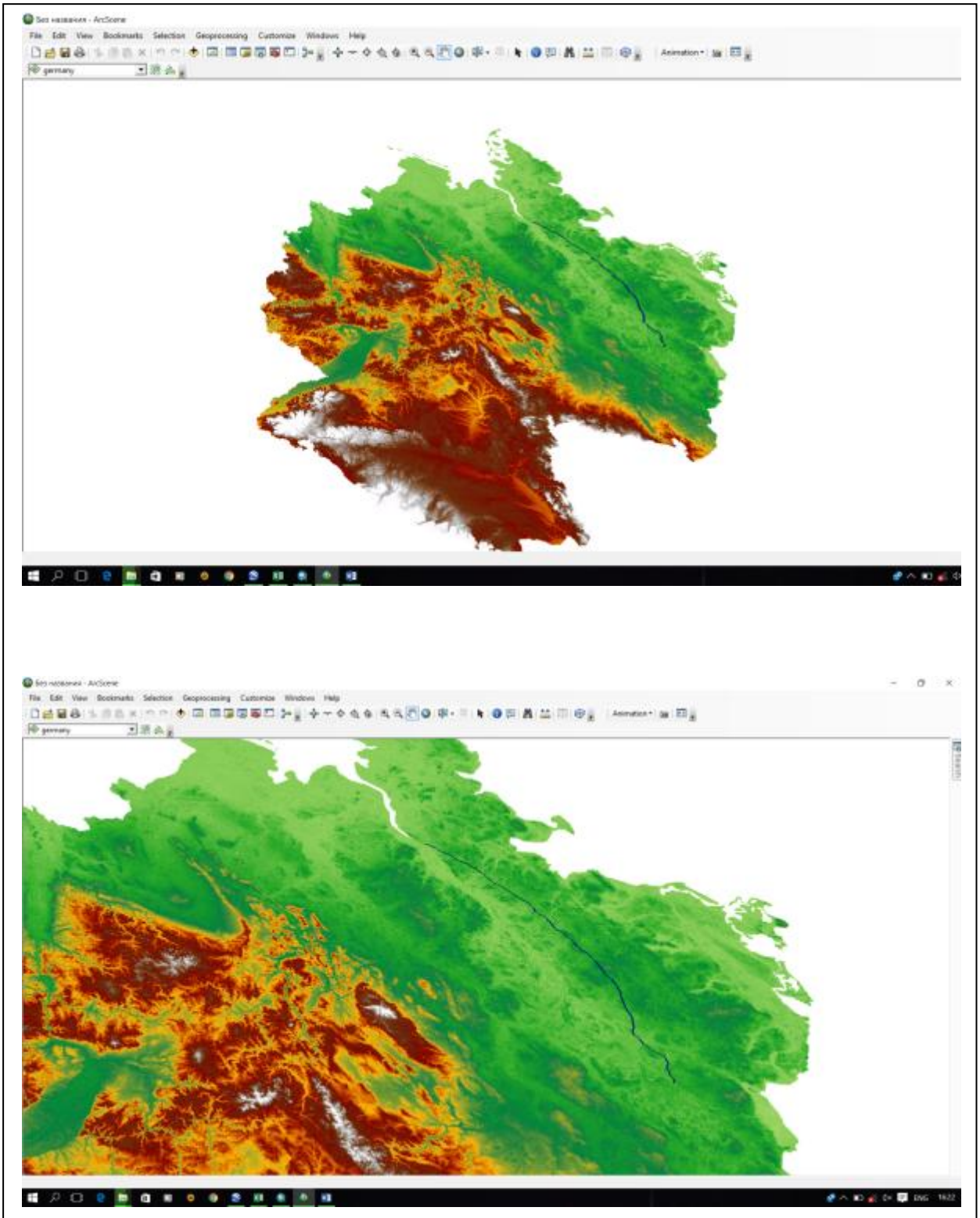

Figure 4.1: 3D representation of road Hamburg-Berlin

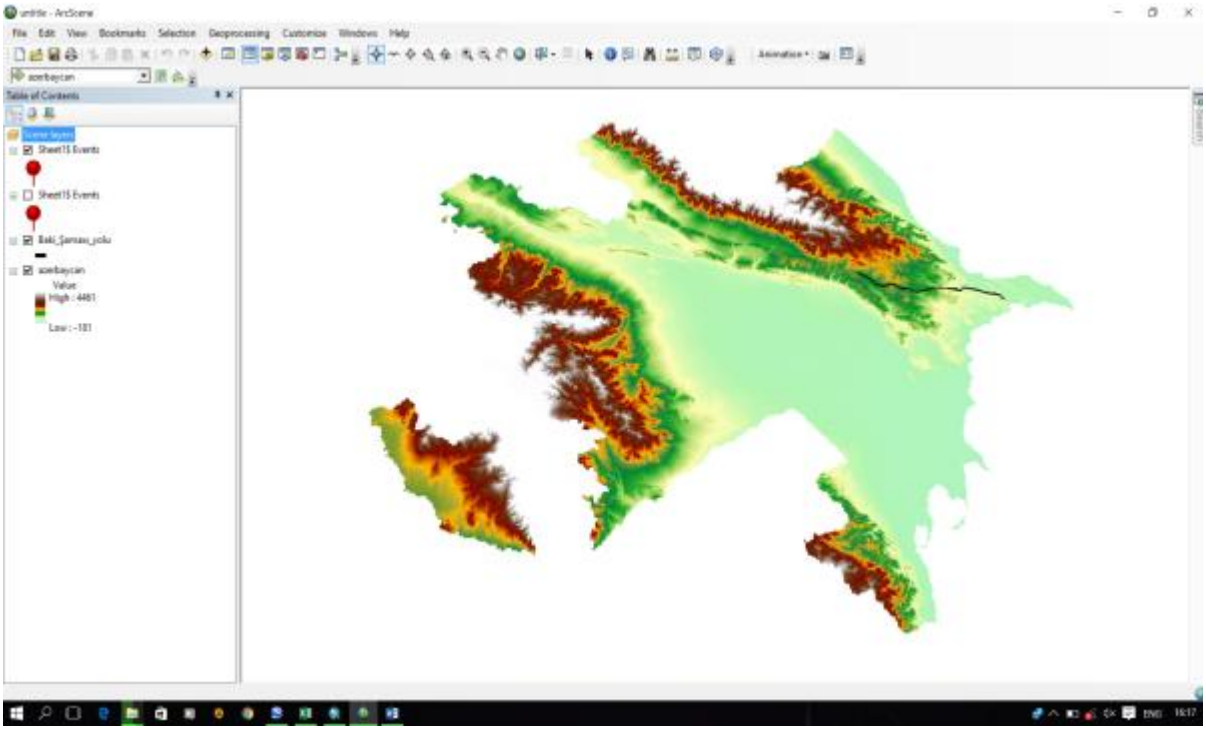

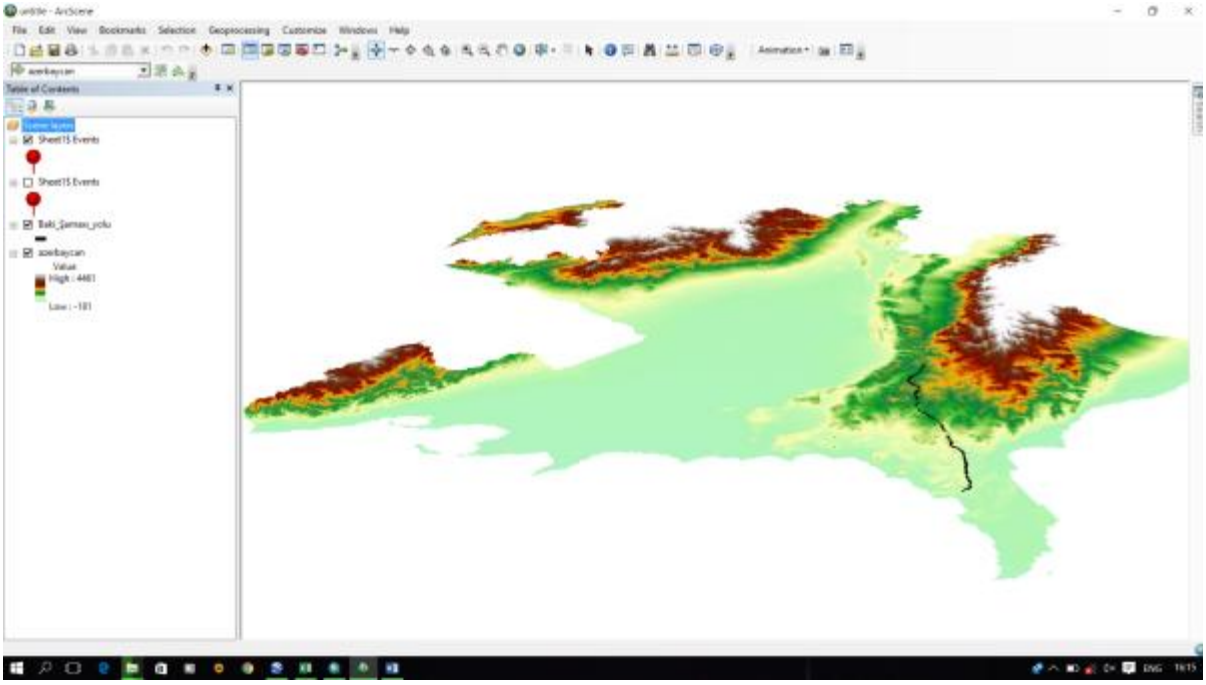

Figure 4.2: The 3D presentation of road Baku-Shamakhi.

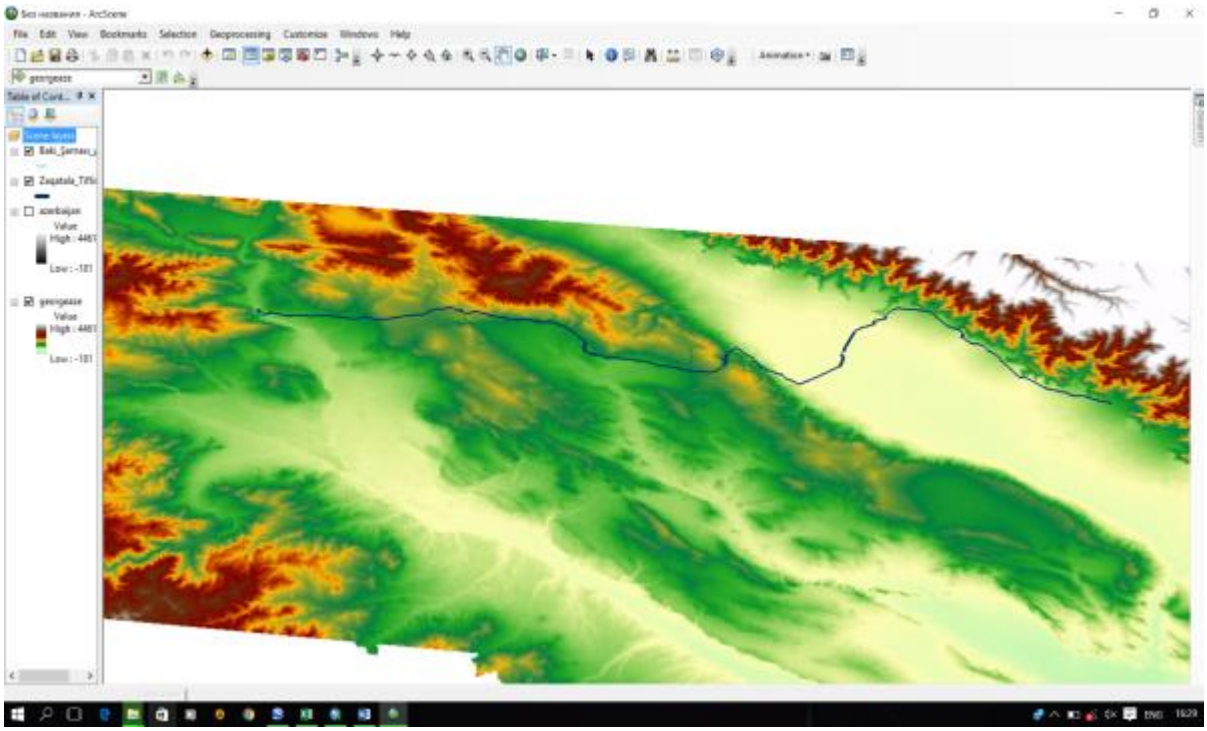

Figure 4.3: The 3D presentation of road Zakatala-Tbilisi.

The stretch of roads Baku-Shamakhi and Zakatala-Tbilisi are about 120 km and 250 km, respectively. Those roads are passing through plain and montane regions and have complex trajectories. For the road Baku-Shamakhi the behaviour of tilt angle along the trajectory is presented in Figure 4.4.

For the chosen type of solar car the low of motion, $v = v(t)$ and $s = s(t)$ essentially depends on two factor: 1) start time ; 2) road tilts. First factor concerns the season of year and determines the power of solar energy falling onto the panel and thereby the input to engine electric power. Second factor either is hastening car motion or decelerating it.

The input parameters of the developed model are:

I. Parameters which determine falling solar radiation:

- Data of starting of car motion (Year, month, hour, minute, second);
- Optical state of atmosphere (optical thicknesses of atmosphere, cloudiness);

II. Parameters characterizing the road:

-Geographical coordinates of road (Latitude, Longitude, Altitude) at the chosen points of road ;

III. Parameters characterizing the car:

- Mass of car;
- Air resistance coefficient;
- Coefficient of rolling friction;
- Solar sell efficiency.

Thus, the model is universal and can be applied to any road and any solar car for any time of year.

The simulation examples provided here were carried out for the solar car "PowerCore SunCruiser" designed by SolarCar Team of the Bochum University of Applied Sciences (Hochschule Bochum) which has the parameters presented in Table 4.1:

Table 4.1: Technical parameters of solar car PowerCore SunCruiser:

Mass of car: *m (kg)*	Air resistance coefficient: C_w	Rolling friction coefficient: C_{rr}	Solar sell efficiency: C_{ef}
340	0.16	0.0025	0.30

4.1.1. Simulation of solar car motion on the road Hamburg-Berlin.

The stretch of road Hamburg-Berlin is about 283 km and is relatively smooth (without hairpin, sharp rise of road and falling gradient). The tilt angle module along the road is less than 10^0 (Figure 4.4).

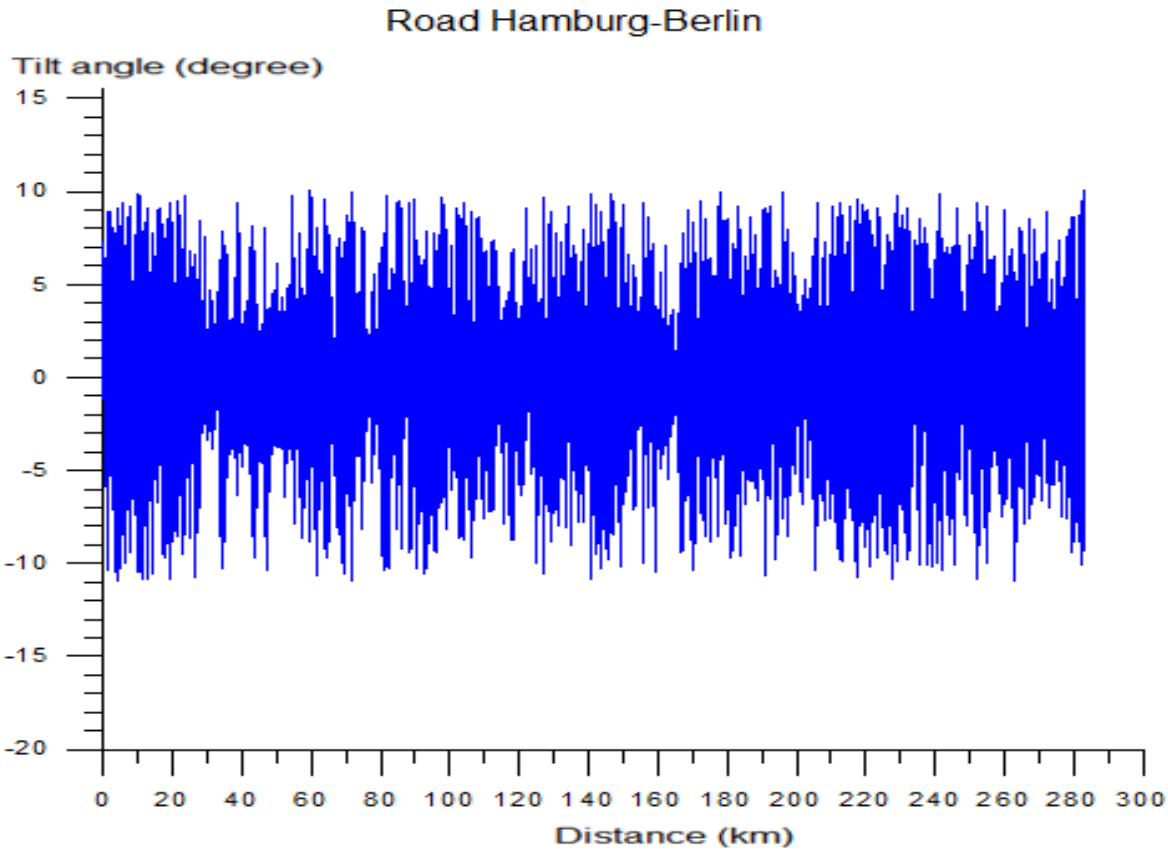

Figure 4.4: The tilt angle dependence on distance along the road.

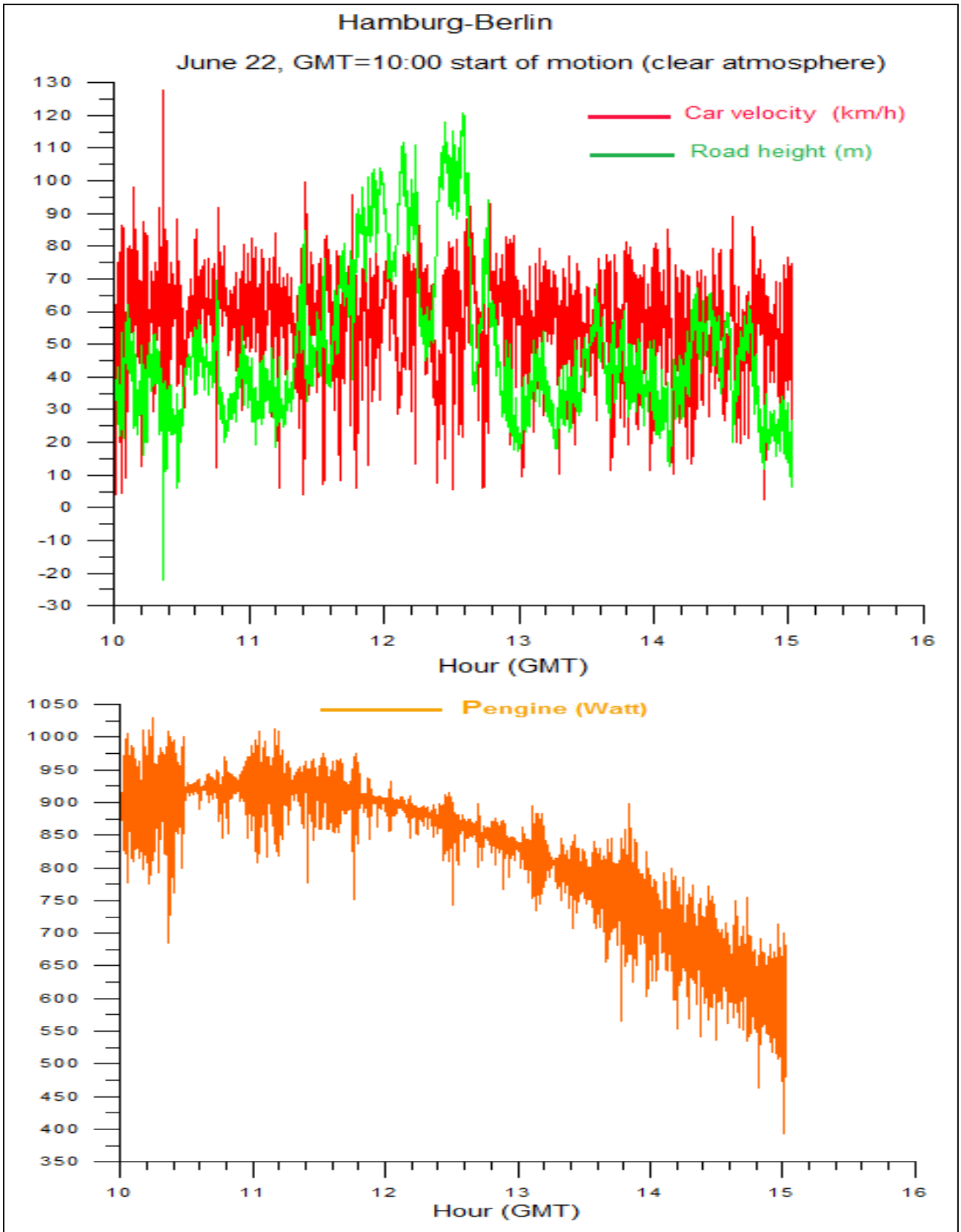

Figure 4.5: The behaviour of motion characteristics.

For the specific day of year, June 22 (summer solstice) the dependences on time of motion characteristics are presented in Figure 4.5. The decreasing trend of transmitted to engine power relates to time of day but its fluctuation is caused by road tilt variance which induces the fluctuation of amount of solar radiation falling onto the solar car panel. The fluctuation of car velocity is caused by composite effect of variance of road tilt and power. As we can see from graphics in Figure 4.5 the velocity rise is sharp when road has falling gradient and increasing input to the engine power and vice-versa.

For other specific days of year and starting time the main parameters of motion are presented in Table 4.2.

Start of motion		**Average velocity (km/h)**	**Course made (km)**	**Travelling time**	**Terminal time Hour:minute (GMT**	**Terminal Solar power (Watt/m^2)**	**NOTE**
Month, Day	**Hour: minute (GMT)**						
March, 21	07:00	41.4	282.8	6 hour 49min	13:49	452	Finished
March, 21	10:00	32.7	232.5	7 hour 8 min	17:08	24	Not finished
June, 22	05:00	42.3	282.8	5 hour 51min	10:51	911	Finished
June, 22	10:00	56.2	282.8	5 hour 7min	15:07	646	Finished
December, 22	10:00	14.0	65.7	4 hour 40min	14:40	0	Not finished

Table 4.2 Characteristics of motion on the road Hamburg-Berlin

In the case of car motion starting at June 22, GMT=10:00 on the route Hamburg- Berlin the total amount of consumption solar energy was:

$E_{total} = 4.16\ kWatt \cdot hour.$

The amount of energy to do the work against gravity force was:

$E_{poten} = mg\left(h_{Hamburg} - h_{Berlinu}\right) \approx 0.01\ kWatt \cdot hour$.

Travel time was 5 *hour* 7 *min* , mean velocity =55.2 *km/h.*

On the back route Berlin-Hamburg with the same starting time the total amount of consumption solar energy also was: $E_{total} = 4.16\, kWatt \cdot hour$. Travel time was 5 *hour* 1 *min* , mean velocity =56.2 *km/h.* The small differences there and back were caused by small fluctuation of road heights.

4.1.2. Simulation of solar car motion on the road Baku-Shamakhi.

The stretch of roads Baku-Shamakhi is about 120 km. The roads are passing through plain and montane regions and have complex trajectories. The behaviour of tilt angle along the trajectory is presented in Figure 4.6.

As we see the road has numerous hairpins, sharp rises of road and falling gradients. The tilt angle module along the road reaches values about 30^0. Therefore, at many points of the road the amount of solar radiation falling onto the car panel essentially differs from that to the horizontal surface.

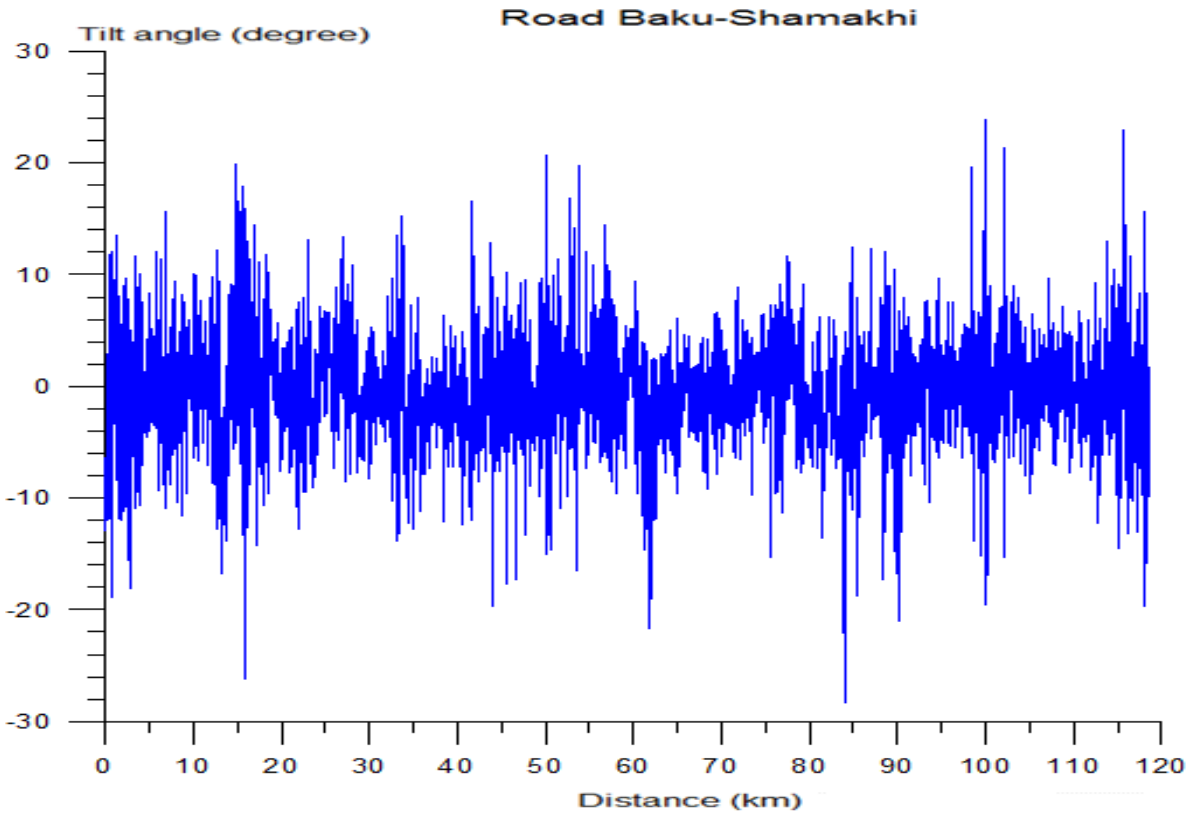

Figure 4.6: The tilt angle dependence on distance along the road.

The dependences on time of motion characteristics for start times GMT=05:00 and GMT=10:00 are presented in Figures 4.7. The analyses of graphics shows that the velocity of car is determined by flow of energy and road tilt. The velocity is very low when power of energy is small and road tilt is high.

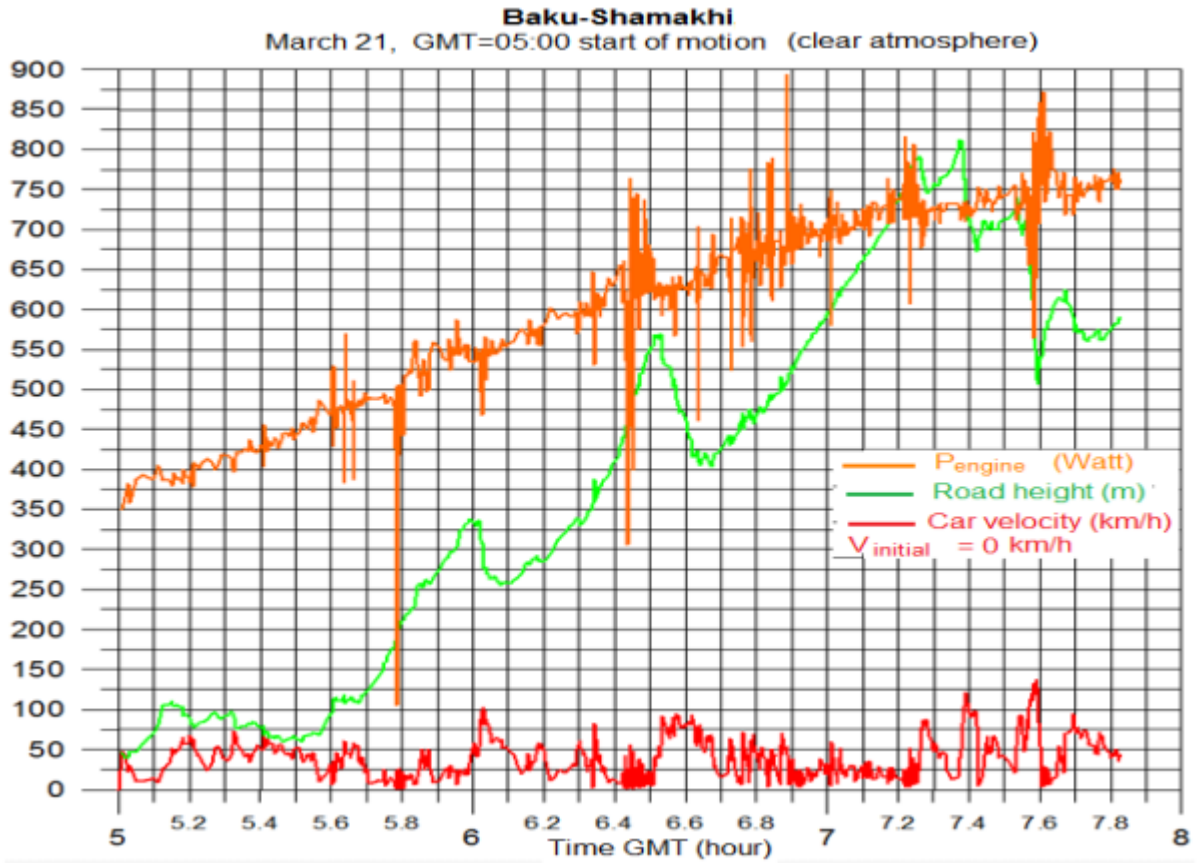

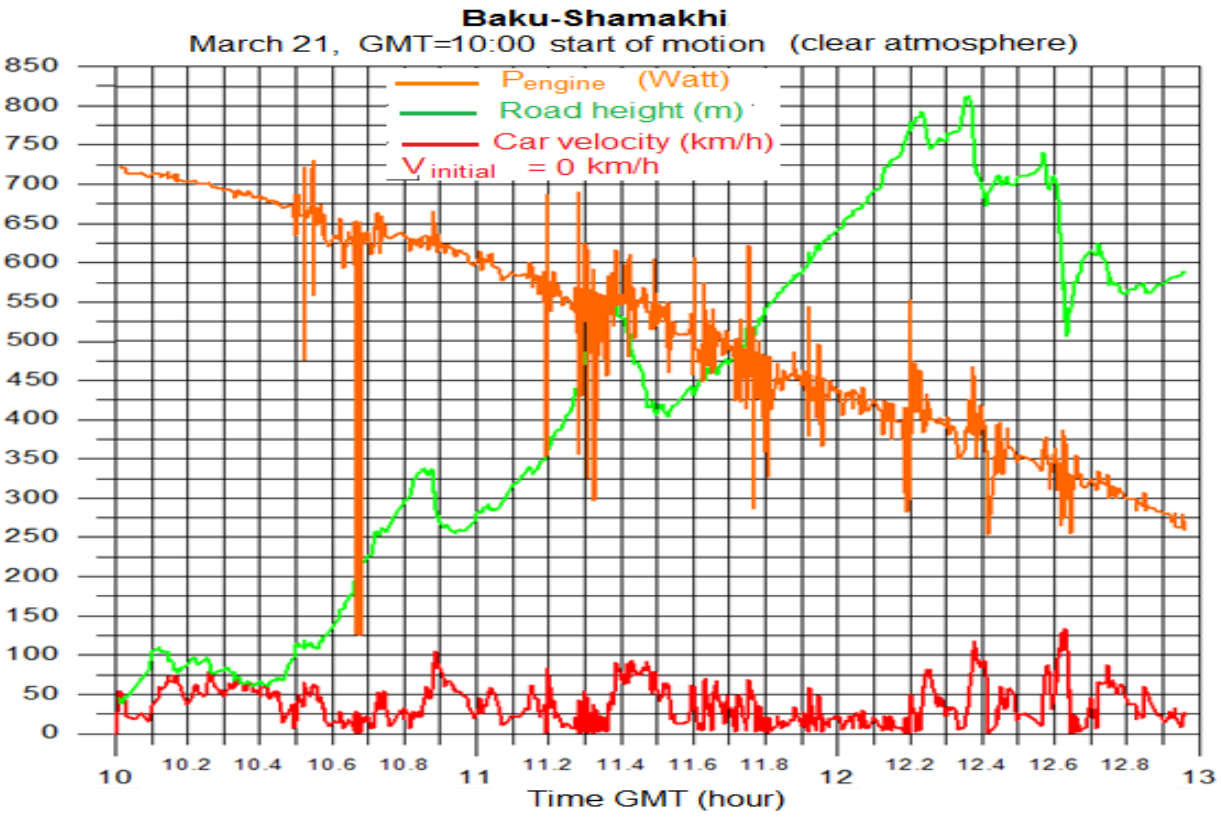

Figure 4.7: The behaviour of motion characteristics.

For other specific days of year and starting time the main parameters of motion are presented in Table 4.3.

Table 4.3: Characteristics of motion on the road Baku-Shamakhi

Start of motion		**Average velocity (km/h)**	**Course made (km)**	**Travelling time**	**Terminal time Hour:minute (GMT**	**Terminal Solar power (Watt/m^2)**	**NOTE**
Month, Day	**Hour:minute (GMT)**						
March, 21	05:00	37.8	118.6	3hour 8min	08:08	752	Finished
March, 21	10:00	35.1	118.6	3hour 22min	13:22	171	Finished
June, 22	05:00	48.7	118.6	2hour 26min	07:26	991	Finished
June, 22	10:00	34.7	118.6	3hour 25min	15:25	627	Finished
December, 22	10:00	8.9	27.5	3hour 5min	13:05	38	Not finished

In the case of car motion starting at June 22, GMT=10:00 on the route Baku- Shamakhi the total amount of consumption solar energy was:

$E_{total} = 2.43\ kWatt \cdot hour.$

The amount of energy to do the work against gravity force was:

$E_{poten} = mg(h_{Shamak\ hi} - h_{Baku})$

$= 340kg \cdot 9.8\ \frac{m}{s^2} \cdot (648.8m - 70.3m) = 1927562\ Joule \approx 0.54\ kWatt \cdot hour$.

Thus, the difference

$$\Delta E = E_{total} - E_{poten} = 2.43 - 0.54 = 1.89\ (kWatt \cdot hour)$$

was used up to do the work against resistance forces. Travel time was 3 *hour* 25 *min* , mean velocity =34.7 *km/h.*

On the back route Shamakhi-Baku with the same starting time the total amount of consumption solar energy was: $E_{total} = 1.98\ kWatt \cdot hour$. Travel time was 2 *hour*

22 *min* , mean velocity =50.0 *km/h.* That was because of the motion was realized from high point (Shamakhi) to low point (Baku).

4.1.3. Simulation of solar car motion on the road Zakatala-Tbilisi.

The stretch of roads Zakatala-Tbilisi is about 200 km. The roads is passing through plain and montane regions and have complex trajectories. The behaviour of tilt angle along the trajectory is presented in Figure 4.8. As we see the road has numerous hairpins, sharp rises of road and falling gradients. The tilt angle module along the road reaches values about 35^0. Therefore, at many points of the road the amount of solar radiation falling onto the car panel essentially differs from that to the horizontal surface.

The dependences on time of motion characteristics for start times GMT=05:00 is presented in Figures 4.9.

The analyses of graphics shows that the velocity of car is determined by flow of energy and road tilt. The velocity is very low when power of energy is small and road tilt is high.

For other specific days of year and starting time the main parameters of motion are presented in Table 4.4.

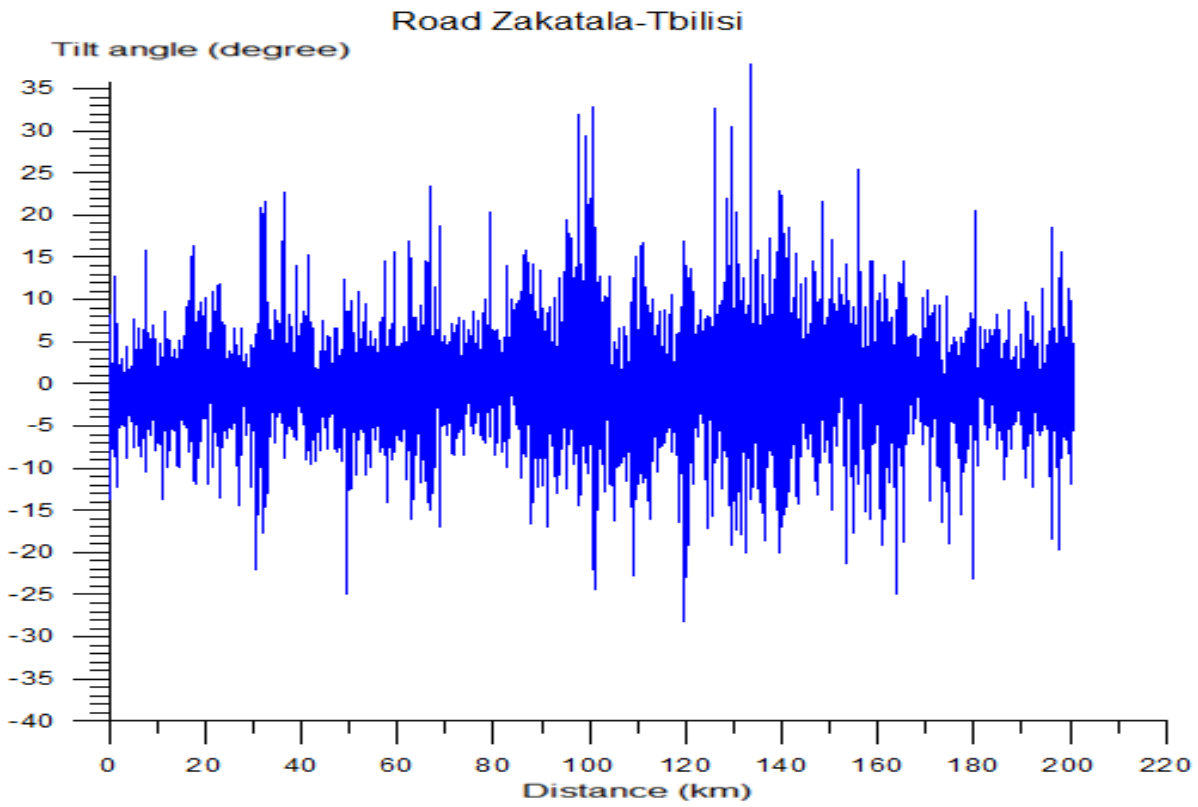

Figure 4.8: The tilt angle dependence on distance along the road.

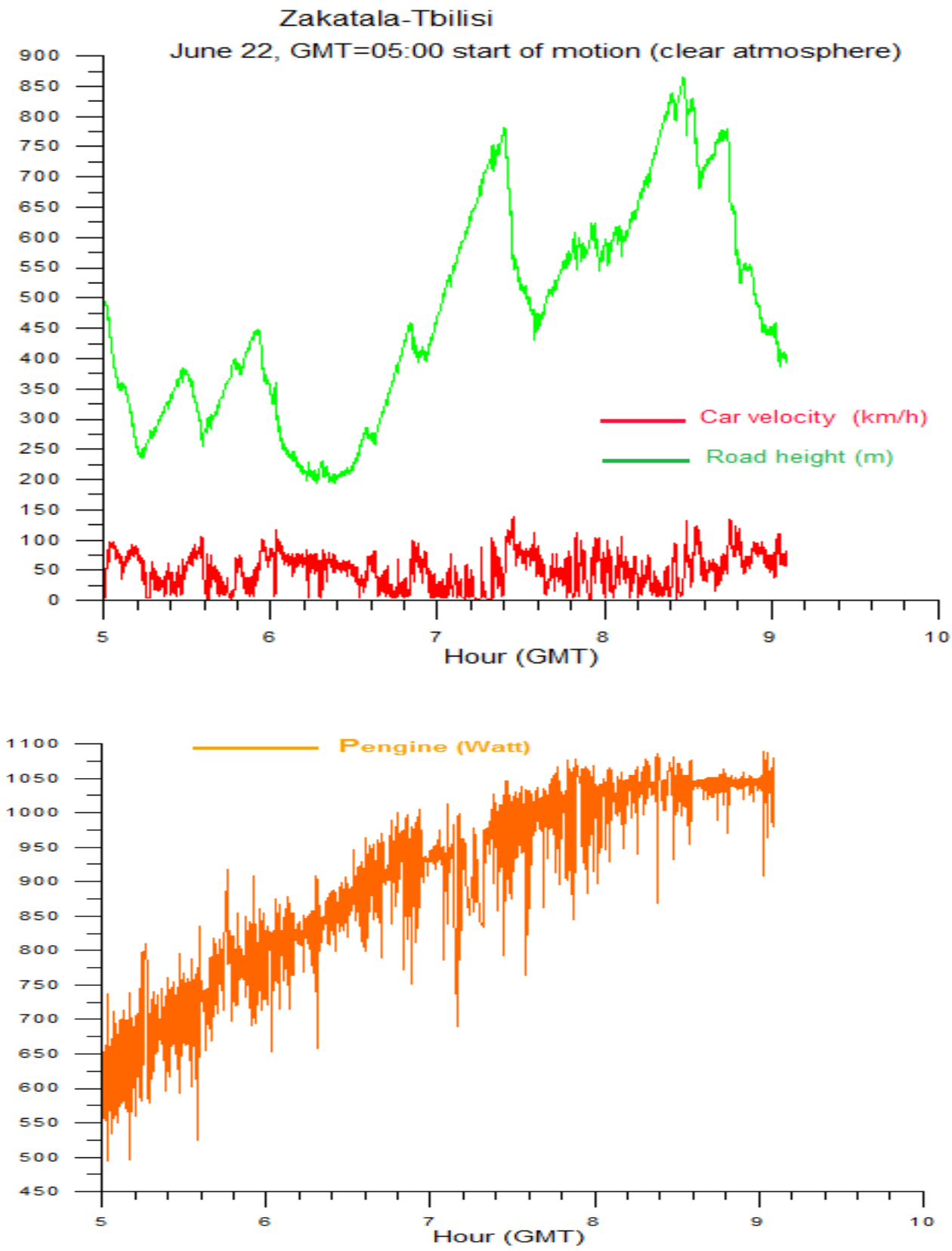

Figure 4.9: The behaviour of motion characteristics.

Table 4.4: Characteristics of motion on the road Zakatala-Tbilisi

Start of motion		**Average velocity (km/h)**	**Course made (km)**	**Travelling time**	**Terminal time Hour:minute (GMT**	**Terminal Solar power (Watt/m^2)**	**NOTE**
Month, Day	**Hour:minute (GMT)**						
March, 21	05:00	39.4	200.7	5 hour 6 min	10:06	691	Finished
March, 21	10:00	21.4	100.8	4 hour 42min	14:42	25	Not finished
June, 22	05:00	49.0	200.7	4 hour 5min	09:05	1016	Finished
June, 22	10:00	25.1	159.8	6 hour 21min	16:21	24	Not finished
December, 22	10:00	12.5	40.6	3 hour 14min	13:14	1	Not finished

In the case of car motion starting at June 22, GMT=05:00 on the route Zakatala-Tbilisi the total amount of consumption solar energy was:

$E_{total} = 3.69\ kWatt \cdot hour.$

The amount of energy to do the work against gravity force was:

$E_{poten} = mg(h_{Zakatala} - h_{Tbilisi}) \approx -0.08\ kWatt \cdot hour$.

Travel time was 4 *hour* 5 *min* , mean velocity =49.0 *km/h.*

On the back route Tbilisi-Zakatala with the same starting time the total amount of consumption solar energy also was: $E_{total} = 3.76\ kWatt \cdot hour$. Travel time was 4 *hour* 14 *min* , mean velocity =47.3 *km/h.* The differences there and back were caused by height differences of initial and terminal points.

4.2. Visualisation Of Solar Car Motion

The 3D visualization of the motion of solar car around the road represents an exact replication of real-life object -a solar car and surrounding it real-life terrain into 3D model by means of tools and software. The field of application of the visualization can be very diverse from scientific visualization where the visualization facilitates the exploration, analysis and understanding of data to educational visualization, where visualization gives clearer picture of the events to the learners, or knowledge visualization, where visualization assists to knowledge transfer between the parties. Therefore, we use ArcScene in order to carry out such a visualization of solar car motion on the chosen roads.

Obtaining of high quality visual representation is a process that requires sophisticated tools (programs and program tools) as well high processing resources. It is also required to design an each object and terrain model in the visualization scene.

Like any other process, visualization of the scenes has the following levels:

1) Carrying out 3-dimensional modeling: 3D visualization of the object by creating the exact copy of its real life prototype
2) Selection and customization of the texture of the surface of the object that is selected for the subject imaging
3) Selection of illumination : this is one the most important levels in subjective visualization which defines the level of the comprehension of the object by the viewers
4) View angle selection : During the visualization, only the most relevant view angles should be presented

To create a 3D visualization of a scene it is needed to have a number of primary data. The more data, the faster and better gets the objective visualization. The visualization of solar car motion is provided by using simulation data derived from the mathematical model.
To configure the substantive visualization of solar car motion we take the following into account:

• A detailed description of the visualization scene. Availability of sketches, drawings and photographs can be also become useful. In their presence it is easier to carry out the quality work and compare the scene to its real life prototype.

• The particular requirements of the viewers. When creating the subject of visualization it is necessary to know in detail what the viewer expects from the visualisation

The final visualization work to be done depends on the selected settings. It is necessary to know the desires and expectation of the viewer regarding the scene illuminations, usage of different 3D special effects and the other nuances.
In order to achieve a good 3D spatial visualization, it is possible to combine different visualization tools. These tools can be implemented in order to extract the route and visualize the simulation of the solar car motion under the falling solar energy as given by the mathematical model.

For example, in [16] it is given an example of two ways of road extraction methods, where the first method uses the combination of two different tools, i.e. Photoshop and ArcGIS and the second method is based on combining MapInfo GIS with ArcGIS. The results of the extraction provided in [16] show that along with having such features as simplicity, appropriate and cost effective, the combination of Photoshop and ArcGIS gave more accurate final results.

Another method given in [17] extracts road data from the Google Earth by watershed dual-thresholds algorithm in order to obtain the initial outlines of roads and multi-weighted method to obtain the edges of the roads, and morphology to take away thin lines. Finally, shape index deletes all the areas but the road area. The proposed method suggests that good results will be achieved if more characteristics of the roads will be used during the extraction. The paper provides examples of two different road types which are used for the experiment. In [17] it is given the outcome of the experiment to prove the high accuracy and the robustness of the algorithm.

We obtain the road coordinates (latitude and longitude) and the corresponding elevations using ArcMap. Further, we transform this data into points, for which we specify the distances between the points. For current visualisation purposes we use 30 meters distance between the points. Afterwards, we obtain elevation data from the Digital Elevation Model (DEM) of the corresponding terrain. When we retrieve all the necessary data - latitudes, longitudes and elevations, we can use this data as input to the mathematical model and receive back the simulated data for motion which we can visualise in ArcGIS. More detailed description of the processes carried out are given in further chapters.

4.2.1 3D ArcGIS based visualization of solar car motion along the road

In ArcGIS time data represent the state of an object in relatively to time instance. Time data are collected in order to analyze and visualize the other spatial events, for example to observe the transport flow, study the demographic changes etc.These data can be retrieved from various sources: data that was manually inserted data that was received from the sensors or the data obtained from the mathematical models. The visualization of time data allows to view the data in time frame sequence thereby see the patterns and trends that arise over the time. In ArcMap, ArcGlobe or ArcScene it

is possible to active the time properties of data and carry out the visualization of data by means of time slider which changes the state of the object (in our case 3D solar car) over the instance of time. The time frame instance must reflect the geographical position (latitude, longitude and elevation) of the moving solar car for the given instance of time.Therefore, we first need to visualize the roads (Hamburg-Berlin, Baku-Shemakhi and Zakatala-Tbilisi) which the solar car will move through on ArcScene. When the roads data (latitude, longitude and elevation each in every 30 meters) is acquired, then this data will be an input to the mathematical model, which will give the output file with exact geographical coordinates (latitude, longitude and elevation) for the given instance of time. Further, we derive Digital Elevation Models (DEMs) for the corresponding terrains where the roads pass through. Afterwards, we combine the road, the simulation file of the motion of the solar car and the 3D Digital Elevation Model of the corresponding terrain of the road in order to obtain a high level 3D visualization scene.

4.2.2 Creation of Digital Elevation Models for the terrains of the chosen roads

In order to be able to retrieve the elevations data, it is firstly needed to create the Digital Elevation Model of terrains where the roads pass. For that purpose we use EarthExplorer (http://earthexplorer.usgs.gov/). In the Figure 4.10 below it is shown

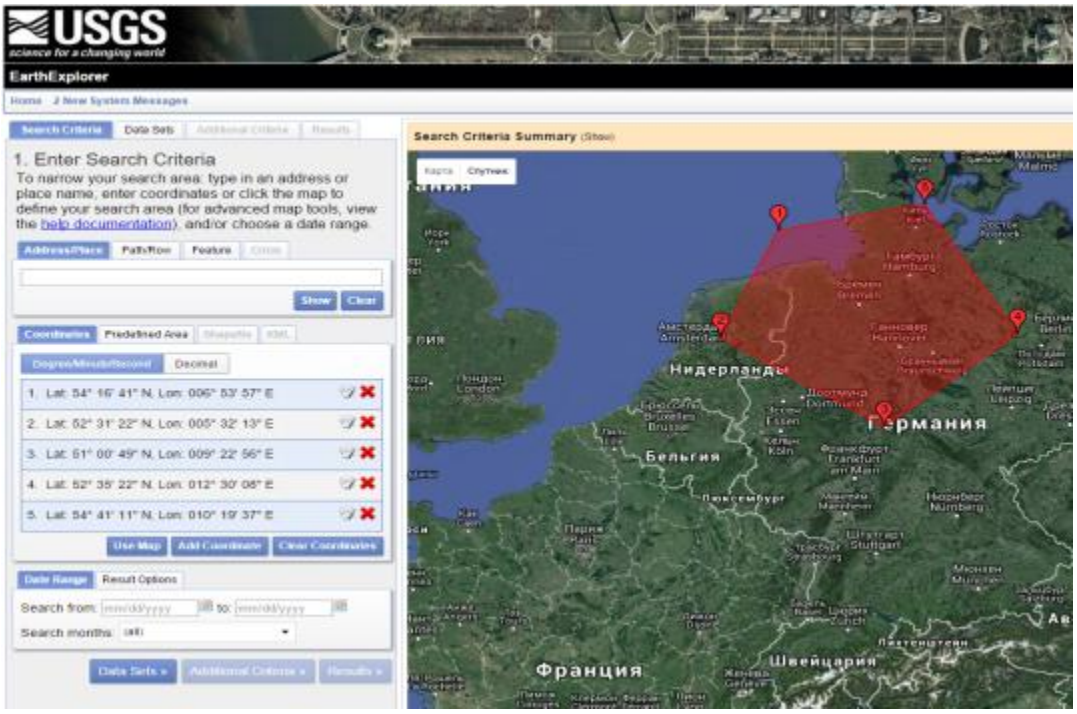

Figure 4.10: Selection of the territory using EarthExplorer.

selection of the needed territory for DEM extraction. Then, from the dataset menu we select *ASTER GLOBAL DEM* option. The results giving the data set and the results is provided in the Figure 4.11 below.

Figure 4.11: Data sets and results from EarthExplorer

Now, it is possible to download and browse the digital elevation and their data. As it can be seen from the *table of contents* window, the obtained DEMs represent separate

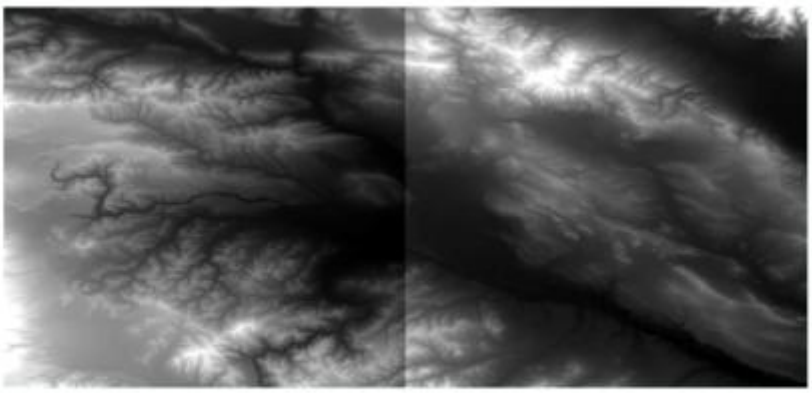

Figure 4.12: Composition of DEMs

parts of the selected area (Figure 4.12) and therefore, we will assemble them together using Arctoolbox. In Arctoolbox we follow the path (Figure 4.13):

Data management tools/raster/rasterdatasets/mosaic to new raster/

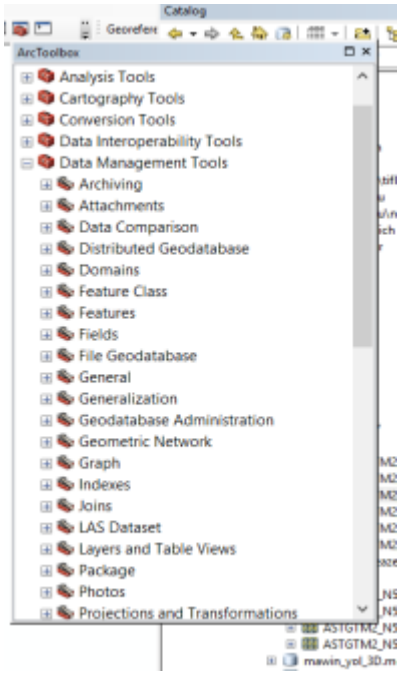

Figure 4.13: Arctoolbox implementation

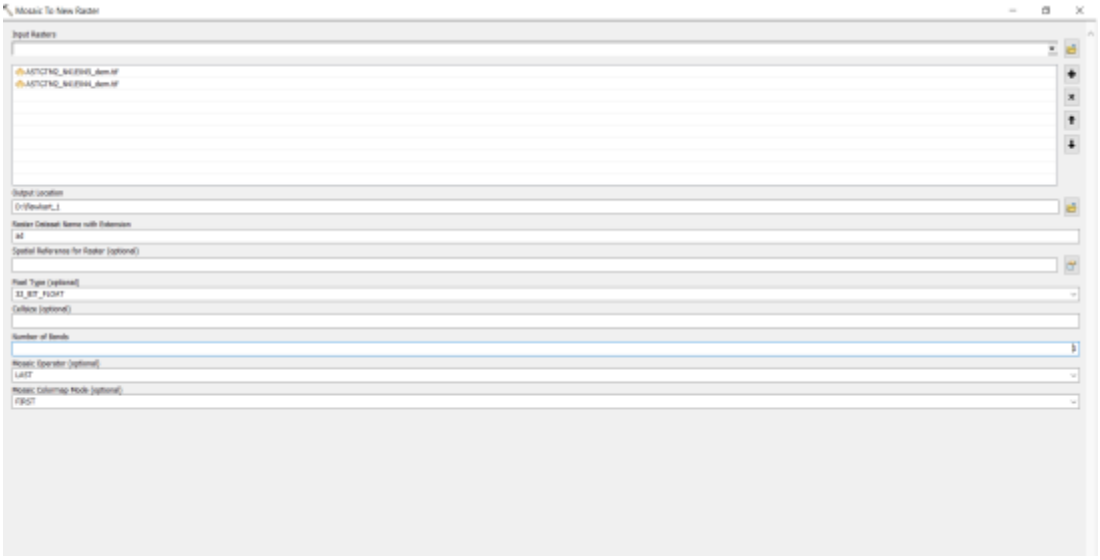

Figure 4.14: Assembly of DEMs with Arctoolbox

We assemble the obtained DEMs of the terrain using Arctoolbox as shown in Figure 4.14. We may now select different color composition (Figure 4.14 (b)) in order to

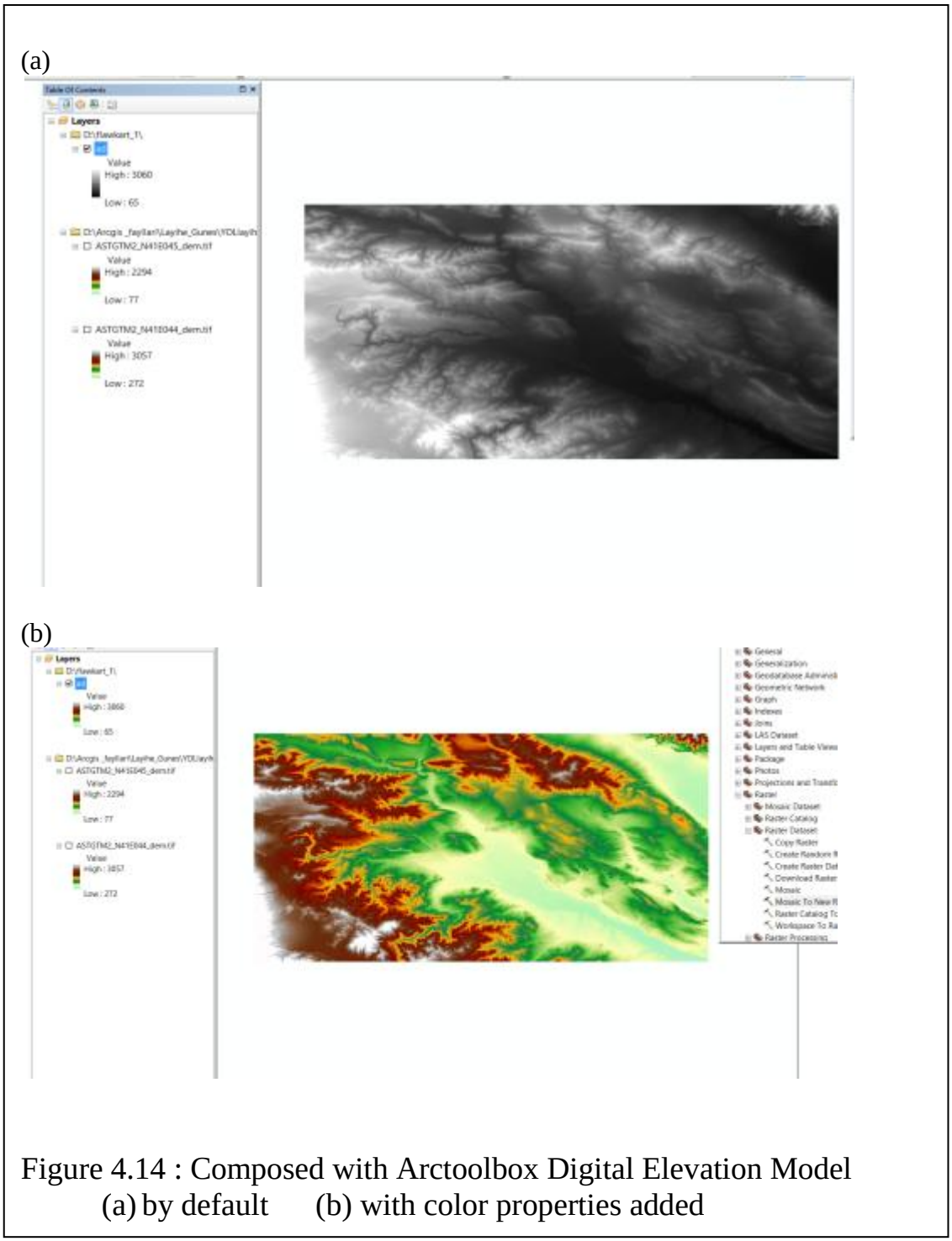

Figure 4.14 : Composed with Arctoolbox Digital Elevation Model
(a) by default (b) with color properties added

obtain better a better view of elevations. We carry out the abovementioned operation for the terrains of the three chosen roads.

4.2.3 Acquisition of roads data using ArcMap and their transformation to points

In order to acquire the roads, we use ArcMap. On standard menu we select Add Basemap. We use Open Street Map, since this option offers various types of maps (Figure 4.15).

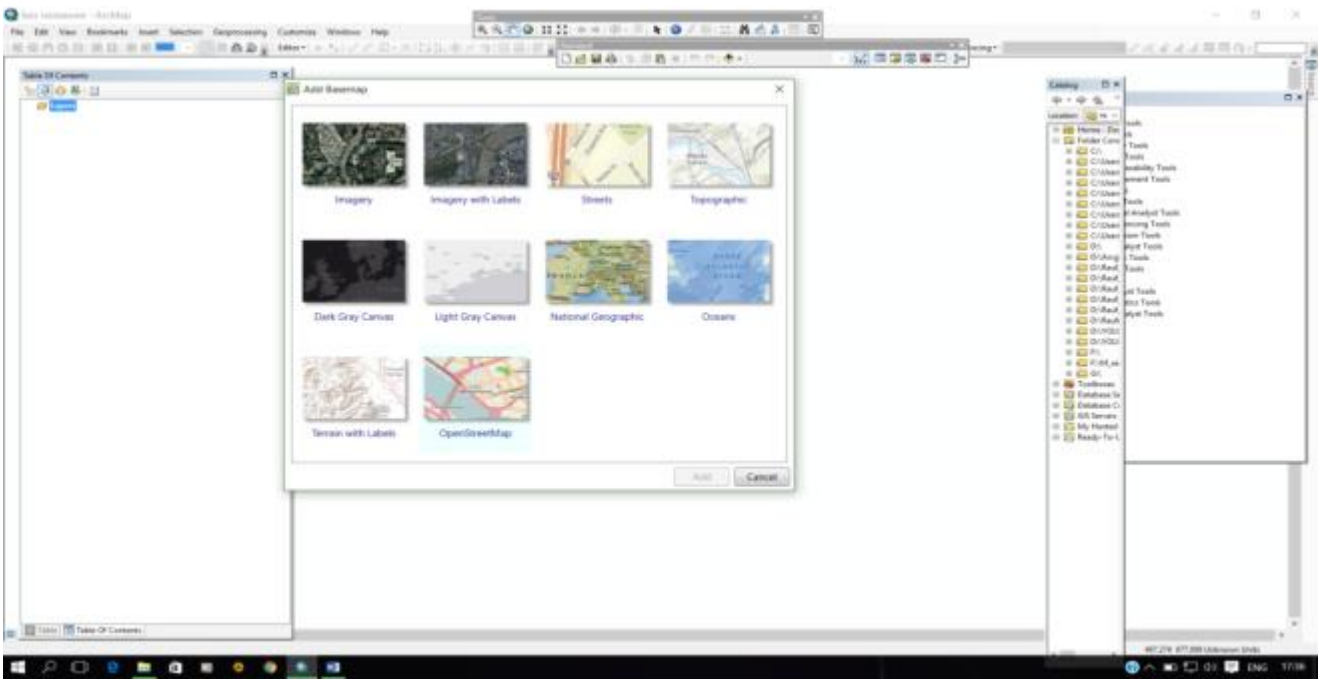

Figure 4.15: ArcMap basemap options

We zoom down the view so we can clearly see the two cities area (in current example Hamburg-Berlin) we are interested to acquired the road for (Figure 4.16).

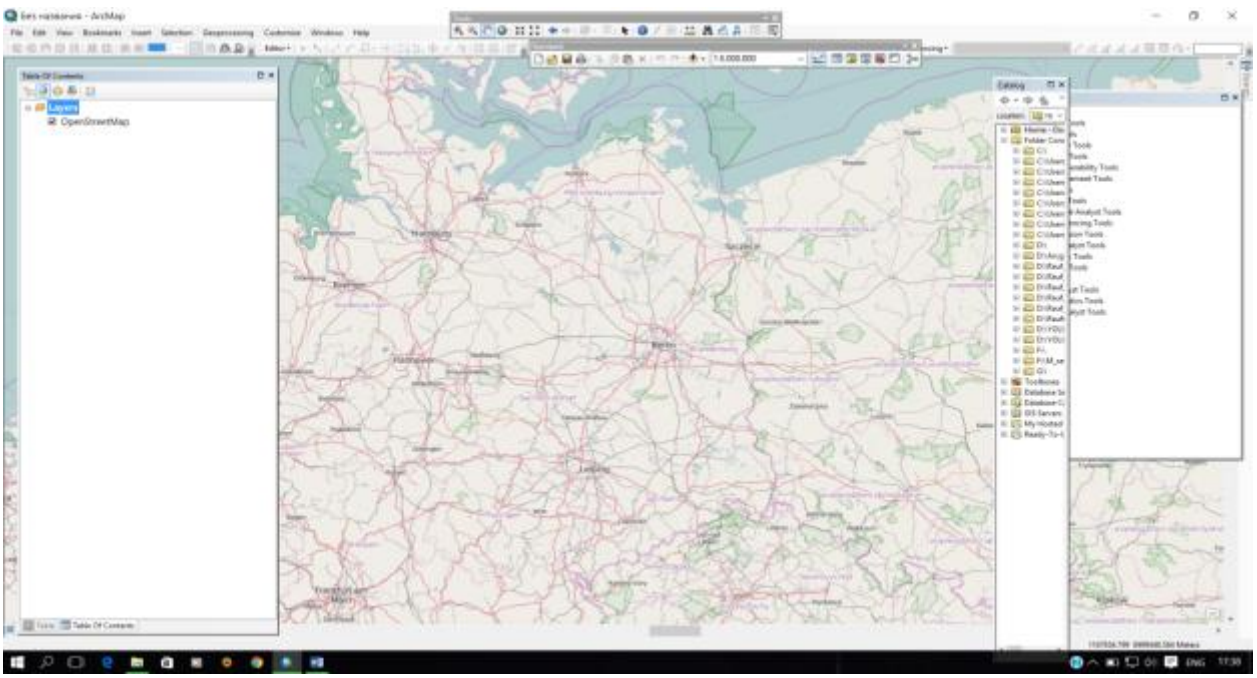

Figure 4.16: Hamburg and Berlin cities in ArcMap

In the next step we have to create the roads shapefile. We select *New* and then *Shapefile* and then *Start Editing (*Figure 4.17).

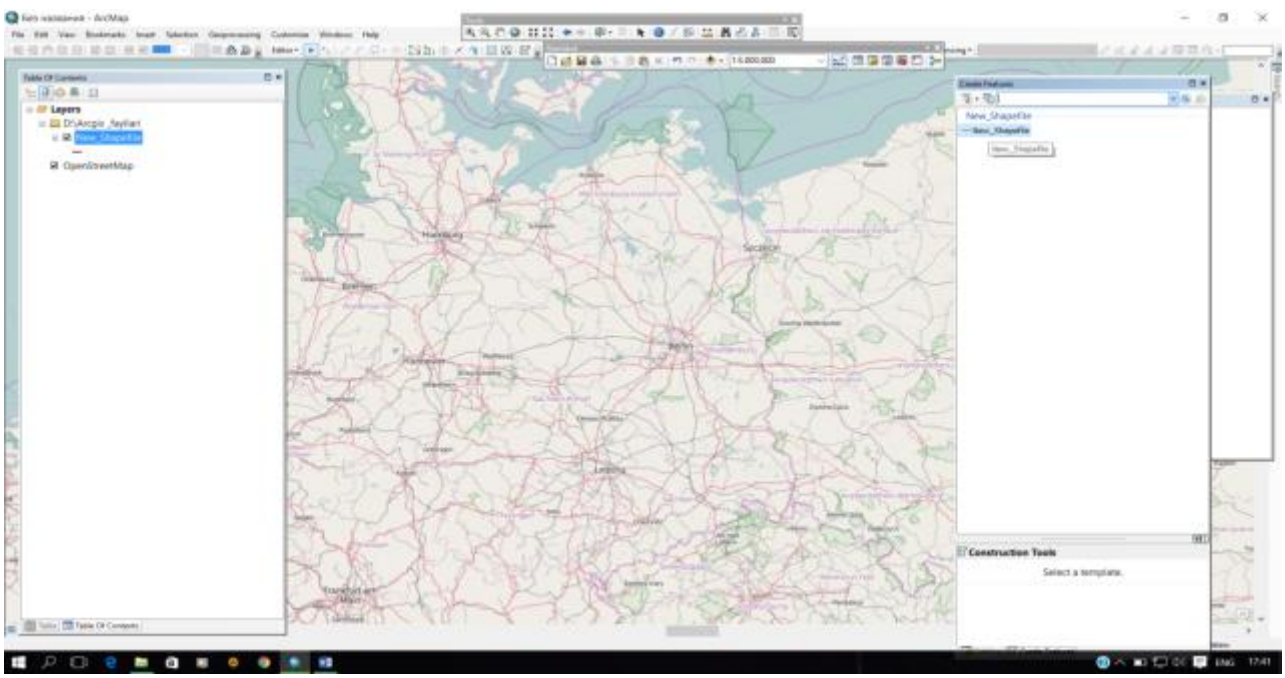

Figure 4.17: Creating a new Shapefile in Layers

By selecting *Create Features* we draw/fixate select the road (Figure 4.18).

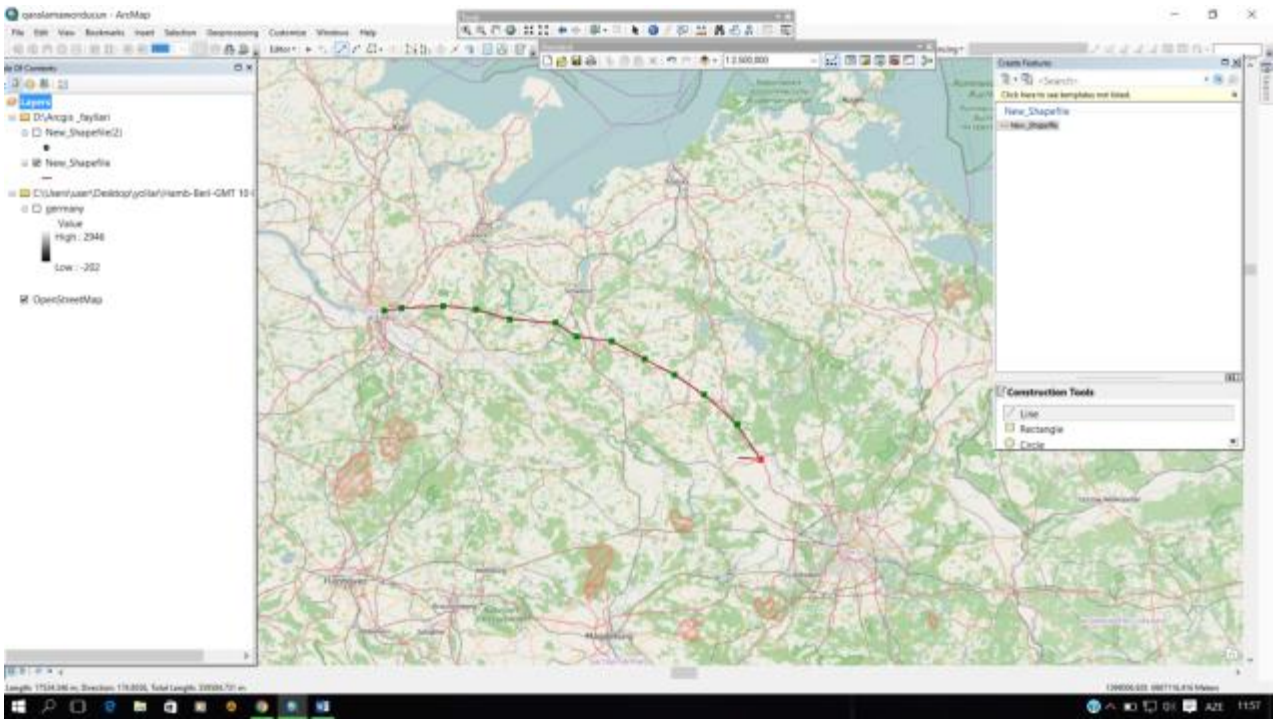

Figure 4.18: Fixating the road on ArcMap

Finally, we select the option *Finish Sketch*.

Further, we again create a Shapefile, but this time we specify it to be of point type. It is needed to specify in how many meters (the distances between the points) do we need to have the points and we give the value 30 meters (Figure 4.19).

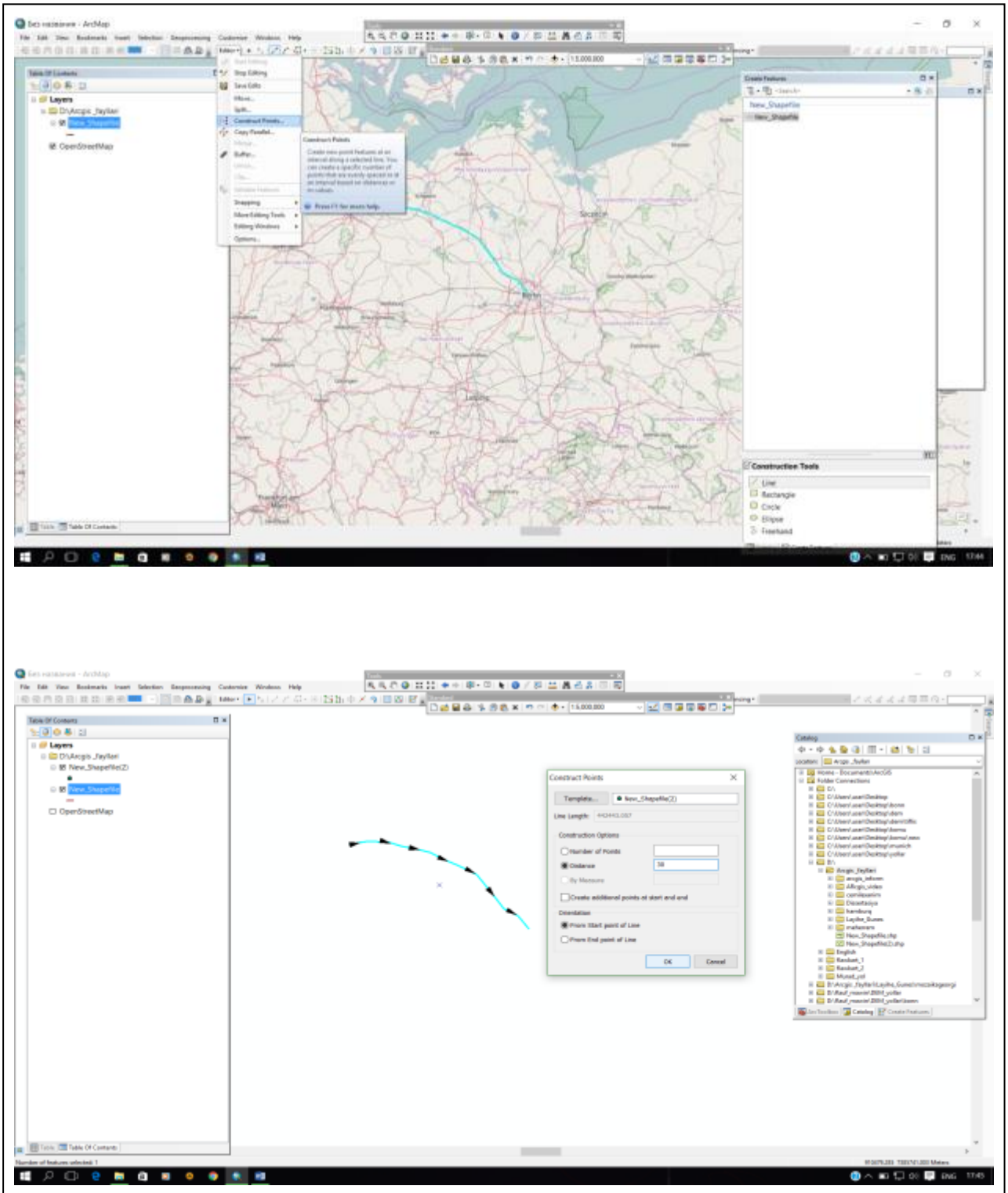

Figure 4.19: Creation of points and specification of distances

Then, we open right click on the newly created Shapefile select *Add Field*. We call the new field Lat (which stands for Latitude).We do the same operation to create Lon and Alt (which stands for elevation values) fields. Then, we select the added fields, and by right click open dropdown menu and select *Calculate Geometry* (Figure 4.20).

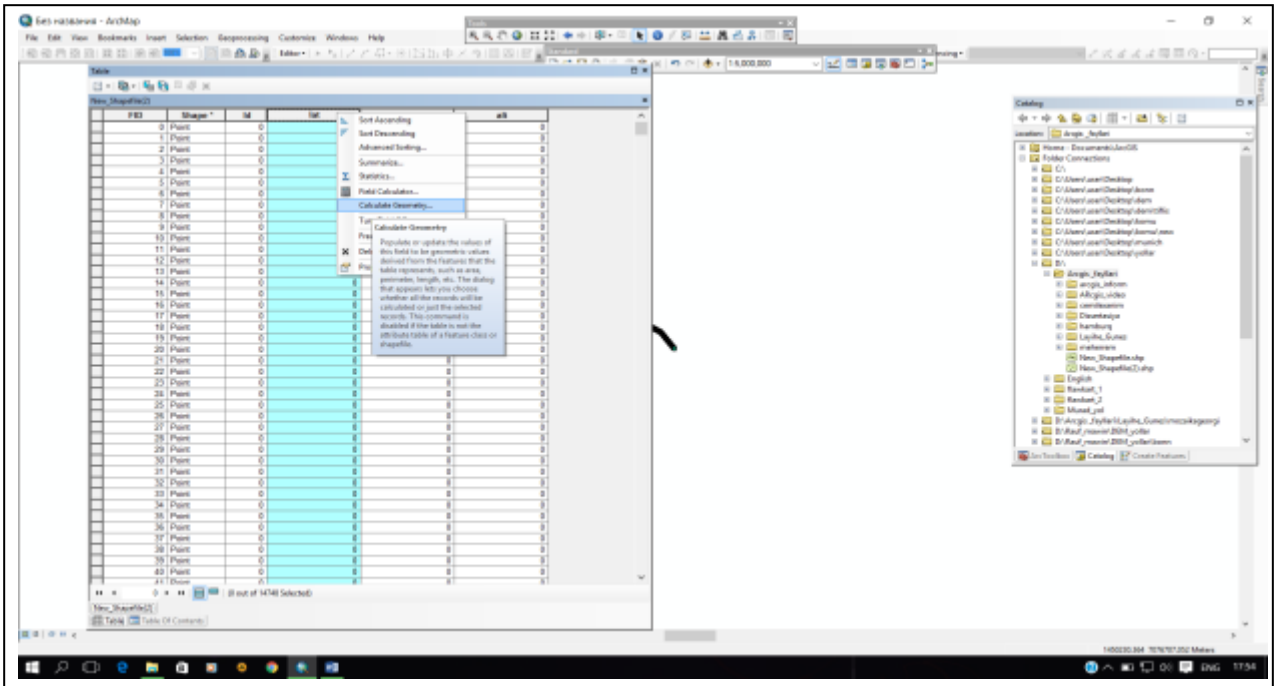

Figure 4.20: Retrieving latitude and longitude on ArcMap

For retrieving elevations data, we call corresponding previously created DEM of the territory to the ArcMap and select *Add Surface Information* as shown in Figure 4.21.

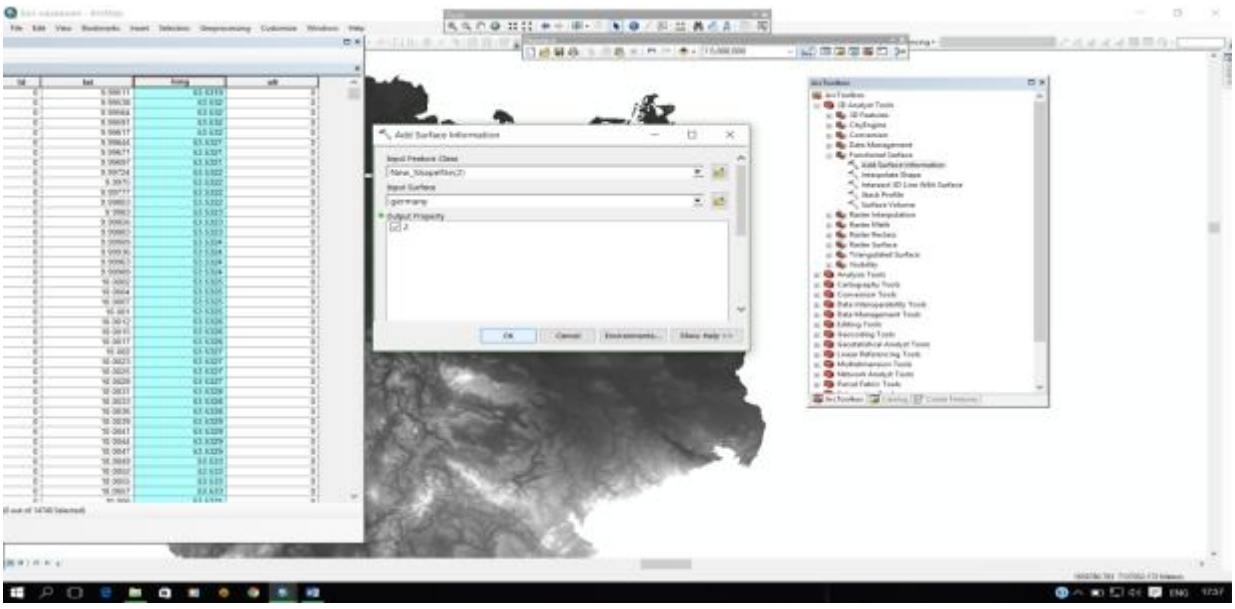

Figure 4.21: Extracting the elevations data from DEM

When all the necessary data (latitude, longitude and elevation) is obtained, the data is to be saved as .xlsx extension, so that it can be used as input data file to the mathematical model of motion.

4.2.4 Visualization

In ArcScene, combining the obtained previously DEM of the terrain, the shapefile representing the road on the DEM and the .xlsx output file obtained from the mathematical model of motion allows to carry out the visualization scene. It is possible to add various Viewers to the visualization scene in order to achieve different points of view. In Figure 4.22 below its shown the final visualization of solar car motion along the road Baku-Shamakhi (start of motion: June 22, GMT 10:00):

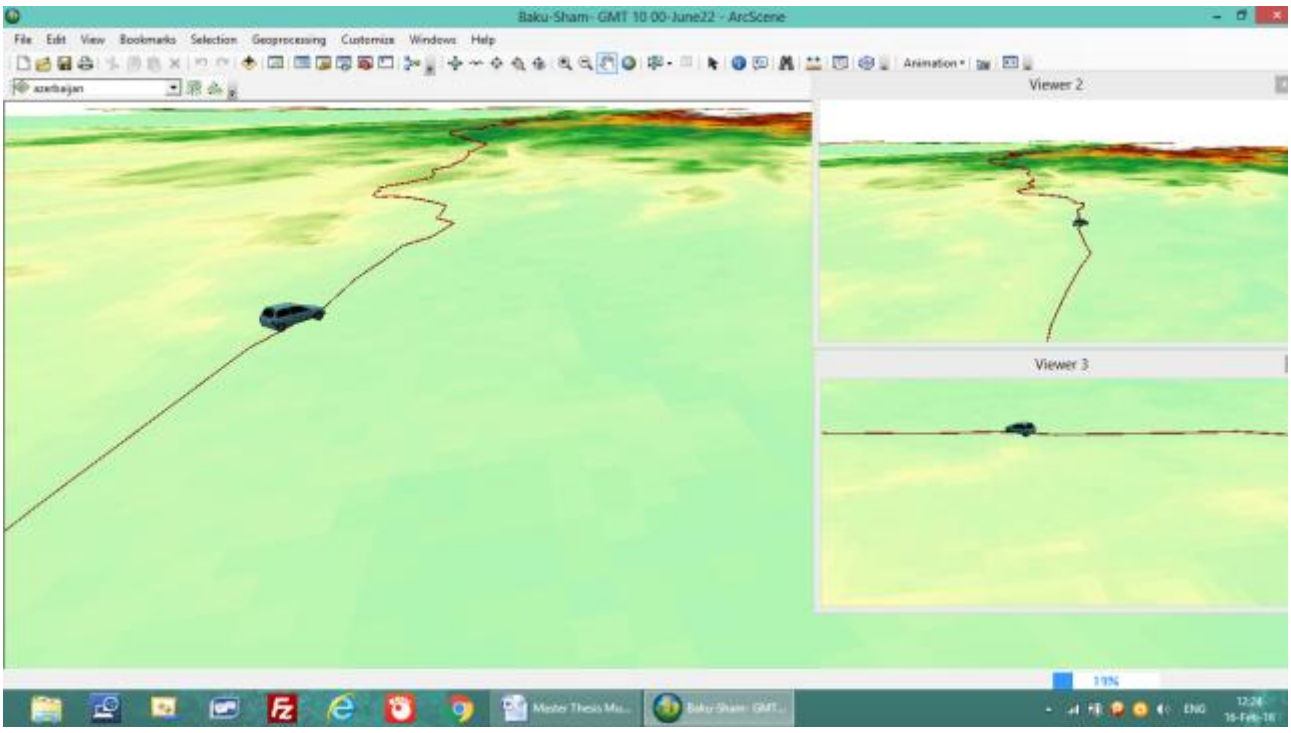

Figure 4.22: Visualization of solar car motion on the road Baku-Shamakhi (start of motion: June 22, GMT 10:00)

The visualizations for the solar car motions for the roads Hamburg-Berlin and Zakatala-Tbilisi with start of motion times (March 21, GMT 10:00) and (June 22, GMT 05:00) respectively, is given in the Figure 4.23 and 4.24 below.

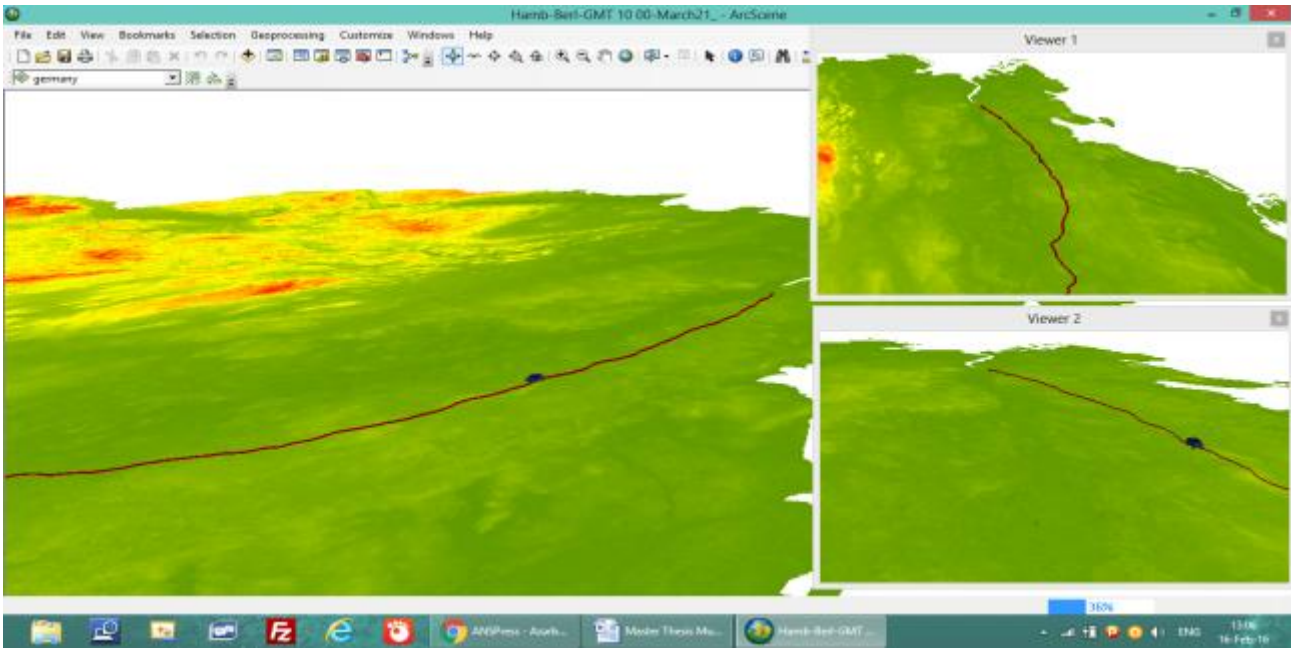

Figure 4.23: Visualization of solar car motion on the road Baku-Shamakhi (start of motion: March 21, GMT 10:00)

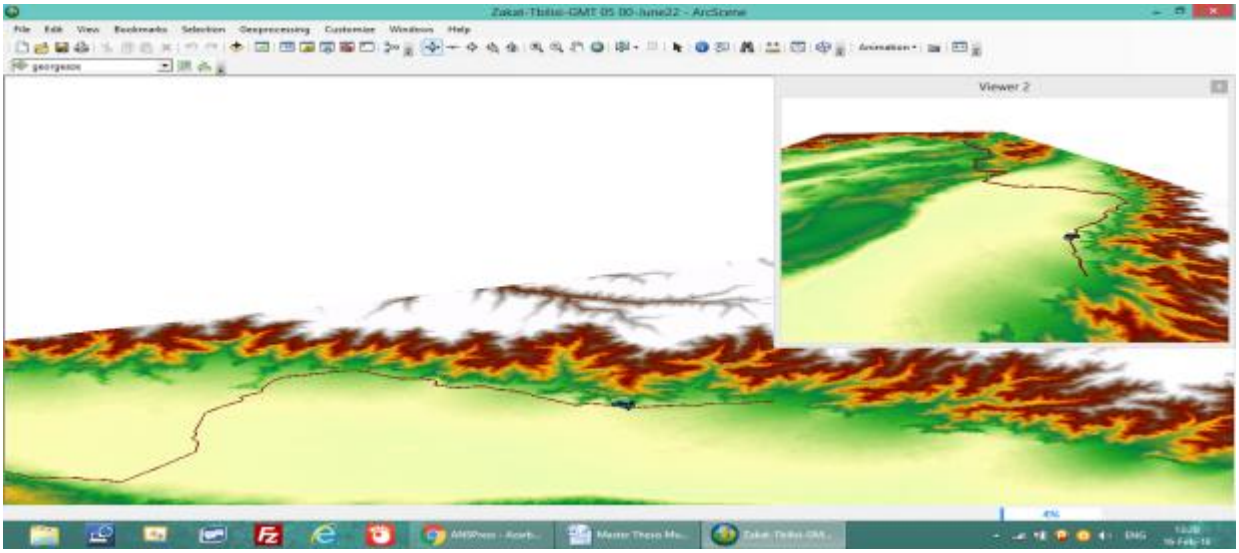

Figure 4.24: Visualization of solar car motion on the road Zakatala-Tbilisi (start of motion: June 22, GMT 05:00)

CHAPTER 5

CONCLUSIONS

Apparently, now the world is at the beginning stage of transition from cars with internal-combustion engine to electro mobiles working by using hybrid energy - solar and accumulator. Evidently, this transition will happen quickly and in next decade we will witness the mass production of hybrid cars and disappearance of conventional cars. There are two main reasons for such an optimistic prognosis. First, the pollution of environment by exhaust gases emitting from conventional cars becomes tragically dangerous for human life. Second, year after year the photoelectric cells with high efficiency are discovered and their widely use becomes available. The main feature of solar car working only with solar energy, which distinguishes it from conventional car, is the reality that the origin of driving energy is located outside the car and cannot be controlled by user. Therefore, the problem of optimal energy consumption becomes very important for management of solar car. In turn, the optimal energy consumption requires knowledge about solar energy potential. The amount of solar energy falling onto the panel of solar car along the road mainly depends on 1) time of year; 2) weather condition (cleanest and turbidity of atmosphere); 3) geographical location of road; 4) road characteristics (tilt, surrounding relief). Except for the “weather condition”, the effect of other parameters is deterministic and can be taken into account exactly. Until now, the roads had been constructed under the requirements which did not include “more sunlight” and it doesn’t seem realistic the reconstruction of roads to make them “more sunny”. Therefore, it is important the assessment of “solar energy potential” of the existing roads.

5.1 Essence of the model and results.

The “solar radiation model” developed in current work calculates the amount of solar radiation falling onto road surface (i.e. onto solar car panel) for so called “standard atmosphere” (clear atmosphere with optical thicknesses = 0.3) at any moment of time and any point of road. As a study case, the model is applied to three chosen roads: 1) Hamburg-Berlin; 2) Baku-Shamakhi; 3) Zakatala-Tbilisi. The road Hamburg-Berlin is located upward North about 12^0 as against second and third roads and therefore its solar energy potential is differing than others.

Knowledge of solar energy falling onto panel of car allows us to determine the law of motion (i.e. the dependences on time of course made and velocity) by solving the differential equation of motion. In present work the differential equation of motion which takes into account all the forces acting to the car, was exactly solved for straight-line road. The analyses of solution show that the features of motion are determined by alignment of driving, gravity, reaction and resistance forces. In general case, the curved road is presented as a chain of straight-line segments and solution obtained for straight-line road is applied to an each segment. The Cartesian coordinate system with origin at the Earth centre is used which allows taking into account the Earth curvature and consider the roads connecting starting and terminating points on the Earth surface regardless of distance between them. Thus, presented here model is a composition of “solar radiation model” and “model of car motion” and is sufficiently universal.

The calculations on the model for the chosen roads show that the features of motion depend on 1) time of year and geographical location of road, which determine the flow of solar energy and thereby the driving force; 2) road tilt, which determine the reaction force; 3) car technical characteristics which determine the resistance force. In study cases the technical characteristics (coefficients of aerodynamic and

rolling resistances) for solar car “PowerCore-SunCruiser” are used and simulation of car motion is provided by solving the differential equation of motion. Using the simulated data (time, latitude, longitude, altitude) the 3D visualization of car is performed in ArcGIS.

5.2 Further improvement of the model

The blind spot of the model is its impossibility to exactly evaluate the random events “weather condition”. The model can be improved by entering the random quantities- atmosphere turbidity and cloudiness parameters from prognostic or real time georeferenced satellite data for every considered case. Additionally, during the travelling period the update of the data can be processed and the necessary corrections be made.

The model can be expanded for the case when hybrid (solar and accumulator) energy consumption is used.

The model presented here can also be applied for solution of various optimal control problems for solar cars, for instance, such as: minimising the travel time; minimising the energy consumption from accumulator; minimising both the travel time and energy simultaneously.

Additionally, the road signs restricting the car motion can be easily taken into account in this model.

Among the input parameters of model there are the tilt and shadow characteristics at the points of road. For the roads those characteristics are determined by using 3D digital elevation model of the territory. Thus, for an each road the determination of those characteristics must be carried out and a data base needs to be created. The information from this database will serve for development of various optimal control problems for the certain type of solar cars with fixed controlled parameters. The program package which realizes this model will be an important part of navigation

system of solar cars and will implement the optimal management (choosing the time of start of motion, speed which must be kept along the road, instant of time of arriving to the mountain pass, where huge amount of solar radiation or fully charged accumulators are needed, choosing the time of start using the accumulators and their charging, and etc.) of solar cars.

REFERENCES

[1] UDO BACHHIESL. MEASURES AND BARRIERS TOWARDS A SUSTAINABLE ENERGY SYSTEM. 19th World Energy Congress – Youth Symposium. Graz University of Technology. Institute of Electricity Management and Energy Innovation

[2] V. Jurić, D. Županović. ECOLOGICAL IMPACTS OF DIESEL ENGINE EMISSIONS. Human - Transport Interaction Review, 2012

[3] International Energy Agency (2011) *Solar Energy Perspectives*, 9 rue de la Fédération 75739 Paris Cedex 15, France: OECD/IEA.

[4] T.S. Ravi. Technology development for high-efficiency solar cells and modules using thin (<80 μm) single-crystal silicon wafers produced by epitaxy. Subcontract Report, (2013) NREL/SR-5200-58593

[5] Liu, Piao. Heterojunctions and Schottky Diodes on Semiconductor Nanowires for Solar Cell Applications (2010). University of Kentucky, Doctoral Dissertations.

[6] Haspert, Lauren C; Gillette, Eleanor; Lee, Sang Bok; and Rubloff, Gary W. Perspective: hybrid systems combining electrostatic and electrochemical nanostructures for ultrahigh power energy storage Energy and Environmental Science, 6, 2578 (2013). [DOI:10.1039/c3ee40898a]

[7] Sioe Yao Kan, Verwaal M., Broekhuizen H. The use of battery-capacitor combinations in photovoltaic powered products. Journal of Power Sources, (2006), 162(2), 971-974

[8] Solar Energy Development Programmatic EIS (2012) *Solar Cells*, Available at:*http://solareis.anl.gov/guide/solar/pv/index.cfm* (Accessed: 16 February 2016).

[9] Ranjeet Singh, Manoj Kumar Gaur, Chandra Shekhar Malvi. A Study and Design Based Simulation of Hybrid Solar Car. International Journal of Emerging Technology and Advanced Engineering. ISSN 2250-2459, ISO 9001:2008 Certified Journal, Volume 3, Issue 1, January 2013

[10] Yogesh Sunil Wamborikar, Abhay Sinha. Solar Powered Vehicle. Proceedings of the World Congress on Engineering and Computer Science 2010 Vol II WCECS 2010, October 20-22, 2010, San Francisco, USA

[11] SolarCar Team of Bochum University of Applied Sciences (2016) *SolarCar Team,*Available at: *http://www.bosolarcar.de* (Accessed: 16 February 2016).

[12] R.Gardashov, M.Eminov. Modelling of the Solar Energy Falling onto the Panel of Solar Car and Web-Aplication for Simulating the Car Motion along the Road, 31st European Photovoltaic Solar Energy Conference and Exhibition,p. 2253 – 2256, ISBN: 3-936338-39-6, DOI: 10.4229/EUPVSEC20152015-5BV.2.25

[13] Emegen G., Gokhan K., Erdogmus F., Gardashov R. The determination of sunglint location on the ocean surface by observing from the geostationary satellites. *Terrestrial, Atmospheric and Oceanic Sciences (TAO), Vol*. 17, No.1, 253-261, 2006

[14] Gardashov R .H, Eminov M.Sh. 2013, The Determination of the Sun Glint Geographical Coordinates by Observing from Meteosat 9 Satellite. *Proceedings VII International Conference "Current Problems in Optics of Natural Waters",* 10-14 September. St.-Petersburg. 154-158.

[15] Gardashov R.H.,Eminov M.Sh. The determination of the sunglint location and its characteristics by observing from Meteosat 9 satellite. *International Journal of Remote Sensing,p.*2584- 2598.DOI**:**10.1080/01431161.2015.1042119

[16] W.Zhao, J.Liu, J.Xiao. Two methods of urban road area extraction based on Google Earth. Chinese Journal of Environmental Engineering 07/2015; 9(7):3400-3404.

[17] Gang Xu, Dawei Zhang, Xinyu Liu.Road extraction in high resolution images from Google Earth.ICICS'09 Proceedings of the 7th international conference on Information, communications and signal processing, pages 556-560.EEE Press Piscataway, NJ, USA ©2009.ISBN: 978-1-4244-4656-8

[18] Bose, Bimal K. (2006). Power Electronics and Motor Drives : Advances and Trends. Academic Press.

[19] Harris Benson. (1991) University physics. John Wiley&Sons,Inc.

[20] Taylor, John R. (2005). *Classical Mechanics*. University Science Books.

[21] G. Falkovich (2011). Fluid Mechanics (A short course for physicists). Cambridge University Press. ISBN 978-1-107-00575-4.

[22] Hibbeler, R.C. (2007). Engineering Mechanics: Statics & Dynamics (Eleventh ed.). Pearson, Prentice Hall.

APPENDIX A

FORTRAN CODE PROGRAM FOR SIMULATION OF SOLAR CAR MOTION ON THE ROAD

```
C      MAIN PROGRAAM
C      PROGRAMME for SIMULATION OF SOLAR CAR MOTION ALONG THE ROAD
c      Calculation of time {ti} when Solar car are passing from point Mi(xi,yi,zi) of road.
c      On the massive {ti,Mi) the visualiation of Solar car motion is carred out.
c     APhiD(72),AGamSh(72) - massive of Shadow function GamSha=GamSh(Phi)  (unite: degrees)
with ptep 5         c
          use msimsl
          Parameter(NM=3904)
          Parameter(CarMas=340.,Cx=0.16,Crr=0.0025,Cef=0.3,Eef=0.9)
          Parameter(Key=0,Imonth=6,Iday=22,Ihour=10,Iminut=0,Isec=0)
          Parameter(airDen=1.22,Scross=1.6,Spanel=3.)
          Parameter(V0_kmh=0.)
c
c     "Spanel" - area of panel [m2]  ; "CarMas"- mass of Car [kg] ; "Cef"-[nondemensional]
coefficient of efficiency (Solar power to driving force
c      airDen=1.2041 [kg/m3]- air density
c     Scross=2. [m2]- area of crosssection of car
c     "Cx" - [nondemensional] coefficient of air resistance;
c     "Crr - [nondemensional] coefficient of rolling resistance;
c     "Eef" - [nondemensional] coefficient of effisiency of electrical engine;
c      "V0_kmh" - [km/h] initial speed;
c      "Imonth_0=3,Iday_0=21,Ihour_0=7,Iminut_0=00,Isec_0=00"- initial moment of time of
motion;
c           "WsolP"- [1/m2] Solar energy fallin gonto panel ;
c      massives AlatM(NM),AlonM(NM),AhM(NM) - geographical coordinaters of point Mi on the
road i=1,...NM ;
c      massive AT(i) =ti - instant of times when car is passing from point Mi. The quantity {ti} is
calculated by solution differential exactiteration;
c      massive AV(i) - speed of car  at the moment ti (or at the Mi);
c      massives  ADis(i)- distance between Mi and Mi+1; ADisL(i)- distance between Mi and M1
c      Ppanel- power of electrical energy output by panel [Ppanel]=Watt
c-----------------------------------------------------------------------------------------------------------------
-------------------
c
           DOUBLE PRECISION AlonM(NM),AlatM(NM),AhM(NM)
          DOUBLE PRECISION LatM1,LonM1,hM1,LatMn,LonMn,hMn
            DOUBLE PRECISION LatMD,LonMD,LatM,LonM,hM
          DOUBLE PRECISION Teq,TG0,Tt,t0,V0,t_end,V_end,S_end
          DOUBLE PRECISION pi,Del
```

```
      DOUBLE PRECISION tau,pCloud,WsolP,Wsol_panel
c     Adis(i) - distance between road points Mi and Mi+1
c
      OPEN(10,FILE='ti,Vi.DAT')
      OPEN(11,FILE='ti,Si.DAT')
      OPEN(4,FILE='ti,SiC.DAT')
      OPEN(5,FILE='Si,alfaDi.DAT')
      OPEN(6,FILE='ti,hMi.DAT')
      OPEN(9,FILE='ti,Ppanel.DAT')

c-------------------------------------------------------------------------Optical parameters of ATMOSPHERE
          tau=0.3
      pCloud=0.
c-------------------------------------------------------------------------------------------------
c Reading  from FILE='Lat,Lon,Alt(Baku-Shemaxi).DAT') - (lat,lon,alt) along the road BAKU-
SHEMAXI
c
c     OPEN(1,FILE='Lat,Lon,Alt(Hamburg_Berlin).DAT')
      OPEN(1,FILE='Lat,Lon,Alt(Baku-Shemaxi).DAT')
c     OPEN(1,FILE='Lat,Lon,Alt(Zakatala_Tbilisi).DAT')
c     OPEN(2,FILE='Lat,Lon,Alt,W(Hamburg_Berlin).DAT')
      OPEN(2,FILE='Lat,Lon,Alt,W(Baku-Shemaxi).DAT')
c     OPEN(2,FILE='Lat,Lon,Alt,W(Zakatala_Tbilisi).DAT')
      OPEN(7,FILE='INF.DAT')
c-------------------------------------------------------------------------------------------------
      pi=3.141592653589793
      Del=pi/180.
c-------------------------------------------------------------------------------------------------
    V0=V0_kmh*0.2777777
      Do 11 i=1,NM
      Read(1,*) RlatMD,RlonMD,hMi
c
      AlatM(i)=RlatMD*Del
      AlonM(i)=RlonMD*Del
      AhM(i)=hMi
c     AhM(i)=40.
c     AlatM(NM-i+1)=RlatMD*Del
c     AlonM(NM-i+1)=RlonMD*Del
c     AhM(NM-i+1)=hMi
c
      Write(2,54) AlatM(i)/Del,AlonM(i)/Del,AhM(i)
 11   Continue
 54   Format(3F12.6)
      CALL MotLaw(t_end,V_end,S_end,CarMas,Cx,Crr,Cef,airDen,
      *Scross,Spanel,P_panel,V0,t0,LatM1,LonM1,hM1,LatMn,LonMn,hMn,alfaDi
   *,tau,pCloud,Wsol_panel,dis_M1Mn)
      T_M1Mi=T_M1Mi+t_end
      Dist_M1Mi=Dist_M1Mi+S_end
      DisC_M1Mi=DisC_M1Mi+dis_M1Mn
c
```

```
          V0=V_end
          t0=T_M1Mi
          ti_hour=1.*Ihour+(T_M1Mi-t_begin)/3600.
c         IF(abs(alfaDi).gt.29) alfaDi=29.*abs(alfaDi)/alfaDi
      write(11,52) ti_hour,Dist_M1Mi/1000.
          write(4,52) ti_hour,DisC_M1Mi/1000.
          write(10,52) ti_hour,V_end/0.277777
          write(5,52) Dist_M1Mi/1000.,alfaDi
          write(6,52) ti_hour,AhM(i)
          write(9,52) ti_hour,P_panel
c
  12  Continue
      t0_begin=1.*Ihour
          Time_Terminal=ti_hour
          ITime_Terminal_hour=int(Time_Terminal)
          ITime_Terminal_minute=int((Time_Terminal-int(Time_Terminal))*60.)
          Time_travel=ti_hour-t0_begin
          ITime_travel_hour=int(Time_travel)
          ITime_travel_minute=int((Time_travel-int(Time_travel))*60.)
      Vmean=(Dist_M1Mi/1000.)/Time_travel
          Write(7,153) t0_begin,Time_Terminal, Dist_M1Mi/1000.,Vmean,
     *ITime_Terminal_hour,ITime_Terminal_minute
     *,ITime_travel_hour,ITime_travel_minute,P_panel
c-----------------------------------------------------------------------------------------------------
 9999   CONTINUE
      Stop
      End
C*********************************************************************
          SUBROUTINE MotLaw(t_end,V_end,S_end,CarMas,Cx,Crr,Cef,airDen,
          *Scross,Spanel,P_panel,V0,t0,LatM1,LonM1,hM1,LatMn,LonMn,hMn,alfaD
     *,tau,pCloud,Wsol_panel,dis_M1Mn)
c
          DOUBLE PRECISION  SIMPS,F3,FtD3p,FtD3n,FsD3p,FsD3n
          DOUBLE PRECISION LatM1,LonM1,hM1,LatMn,LonMn,hMn,Delh
          DOUBLE PRECISION t_end,V_end,S_end
          DOUBLE PRECISION xM1,yM1,zM1,xMn,yMn,zMn
          DOUBLE PRECISION r0xM1,r0yM1,r0zM1,r0xMn,r0yMn,r0zMn
          DOUBLE PRECISION lxM1,lyM1,lzM1,l_modM1
          DOUBLE PRECISION mxM1,myM1,mzM1,m_modM1
          DOUBLE PRECISION nxM1,nyM1,nzM1,n_modM1,r0n,r0l
          DOUBLE PRECISION r0xl_mod,r0xl_x,r0xl_y,r0xl_z
          DOUBLE PRECISION V0,Vk,aa,bb,cc,Vroot,pp,qq,DelV
          DOUBLE PRECISION VVk,SqPP,t0,V1,V2,V3
          DOUBLE PRECISION tau,pCloud,Wsol_panel
          EXTERNAL FV
c    "CarMas"- mass of Car [kg] ;
c     airDen=1.2041 [kg/m3]- air density
c     Scross=2. [m2]- area of crosssection of car
c     "Cx" - [nondemensional] coefficient of air resistance;
c     "Crr" - [nondemensional] coefficient of rollong resistance;
```

```
c     "V0" - [km/h] initial speed; "Vmax_km/h" - [km/h] maximal speed;
c     LatM1,LonM1,hM1,LatMn,LonMn,hMn - geographical coordinaters of point initial point M1
and end point Mn ;
c      ti - instant of times when car is passing from point Mi . The quantity {ti} is calculated by
integration;
c      Vi - speed of car  at the moment ti (or at the Mi);
c      massives  Dis_i- distance between Mi and Mi+1;
c-----------------------------------------------------------------------------------------------------------------
------------------
           OPEN(8,FILE='Infor.DAT')

          c-----------------------------------------------------------------------------------------------------------
---------------------------          g=9.8
c                  g=9.8 [m/sec2] gravitational constant
c
c                                    Reath=6371000 meter- Volumetric mean radius of Earth
              REarth=6371000.
          pi=3.141592653589793
          del=pi/180.
c
          Cx0=Cx/CarMas
          Delh=hMn-hM1
          r1=REarth+hM1
          rn=REarth+hMn
          xM1=r1*dcos(LatM1)*dcos(LonM1)
          yM1=r1*dcos(LatM1)*dsin(LonM1)
          zM1=r1*dsin(LatM1)
          xMn=rn*dcos(LatMn)*dcos(LonMn)
          yMn=rn*dcos(LatMn)*dsin(LonMn)
          zMn=rn*dsin(LatMn)
          dis_M1Mn=REarth*dsqrt(((xMn-xM1)/REarth)**2+((yMn-yM1)/REarth)**2
          *+((zMn-zM1)/REarth)**2)
          sin_alfa=Delh/dis_M1Mn
          alfa=asin(sin_alfa)
          alfaD=alfa/del
c         IF(dis_M1Mn.gt.300.) GOTO 8
c-------------------------------------------------------------------------------
c
c          xM1,yM1,zM1 and xMn,yMn,zMn -  coordinates of point M1 and Mn with coordinat center
"O" is Earth center ("central coordinate system"),
c       "OX" - on equatorial plane with direction longitude=0 ; "OY" - on equatorial plane with
direction longitude=90 ;
          rModM1=dsqrt(xM1**2+yM1**2+zM1**2)
          rModMn=dsqrt(xMn**2+yMn**2+zMn**2)
      r0xM1=xM1/rModM1
          r0yM1=yM1/rModM1
          r0zM1=zM1/rModM1
          r0xMn=xMn/rModMn
          r0yMn=yMn/rModMn
          r0zMn=zMn/rModMn
```

```
          r0M1_mod=dsqrt(r0xM1**2+r0yM1**2+r0zM1**2)
          r0Mn_mod=dsqrt(r0xMn**2+r0yMn**2+r0zMn**2)
c
          Write(8,57) r0xM1,r0yM1,r0zM1,r0M1_mod
     *,r0xMn,r0yMn,r0zMn,r0Mn_mod,alfaD,dis_M1Mn,Delh
  57      Format
     *('r0xM1='F12.8,5x,'r0yM1='F12.8,5x,'r0zM1='F12.8,5x,'rModM1='F12.8
     *,/,
     *'r0xMn='F12.8,5x,'r0yMn='F12.8,5x,'r0zMn='F12.8,5x,'rModMn='F12.8
     *,/,'alfaD='F12.8,5x,'dis_M1Mn='F18.4,5x,'Delh='F16.2)
c-----------------------------------------------------------------
c
          lxM1=(xMn-xM1)/dis_M1Mn
          lyM1=(yMn-yM1)/dis_M1Mn
          lzM1=(zMn-zM1)/dis_M1Mn
          l_modM1=dsqrt(lxM1**2+lyM1**2+lzM1**2)
c
c
          r0xl_x=r0yM1*lzM1-r0zM1*lyM1
          r0xl_y=-r0xM1*lzM1+r0zM1*lxM1
          r0xl_z=r0xM1*lyM1-r0yM1*lxM1
          r0xl_mod=dsqrt(r0xl_x**2+r0xl_y**2+r0xl_z**2)
c
      mxM1=r0xl_x/r0xl_mod
          myM1=r0xl_y/r0xl_mod
          mzM1=r0xl_z/r0xl_mod
          m_modM1=dsqrt(mxM1**2+myM1**2+mzM1**2)
      nxM1=lyM1*mzM1-lzM1*myM1
          nyM1=lzM1*mxM1-lxM1*mzM1
          nzM1=lxM1*myM1-lyM1*mxM1
          n_modM1=dsqrt(nxM1**2+nyM1**2+nzM1**2)
          r0n=r0xM1*nxM1+r0yM1*nyM1+r0zM1*nzM1
          r0l=r0xM1*lxM1+r0yM1*lyM1+r0zM1*lzM1
c
          aa=Cx0*airDen*Scross/2.
          bb=-Crr*g*r0n-g*r0l
c         bb=ISIGN*g*sin_alfa-Crr*g*cos(alfa)
c-----------------------------------------------------------------
      Call Solar
          *(t0,latM1,lonM1,hM1,ZeSunD,AzSunD,tau,pCloud
     *,nxM1,nyM1,nzM1,Wsol_panel)
c
          P_panel=Cef*Spanel*Wsol_panel
C  Conversion from Joule to Watt.hour:  E_poten_Watt.hour=E_poten*2.777778E-4
c-----------------------------------------------------------------
      cc=P_panel/CarMas
c
          Write(8,72) aa,bb,cc
  72  Format('aa='E12.6,5x,'bb='E12.6,5x,'cc='E12.6)
c
```

```
c      ---------------------------------------  Cubic equation coefficients: pp=-(bb/aa) and  qq=-(cc/aa)
and finding roots: z1, z2, z3
     pp=-(bb/aa)
          qq=-(cc/aa)
          D3_discriminant=-(qq**2/4.+pp**3/27.)
          Call Cubic(pp,qq,z1r,z1i,z2r,z2i,z3r,z3i)
          IF(D3_discriminant.lt.0.) Vroot=amax1(z1r,z2r,z3r)
          IF(D3_discriminant.gt.0.) Vroot=amax1(z1r,z2r,z3r)
          V_terminal velocity=Vroot/0.2777777
          write(8,58) pp,qq,D3_discriminant,z1r,z1i,z2r,z2i,z3r,z3i,
     *V_terminal velocity,Vroot,V0
          V1=z1r
          V2=z2r
          V3=z3r
c
c         ---------------------------------------------------------------------------------------------
c                                                                  1 km/h = 0.2777777 m/sec.
     DelV=abs(Vroot-V0)/10000.
c
          Distk=0.
          k=1
          t00=0.
c
8888  Continue
     IF(Vroot.gt.V0) Vk=V0+DelV*k
          IF(Vroot.lt.V0) Vk=V0-DelV*k
c
c     IF(Vroot.gt.V0) Vk=V0+DelV/sqrt(k+1.)
c         IF(Vroot.lt.V0) Vk=V0-DelV/sqrt(k+1.)
c
          DelVV=DelV/10.
          NV1Vk=int(dabs(Vk-V0)/DelVV)
          If(NV1Vk.lt.4) NV1Vk=4
c    ---------------------------------------------------------------------------------------------------------------
-----------
c         General case: all forces taken into account [al , be, ce  is not 0 ] => [pp , qq  is not 0 ]

     IF(D3_discriminant.lt.0.) tkf=-FtD3n(V0,Vk,Vroot,pp)/aa
     IF(D3_discriminant.gt.0.) tkf=-FtD3p(V0,Vk,V1,V2,V3)/aa
     IF(D3_discriminant.lt.0.) Distkf=-FsD3n(V0,Vk,Vroot,pp)/aa
     IF(D3_discriminant.gt.0.) Distkf=-FsD3p(V0,Vk,V1,V2,V3)/aa
c    ---------------------------------------------------------------------------------------------------------------
-----------
          tk=tkf
          Del_tk=tk-t00
          sk=Vk*Del_tk
          Distk=Distk+sk
          hMk=Distk*sin_alfa
          IF(Distk.ge.dis_M1Mn) Goto 8
c         IF(Distkf.gt.dis_M1Mn) Goto 8
```

```
          Ddisk=dis_M1Mn-Distk
          IF(dabs(Vk-Vroot).lt.0.27777777) then
          tdk=Ddisk/Vroot
          tk=tk+tdk
          Distk=Distk+Ddisk
          goto 8
          EndIf
          t00=tk
          k=k+1
c         IF(k.ge.10000) Goto 8
          Goto 8888
  8   Continue
          V_end=Vk
          t_end=tk
          S_end=Distk
c      IF(D3_discriminant.lt.0.) Distkf=-FsD3n(V0,Vk,Vroot,pp)/aa
c      IF(D3_discriminant.gt.0.) Distkf=-FsD3p(V0,Vk,V1,V2,V3)/aa
C-------------------------------------------------------
c
  52  Format(E12.6,F12.6)
  59  Format
     *('tk [sec]='F16.6,5x,'Vk [km/h]='F12.6,5x,
     *'Distk [km]='F12.6,5x,'Distkf [km]='F12.6,5x,'hMk [km]='F12.6,5x,
     *'k='I9,/)
  55  Format(F16.4,F16.4)
c-------------------------------------------------------------------------------------------------------
 999     CONTINUE
        RETURN
         END
C*************************************************************************************
```

APPENDIX B

SUBROUTINE FOR SIMULATION OF SOLAR RADIATION FALLING ONTO SOLAR CAR PANEL

```
SUBROUTINE Solar(T,LatM,LonM,hM,ZeSunD,AzSunD,tau,pCloud
     *,nxM,nyM,nzM,WsolP)
c-------------------------------------------------------------------------
c     Parameter(Kyear=0) ;  For  leap year: Kyear=1
      Parameter(Kyear=0)
c-------------------------------------------------------------------------
      DOUBLE PRECISION T,PI,PIH,PI2,ECCEN,EPIS,TM
     *,ER,TER,SE,DelE,OMEGA0,TeS,FiS,phiS
     *,EPISR,SunLoD,SunLaD
     *,BB,AA,CC,EROOT,CONST
     *,SUNMAS,GRAV,DAA,E0,alf
      *,nxM,nyM,nzM,nMmod,s0x,s0y,s0z,s0mod,cos_Capn
      DOUBLE PRECISION LatM,LonM,SunLat,SunLon,CosZeS,CosAzS,ZeSun,AzSun
      DOUBLE PRECISION hM,tau,tauh,pCloud,WsolP
c-------------------------------------------------------------------------------------------------------
c     Finding the Azimuth and Zenith angles of Sun  on 1) Time t (T) reckoned  from the moment
GMT=00.00, March 21
c                                   2) Point M on Earth surface with LatM,LongM
c     The Sun latidue and longitude with time step dt=2 minute and recorded to file "t,Slat,Slon.dat"
c     The number of time points: Nt=(86400sec/120sec)*365=262800  "
C-------------------------------------------------------------------------------------------------------
C      I=0 Day = 21 March,   GMT=00.00
C     + 31 DAY = 21 April       : 31 DAY
C     + 30 DAY = 21 May         : 61 DAY
C     + 31 DAY = 21 June        : 92 DAY
C     + 30 DAY = 21 July        :122 DAY
C     + 31 DAY = 21 August      :153 DAY
C     + 31 DAY = 21 September   :184 DAY
C     + 30 DAY = 21 October     :214 DAY
C     + 31 DAY = 21 November    :245 DAY
C     + 30 DAY = 21 December    :275 DAY
C     + 31 DAY = 21 January     :306 DAY
C     + 31 DAY = 21 Febrary     :338 DAY
C     + 28 DAY = 21 March       :365 DAY
C-------------------------------------------------------------------------
c
          PI=3.1415926536D+0
        PIH=PI/2.
     PI2=2.*PI
     DEL=PI/180.
     PP=149.55E+6
```

```
      HH=43.5192E+8
      SUNMAS=1.989D+30
      GRAV=6.667D-20
      DAA=149.6D+6
          LatMD=LatM/DEL
          LonMD=LonM/DEL
c-------------------------------------------------------------------------------
c     ECCEN=0.01671022                from  NASA
      DelE=23.433333333*DEL
c
      SE=DSQRT((1.+ECCEN)/(1.-ECCEN))
      EPIS=1.D-12
      EPISR=1.D-11
      HP2=(43.5192/14955.)/14955.
c
c     TSPD=24*3600=86400      - "Synodic period" of Earth rotation
      TSPD=86400.
c     TSID=23.9344699*3600=86164.09164 - "Sideral period" of Earth rotation
      TSID=86164.09164
      OMEGA0=PI2/TSID
C       OMSUN=0.199E-6
      OMSUN=DSQRT(GRAV*SUNMAS/DAA)/DAA
      AA=149.6E+6
      BB=AA*DSQRT(1.-ECCEN**2)
      CC=AA*ECCEN
c-----------------------------------------------------------------------------------------
c Time T [sec] reckoned         from the moment: GMT=00.00 March,21 ,
c  If parametr Kyear=0 then J=1,365 ; if        Kyear=1 then J=1,366 days of year (leap year);
c     Kyear=0 then IdEnd=365 ; if       Kyear=1 then IdEnd=366 days of year
c     ------------------------------------------------------
      IdEnd=364
          If(Kyear.eq.1) IdEnd=365
      alf=0.20647
          E0=2.*DATAN(DTAN(PI/4.-alf/2.)/SE)
          CONST=E0-ECCEN*DSIN(E0)

      TM=OMSUN*T+CONST
          TMD=TM/DEL
c
      ER=EROOT(TM,ECCEN,EPIS)
      ERD=ER/DEL
      TER=2.*DATAN(SE*TAN(ER/2.))+alf
      IF(ER.GT.PI) TER=TER+PI2
c       IF(TER.GT.PI2) TER=TER-PI2
      TERD=TER/DEL
      ROU=PP/(1.+ECCEN*DCOS(TER))
      XX=(CC+ROU*DCOS(TER))*1.E-6
      YY=ROU*DSIN(TER)*1.E-6
c
           Day_ofYear=T/TSPD
```

```
c
      TeS=DASIN(-DSIN(DelE)*DCOS(TER))
          TeSD=TeS/DEL
          SunLat=TeS
      SunLaD=TeSD
c
      FiS=DACOS(-DSIN(TER)/DCOS(TeS))
          IF((TER.gt.PI2).and.(TER.le.2.5*PI)) FiS=PI2+FiS
          IF((TER.gt.PIH).and.(TER.le.PI)) FiS=PI2-FiS
          IF((TER.gt.PI).and.(TER.le.1.5*PI)) FiS=PI2-FiS
          IF((TER.gt.1.5*PI).and.(TER.le.PI2)) FiS=PI2+FiS
c
      FiQ0=OMEGA0*T
          FiQ0r=FiQ0-int(FiQ0/PI2)*PI2
c
          FiQ0D=FiQ0/DEL
          FiQ0rD=FiQ0r/DEL
c
          IF(FiS.gt.PI2) FiS=FiS-PI2
          FiSD=FiS/Del
          phiS=FiS-FiQ0r
          phiSD=phiS/DEL
          SunLon=phiS
      SunLoD=phiSD
c
          WRITE(106,57) SunLaD,SunLoD
c
   6  CONTINUE
c
   5  CONTINUE
c-------------------------------------------------------------------------------------
          sLatM=DSIN(LatM)
          cLatM=DCOS(LatM)
          sLonM=DSIN(LonM)
          cLonM=DCOS(LonM)
          sSlat=DSIN(SunLat)
          cSlat=DCOS(SunLat)
          sSlon=DSIN(SunLon)
          cSlon=DCOS(Sunlon)
c
      CosZeS=sLatM*sSlat+cLatM*cSlat
     **(cSlon*cLonM+sSlon*sLonM)
c      If(dabs(CosZeS).ge.1.) CosZeS=dabs(CosZeS)/CosZeS
      ZeSun=DACOS(CosZeS)
          ZeSunD=ZeSun/DEL
          CosAzS=(sSlat-sLatM*CosZeS)/(cLatM*DSIN(ZeSun))
          If(dabs(CosAzS).ge.1.) CosAzS=dabs(CosAzS)/CosAzS
          AzSun=DACOS(CosAzS)
          IF(SunLon.lt.LonM)AzSun=PI2-AzSun
          AzSunD=AzSun/DEL
```

```
c-------------------------------------------------------------------------------------------
          WRITE(199,57) T,AzSunD
      WRITE(100,57) T,ZeSunD
c         WRITE(99,57) Day_ofYear,AzSunD
c      If(ZeSunD.le.90.) Day_ofYear,ZeSunD
c-------------------------------------------------------------------------------------------
  57  FORMAT(2E16.6)
c  60  FORMAT('I='I5,3X,'T='E16.10,3X,'SunLon='F8.2,3X,'SunLat='F8.2)
   60  FORMAT(E16.6,F8.2,F8.2)
c
  58  FORMAT('Thour='E12.6,3X,'DAY='F6.2,3X,'I='I8,3X,'ERD='F8.2,
     *3X,'TERD='F8.2,3X
     *,/,3X,
     */,3X,'SunLoD='F8.2,3X,
     *'SunLat='F6.2
     */,'FiSD='F10.2,3x,'FiQ0rD='F10.2,3X,'FiQrD='F10.2,3X,
     *'phiSD='F10.2,/,3X, /)
c    ---------------------------------------------------------------------------
c      WRITE(108,59) CONST,OMSUN
 59   FORMAT('CONST='E12.4,5x,'OMSUN='E12.4)
 511  Format(F12.6,F12.6,F12.1)
c
c-------------------------------------------------------------------------------------------
 999     CONTINUE
c                Hatm=7995.8 meter
          Hatm=7995.8
c                 GamD - shadow angle for direct Sun beams caused by relief  .
          GamD=0.
      tauh=tau*dexp(-hM/Hatm)
      Call SolDir(ZeSun,tauh,SolPer,GamD)
c                                 unite vector of Sun beam: s0=(s0x,s0y,s0z)
            s0x=-cSlat*cSlon
          s0y=-cSlat*sSlon
          s0z=-sSlat
          s0mod=dsqrt(s0x**2+s0y**2+s0z**2)
          cos_Capn=-(nxM*s0x+nyM*s0y+nzM*s0z)
          nMmod=dsqrt(nxM**2+nyM**2+nzM**2)
          CapnD=dacos(cos_Capn)/DEL
          SolDir_Panel=SolPer*cos_Capn
          If(CapnD.ge.90.) SolDir_Panel=0.
          EtaM=EtahM(ZeSun,hM,Hatm)
          SolDif_Panel=(EtaM/(1.-EtaM))*SolPer*CosZeS
            WsolP=SolDir_Panel+SolDif_Panel
          Write(108,158) T/3600.,CapnD,WsolP,SolDif_Panel
          *,nxM,nyM,nzM,nMmod,s0x,s0y,s0z,s0mod
 158     Format
     *('T='F12.4,5x,'CapnD='F12.4,5x,'WsolP='F12.4,5x,
     *'SolDif_Panel='F12.4,/,
     *'nxM='F12.4,5x,'nyM='F12.4,5x,'nzM='F12.4,5x,'nMmod='F12.4,/,
     *'s0x='F12.4,5x,'s0y='F12.4,5x,'s0z='F12.4,5x,'s0mod='F12.4)
```

```
C
      RETURN
      END
C*********************************************************************
```